IAEA TECDOC SERIES

IAEA-TECDOC-1981

IAEA-TECDOC-1981

Compact Accelerator Based Neutron Sources

IAEA
International Atomic Energy Agency

COMPACT ACCELERATOR BASED NEUTRON SOURCES

The following States are Members of the International Atomic Energy Agency:

AFGHANISTAN
ALBANIA
ALGERIA
ANGOLA
ANTIGUA AND BARBUDA
ARGENTINA
ARMENIA
AUSTRALIA
AUSTRIA
AZERBAIJAN
BAHAMAS
BAHRAIN
BANGLADESH
BARBADOS
BELARUS
BELGIUM
BELIZE
BENIN
BOLIVIA, PLURINATIONAL STATE OF
BOSNIA AND HERZEGOVINA
BOTSWANA
BRAZIL
BRUNEI DARUSSALAM
BULGARIA
BURKINA FASO
BURUNDI
CAMBODIA
CAMEROON
CANADA
CENTRAL AFRICAN REPUBLIC
CHAD
CHILE
CHINA
COLOMBIA
COMOROS
CONGO
COSTA RICA
CÔTE D'IVOIRE
CROATIA
CUBA
CYPRUS
CZECH REPUBLIC
DEMOCRATIC REPUBLIC OF THE CONGO
DENMARK
DJIBOUTI
DOMINICA
DOMINICAN REPUBLIC
ECUADOR
EGYPT
EL SALVADOR
ERITREA
ESTONIA
ESWATINI
ETHIOPIA
FIJI
FINLAND
FRANCE
GABON
GEORGIA
GERMANY
GHANA
GREECE
GRENADA
GUATEMALA
GUYANA
HAITI
HOLY SEE
HONDURAS
HUNGARY
ICELAND
INDIA
INDONESIA
IRAN, ISLAMIC REPUBLIC OF
IRAQ
IRELAND
ISRAEL
ITALY
JAMAICA
JAPAN
JORDAN
KAZAKHSTAN
KENYA
KOREA, REPUBLIC OF
KUWAIT
KYRGYZSTAN
LAO PEOPLE'S DEMOCRATIC REPUBLIC
LATVIA
LEBANON
LESOTHO
LIBERIA
LIBYA
LIECHTENSTEIN
LITHUANIA
LUXEMBOURG
MADAGASCAR
MALAWI
MALAYSIA
MALI
MALTA
MARSHALL ISLANDS
MAURITANIA
MAURITIUS
MEXICO
MONACO
MONGOLIA
MONTENEGRO
MOROCCO
MOZAMBIQUE
MYANMAR
NAMIBIA
NEPAL
NETHERLANDS
NEW ZEALAND
NICARAGUA
NIGER
NIGERIA
NORTH MACEDONIA
NORWAY
OMAN
PAKISTAN
PALAU
PANAMA
PAPUA NEW GUINEA
PARAGUAY
PERU
PHILIPPINES
POLAND
PORTUGAL
QATAR
REPUBLIC OF MOLDOVA
ROMANIA
RUSSIAN FEDERATION
RWANDA
SAINT LUCIA
SAINT VINCENT AND THE GRENADINES
SAMOA
SAN MARINO
SAUDI ARABIA
SENEGAL
SERBIA
SEYCHELLES
SIERRA LEONE
SINGAPORE
SLOVAKIA
SLOVENIA
SOUTH AFRICA
SPAIN
SRI LANKA
SUDAN
SWEDEN
SWITZERLAND
SYRIAN ARAB REPUBLIC
TAJIKISTAN
THAILAND
TOGO
TRINIDAD AND TOBAGO
TUNISIA
TURKEY
TURKMENISTAN
UGANDA
UKRAINE
UNITED ARAB EMIRATES
UNITED KINGDOM OF GREAT BRITAIN AND NORTHERN IRELAND
UNITED REPUBLIC OF TANZANIA
UNITED STATES OF AMERICA
URUGUAY
UZBEKISTAN
VANUATU
VENEZUELA, BOLIVARIAN REPUBLIC OF
VIET NAM
YEMEN
ZAMBIA
ZIMBABWE

The Agency's Statute was approved on 23 October 1956 by the Conference on the Statute of the IAEA held at United Nations Headquarters, New York; it entered into force on 29 July 1957. The Headquarters of the Agency are situated in Vienna. Its principal objective is "to accelerate and enlarge the contribution of atomic energy to peace, health and prosperity throughout the world''.

IAEA-TECDOC-1981

COMPACT ACCELERATOR BASED NEUTRON SOURCES

INTERNATIONAL ATOMIC ENERGY AGENCY
VIENNA, 2021

COPYRIGHT NOTICE

For further information on this publication, please contact:

Physics Section
International Atomic Energy Agency
Vienna International Centre
PO Box 100
1400 Vienna, Austria
Email: Official.Mail@iaea.org

Printed by the IAEA in Austria
September 2021

IAEA Library Cataloguing in Publication Data

Names: International Atomic Energy Agency.
Title: Compact accelerator based neutron sources / International Atomic Energy Agency.
Description: Vienna : International Atomic Energy Agency, 2021. | Series: IAEA TECDOC series, ISSN 1011–4289 ; no. 1981 | Includes bibliographical references.
Identifiers: IAEAL 21-01449 | ISBN 978-92-0-133221-9 (paperback : alk. paper) | ISBN 978-92-0-133321-6 (pdf)
Subjects: LCSH: Neutron sources. | Particle accelerators. | Nuclear physics.

FOREWORD

Since the discovery of the neutron in 1932, neutron beams have been used in a broad range of applications. Neutrons are an essential tool in science and research for probing the structure and dynamics of matter from the mesoscale to the nanoscale and from seconds to nanoseconds. The unique properties of neutrons as a powerful probe of matter are particularly well suited to investigating many of the key scientific and societal problems we are facing today and will face in the future, including in the areas of energy, transport, communications, computing technology, environment and health care.

The production of neutrons has been primarily related to the operation of research reactors established in the late 1950s and early 1960s. The production of neutrons by accelerators started later in the 1970s with the construction of large powerful proton accelerators to access neutrons via spallation. At the same time, low energy driven neutron processes emerged for neutron production using electron accelerators, ion beam accelerators, cyclotrons and low energy linear accelerators. This wide variety of accelerator based neutron sources have become known as compact accelerator based neutron sources (CANS). In recent years interest in CANS has increased, partly driven by the closure of aged research reactor based neutron sources, the physical and technical limitations to the power of research reactors and the high cost of megawatt spallation neutron sources. Countries that do not wish to pursue a research reactor neutron source and for which the cost of a spallation source is too high may find one or more CANS technologies of interest.

This publication is the result of a technical meeting held from 4 to 7 November 2019. Twenty-seven representatives of 14 Member States participated: Argentina, Canada, China, France, Germany, Hungary, India, Israel, Japan, Republic of Korea, Russian Federation, Spain, Switzerland and the United States of America.

The IAEA wishes to thank all participants in the technical meeting, in particular, T. Gutberlet (Germany) and F. Ott (France) for their role as Scientific Chairs of the meeting, R. Granada and S. Gossio (Argentina) for their contributions, as well as S.W. Yates (United States of America) and J. Becker (Germany). The IAEA officers responsible for this publication were I. Swainson and S. Charisopoulos of the Division of Physical and Chemical Sciences.

EDITORIAL NOTE

This publication has been prepared from the original material as submitted by the contributors and has not been edited by the editorial staff of the IAEA. The views expressed remain the responsibility of the contributors and do not necessarily represent the views of the IAEA or its Member States.

Neither the IAEA nor its Member States assume any responsibility for consequences which may arise from the use of this publication. This publication does not address questions of responsibility, legal or otherwise, for acts or omissions on the part of any person.

The use of particular designations of countries or territories does not imply any judgement by the publisher, the IAEA, as to the legal status of such countries or territories, of their authorities and institutions or of the delimitation of their boundaries.

The mention of names of specific companies or products (whether or not indicated as registered) does not imply any intention to infringe proprietary rights, nor should it be construed as an endorsement or recommendation on the part of the IAEA.

The authors are responsible for having obtained the necessary permission for the IAEA to reproduce, translate or use material from sources already protected by copyrights.

The IAEA has no responsibility for the persistence or accuracy of URLs for external or third party Internet web sites referred to in this publication and does not guarantee that any content on such web sites is, or will remain, accurate or appropriate.

CONTENTS

1. INTRODUCTION

1.1. BACKGROUND

The ‘traditional’ means of producing moderate to intense neutron beams for research purposes was via a research reactor. Globally, the number of research reactors around the world is falling, particularly in developed Member States. However, a slow growth in the numbers of research reactors is seen in developing Member States. As of September 2020, there were 857 research reactors in the world of which 220 were operational. Over 30 Member States are either developing or have plans to build one, for 10 of which it would be the first reactor in the country [1]. However, it seems certain that there will be a further decrease in the coming 20 years, as two-thirds of the operating research reactors are over 40 years old and are approaching the end of their operational lives [2]. Therefore, many countries are faced with the choice to either build new research reactors or search for alternative technologies to satisfy some of the needs currently fulfilled by reactors.

In the last few decades, spallation neutron sources have emerged as alternatives to research reactors for neutron beam research. Spallation sources for neutron beam research are typically built around proton accelerators with energies from 600 MeV to over 1 GeV. The European Spallation Source [2], expected to be completed in 2025, will be the first accelerator that holds the status of the most intense time-averaged neutron source in the world (overtaking the high flux reactor at the Institut Laue Langevin, France) with an aim of reaching 5 MW of proton beam power, but comes with a capital budget estimate of about €1.8 billion. The cost and complexity of such accelerators means they are not considered a feasible alternative by many countries as national or local neutron sources.

The term ‘compact accelerator based neutron sources’ (CANS) has been coined to describe a variety of different lower energy accelerators that produce neutrons. Recently, based on developments in accelerator, targets and moderator technologies, CANS have emerged as a possible alternatives to research reactors and spallation sources for some applications. The definition of CANS for the purpose of this report is those accelerators based neutron sources whose main purpose is to produce neutrons, but that do not use spallation as the production process (see Section 4.2.1). These processes typically produce one neutron per nuclear reaction, rather than 20–30 that can be achieved by spallation. However, the energy of the neutrons is lower, and the sizes of the moderators and shielding correspondingly smaller. It is the optimization of these factors that enables the CANS to be considered as competitive neutron sources for some applications.

The most common types of accelerators being considered include neutron generators, cyclotrons, electrostatic accelerators, and radiofrequency (RF) linear accelerators, most commonly of electrons or protons (see Section 4.1). As is the case for research reactors, CANS can be constructed in a variety of powers and price ranges, which could serve either an entire nation or a single large research institute. For Member States and their institutions which do not wish to build a nuclear reactor, one or more type of CANS may be a viable alternative.

CANS represent alternatives for some applications, including many of the basic research opportunities for neutron beams, as well as education and training opportunities. They can also provide flexibility to neutron sources: few reactors provide sustained pulsing, and the most notable is the IBR-2 reactor, located at the Frank Laboratory of Neutron Physics, Joint Institute

for Nuclear Research in Dubna, Russian Federation [3], whereas CANS can readily be designed to be continuous (also denoted 'CW') with instruments built around them are similar in design to those at most research reactors. Alternatively, CANS can also be designed to be pulsed, with long, short or mixed pulse durations. Pulsed instruments rely on the time-of-flight ('TOF') method, recording arrival times of neutrons of different energies that were all created by the same pulse on the target.

In general, licensing a CANS is a simpler process than licensing a nuclear reactor (Section 6). As they generally do not involve fissile material and are free from criticality accidents, there are lower safety and security concerns during operation, which makes access by scientists and students easier. For similar reasons, decommissioning at the end of life are usually significantly cheaper (see Section 7.3).

Recently, the conceptual design for a CANS termed NOVA ERA that would be suitable for a research university has been developed by Forschungszentrum Jülich, Germany. The estimate for such a CANS (excluding building) is ca. €4M, with each neutron instrument estimated on average as an additional ca. €900 000 [4]. To date, the highest power CANS to have been operated is ~4 kW power [5]. However, the same laboratory designing NOVA ERA is currently developing the concept for a national CANS, the 7 MW High Brilliance neutron Source (HBS), that would be competitive with research reactors for many techniques but would also be comparable in capital cost [6]. Similar plans of various scales are being developed in several countries, and the IAEA has started to receive requests for assistance from newcomer countries. Hence, it was felt it was timely for the IAEA to produce the report presented here.

An interactive map of CANS has been recently published by the IAEA [7], see Fig. 1. Links within this interactive map lead to further information about individual facilities that may be of interest to those exploring options for CANS.

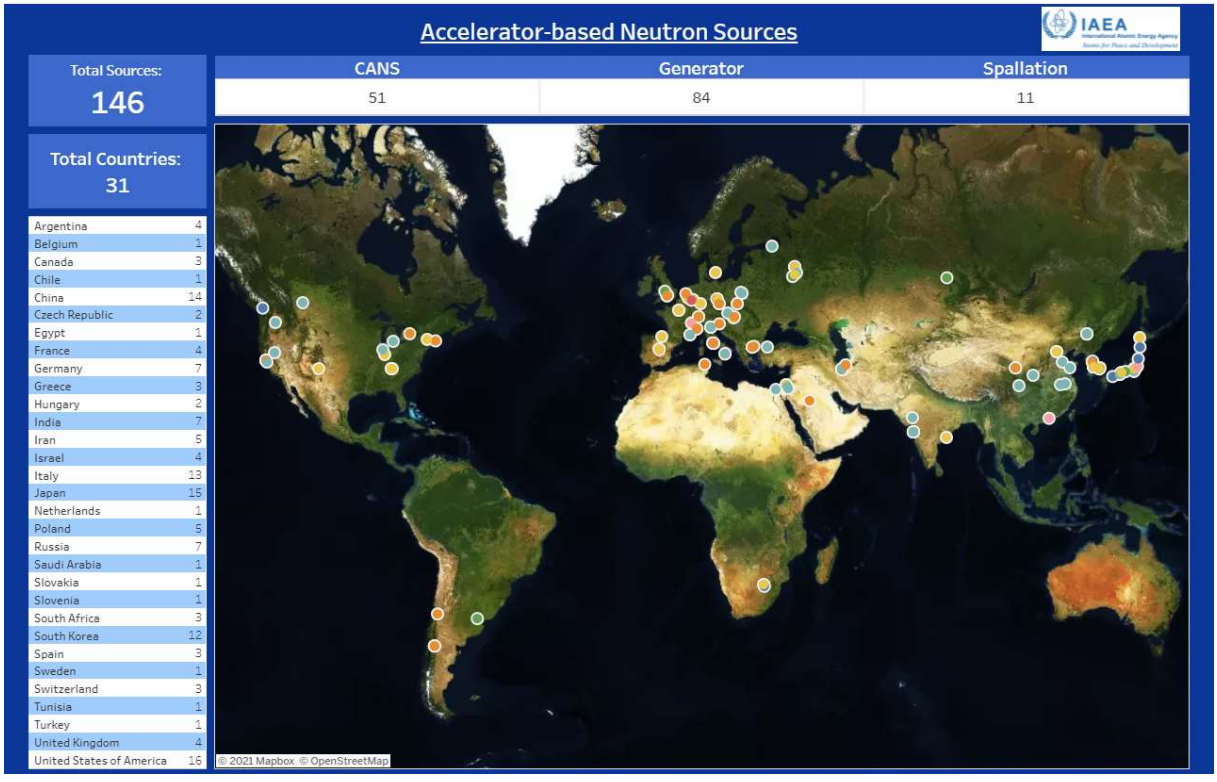

FIG. 1. Interactive visualization of known accelerator based neutron sources used in research from Ref. [7].

1.2. OBJECTIVE

This publication aims to provide an overview of the various types of CANS technologies that are currently available or planned in the near future. It also aims to illustrate many of the analytical and other applications of neutrons that can be used to give a technical justification to a proposal for such a system. Given the wide variety of power and costs, the publication also aims to show that in addition to replacing national medium flux research reactors for certain functions, smaller regional neutron sources may become viable, which may eventually broaden access to neutron facilities.

1.3. SCOPE

The scope of this publication includes a description of research techniques and applications of CANS that can be used as a technical justification for building a facility, technical information regarding the major components of CANS and the supporting infrastructure, as well as the discussion of potential costs and regulatory requirements, which may aid in budgetary planning and decision making for such potential CANS projects.

As boron neutron capture therapy (BNCT) is a growing application for certain classes of CANS, the publication provides a brief overview of this application. A detailed description is beyond the scope of this publication.

1.4. STRUCTURE

The overview given in the next two sections deal with utilization of CANS and may be of interest to both technical experts and decision makers in research funding agencies.

Section 2 provides an overview of the analytical techniques using neutrons that CANS systems could be used for. First, neutron scattering and imaging techniques in condensed matter physics and allied research areas, such as solid state chemistry, structural biology and engineering are illustrated. Next, the use of CANS for cross section measurements in fundamental nuclear physics are discussed. This is followed by a description of neutron activation analysis methods.

In Section 3, an overview of various applications of CANS in other fields that require neutrons is given, including radiation damage to nuclear materials and electronics, radiobiology, radioisotope production, silicon doping, reactor physics, BNCT, and metrology are given.

The neutron analytical techniques and the fields of application outlined above, together with the estimated source strength requirements, may be used to form the basis of the technical justification for the need for a CANS facility.

Section 4 provides technical detail concerning CANS and their current state of development. Neutron generators, cyclotrons and electron linear accelerators that could be used as the basis of a CANS are available as almost ‘commercial off the shelf’ varieties. These three accelerator types are presented in a common format for ease of comparison, including cost guidance, where available. This is followed by a description of a couple of high current electrostatic accelerators that are being developed largely due to the rise in the interest of accelerator based BNCT but will be suitable for many physics applications as well. Next, linear ion (proton/deuteron) accelerators (radiofrequency quadrupoles and drift tube linear accelerators) are briefly described along with some of their main design parameters. The maximum current such accelerators can achieve has been increased by developments in higher powered accelerators;

e.g., spallation sources. These advances promise to also increase the neutron output for CANS designed about this class of accelerator. Finally, the new technology of laser driven neutron sources is introduced. Later in Section 4, the nuclear reactions that lead to neutron production are outlined and some of the target technologies are described. Moderator technologies for the thermalization of high energy neutrons are presented (epithermal, thermal, cold moderators), as are aspects of the neutron reflector systems.

Managers and potential funders may find the later sections the most relevant to them.

The advantages that building a CANS may bring, compared to the alternatives of spallation neutron sources and research reactors, as well as some of their limitations, are outlined in Section 5.

Section 6 gives a light overview of some regulatory issues concerning CANS, and an example of the regulatory situation in Argentina.

In Section 7, the investment requirements for the major components of CANS systems as well as neutron scattering instruments are addressed. The topic of the justification of such facilities on financial, macroeconomic, and broader socio-economic criteria is dealt with, and two examples of investments in Argentina and the Republic of Korea are given.

Section 8 gives a brief summary and conclusions of the publication.

2. NEUTRONS AS ANALYTICAL TOOLS

Since the discovery of the neutron in 1932, neutron beams have been used in a very broad range of applications. Neutrons are an essential tool in science and research for probing the structure and dynamics of matter from the mesoscale to the nanoscale and from seconds to nanoseconds. The unique properties of neutrons as a powerful probe of matter are particularly well aligned with many of the key scientific and societal problems we are facing today and will face tomorrow, including energy, transport, communications and computing technology, as well as environment and healthcare. The fact that neutrons interact strongly with hydrogen nuclei makes them a unique tool for the investigation of organic materials. In addition, the neutron's spin permits the investigation of magnetic structures down to atomic length scales. The high penetration depth of neutrons in the absence of net electric charge allows the non-destructive investigation of objects such as engineering devices or historical artefacts.

Table 1 shows typical source strengths required for specific techniques, together with the preferred neutron energy spectrum (cold, thermal, hot), and whether pulsed or CW operation is preferred. The analytical techniques and methods used in physics are outlined in this section and other applications in Section 3. More discussion on neutron energies and how neutrons may be produced or moderated to obtain them is provided in Section 4.3.

Training and education of the next generation of scientists, engineers and facility staff is often an important aspect of university based sources. For example, the AKR-2 training reactor at TU Dresden is devoted to the training and education of nuclear engineers [8]. The IAEA also offers training for scientists and engineers on nuclear applications at their Seibersdorf laboratories [9]. The main focus is the training of future users of neutron facilities and the education of students as part of their studies in physics, chemistry, material science, geosciences, and related areas. Given their potentially more widespread distribution in the future and their comparatively easy access, CANS may serve as an important training ground for users to learn and become proficient in various techniques. Depending on the demand, they can offer and enlarge the current training possibilities worldwide.

The majority of large neutron scattering facilities organize annual neutron schools (see Table A-1 in the Annex). These provide direct training in the basics of neutron related science and techniques and enhance the multidisciplinary and multi-technique utilization of neutron beams by coordinated thematic training and promoting access for hands-on training. They also provide advanced studies in fields of basic and applied research with neutrons, including instrumentation. These more 'advanced schools' focus on experienced users. Often these schools and training activities build on well-established courses proposed by facilities or universities. Usually the activities include intense hands-on training and experiments at a local neutron source. Participants either do their own experiments or participate in a case study. In particular, smaller facilities with less extensive user service offer broad and in-depth training options. The training of students is either organized by participating in neutron schools or topical summer schools as introductory courses for Masters and PhD students. In addition, Masters and PhD thesis are regularly proposed to students to work with neutrons and learn about the methods and their applications. Training by courses and schools (Table A-1 in the Annex) can also teach young researchers how to prepare experimental proposals and access large scale facilities. Smaller CANS at universities as already established in Japan can offer training grounds for students from undergraduate to PhD level as well as training for industry, professional safety personnel, and regulatory staff.

TABLE 1. TYPICAL SOURCE STRENGTH NECESSARY FOR DIFFERENT TECHNIQUES USING NEUTRONS

Technique	**Source strength n_{fast} [n/s]**	**Time structure**	**Spectrum**	**Use**
		NEUTRON SCATTERING		
Elastic	10^{12}–10^{15}	TOF (preferred) or CW	Thermal Cold Hot	Solid state physics and chemistry, metallurgy, soft matter, chemistry, magnetism
Spectroscopy	10^{15}	TOF (preferred) or CW	Thermal Cold Hot	
eV spectroscopy	10^{14}	TOF (preferred)	Hot	
Instrumentation development	10^{12}	TOF or CW	Thermal Cold	
Multiple scattering and absorption	10^{8}–10^{10}	TOF or CW	Thermal Epithermal Fast	Logging in oil industry
		NEUTRON IMAGING		
Cold – Thermal	10^{11}–10^{13}	CW (preferred) TOF (possible)	Thermal Cold	Qualification of pyrotechnics for propulsion and explosives in space and aerospace systems; nuclear elements (fuel elements activated or not; Boron and U content) Academic (geology, fuel cells, batteries, plants, archeology, metallurgy)
Epithermal	10^{14}		Epithermal (1 eV–50 keV)	Resonance imaging + temperature measurements (in bulk)
Fast	10^{14}		Fast	Nuclear waste barrels (on-site), bridges (in-field)
Time resolved	10^{14}–10^{15}		Thermal Cold	
Energy resolved	10^{14}–10^{15}		Cold	Use of Bragg edges to identify materials (Bragg edges from 2 to 4Å)

TABLE 1. TYPICAL SOURCE STRENGTH NECESSARY FOR DIFFERENT TECHNIQUES USING NEUTRONS (cont.)

Technique	**Source strength n_{fast} [n/s]**	**Time structure**	**Spectrum**	**Use**
			NUCLEAR PHYSICS	
Cross section measurements (Nuclear data)	10^{10}–10^{11}	TOF	Thermal Fast (14–40 MeV)	Thermal neutron resonances for fast breeder reactors / Na cooled reactors Fusion neutrons, resonances, nuclear transmutation Cross section of compounds
Nuclear physics experiments	10^{12}	CW or TOF	Cold Epithermal	Preparation for JPARC experiments (ex. CP violation) Instrumentation development
			ACTIVATION	
Neutron Activation Analysis (NAA)	10^{8}–10^{11}	CW	Thermal Epithermal Fast	Trace elements (off-site + on-site) Authenticity (paintings) Homeland security, Forensics, Legacy materials, Astrogeology
Prompt Gamma Activation Analysis (PGAA)	10^{8} –10^{12}	TOF or CW	Thermal Epithermal Fast	Cement (on-line) Bridge inspection, Mining (on-site) Explosive materials (on-site) Oil well logging
			IRRADIATION	
Software errors	10^{12}	CW	Fast	Aerospace, Chips for satellites & autonomous cars
Hardware errors	10^{10}	CW	Fast	Aerospace Chips for satellites & autonomous cars
Radioisotope production, including medical	10^{13}–10^{14}	CW	Fast Thermal	Direct proton reactions are dominated by cyclotrons and widespread. The direct deuteron (d,p) reaction mimics the (n,γ) reaction. Possible (n,α) or (n,p) etc. reactions are being developed at electron linac (Bremsstrahlung) sources.

TABLE 1. TYPICAL SOURCE STRENGTH NECESSARY FOR DIFFERENT TECHNIQUES USING NEUTRONS (cont.)

Technique	**Source strength n_{fast} [n/s]**	**Time structure**	**Spectrum**	**Use**
Radiobiology	10^{13}		Thermal Epithermal Fast	Mutations Space agencies Cell survival experiments and small animal studies
Silicon doping	10^{16}			CANS not competitive with research reactors. Large homogeneous density is required
Irradiation Metallurgy Plastics	10^{18}		Thermal Specific Fast spectrum (fusion n)	Irradiation of structural materials (metallic alloys) (e.g. IFMIF as test facility for fusion materials or nuclear power plant structural materials)
			REACTOR PHYSICS	
Drive sub-critical reactor assembly Reactor physics	10^{10}	CW		Mostly requires spallation. High powered e-linacs are possible.
			BNCT	
Development	10^{12}–10^{14}	CW	Epithermal	Research reactors played the traditional role. CANS may dominate in the future.
Cancer treatment	10^{13}–10^{15}	CW	Epithermal (0.5 eV–10 keV) Thermal (for skin and explanted organs)	Treatment in hospitals (4 patients /day) It is generally easier to build CANS than research reactors in clinics.

TABLE 1. TYPICAL SOURCE STRENGTH NECESSARY FOR DIFFERENT TECHNIQUES USING NEUTRONS (cont.)

Technique	**Source strength n_{fast} [n/s]**	**Time structure**	**Spectrum**	**Use**
			METROLOGY	
Neutron fields	10^8	CW	Thermal or Mono-energetic (2 keV–20 MeV)	Test and calibration of reference detectors Qualification of dosimetry equipment
			TRAINING	
User training	10^8	CW or TOF	Thermal Cold	User training sessions (1/2 week)

NOTE: “CW” refers to continuous mode operation; “TOF” refers to a pulsed operation for time-of-flight measurements.

2.1. NEUTRON SCATTERING

Neutrons exist over a very wide energy range (Section 4.3). By a coincidence of quantum physics, thermal neutrons (see Section 4.3.2), as moderated in nuclear reactors, have an associated wavelength on the order of a fraction of a nanometre which is ideally suited to study the structural properties of condensed matter. This is a key reason for the early success of neutron scattering techniques, since useful neutrons were readily available around any water-moderated research reactor with beam tubes to supply various instruments for neutron scattering research.

Neutron wavelengths can be increased by using hydrogenous materials at cryogenic temperatures known as 'cold moderators' (see Section 4.3.3). In this case, the useful wavelength range spans from 3 to 20 Å (10^{-10} m). Cold neutrons can be transported in guides outside the main reactor or accelerator building, thus providing a lower background environment and more flexibility to build neutron scattering instruments.

A recent review of neutron scattering instruments suitable for low and medium flux sources has been recently published [10], which provides information on various classes of instruments and techniques, and an interactive map of known neutron scattering and imaging instruments has been published [11], see Fig. 2. The number of instruments has dropped in recent years as neutron scattering facilities in Berlin, Germany, Saclay, France and Chalk River, Canada have been closed. As of February 2021, there were >50 neutron imaging facilities, >120 diffractometers, >100 spectrometers and around 130 other instruments, including small angle neutron scattering (SANS) instruments, reflectometers, interferometers etc. Some of the major neutron techniques and applications are outlined below.

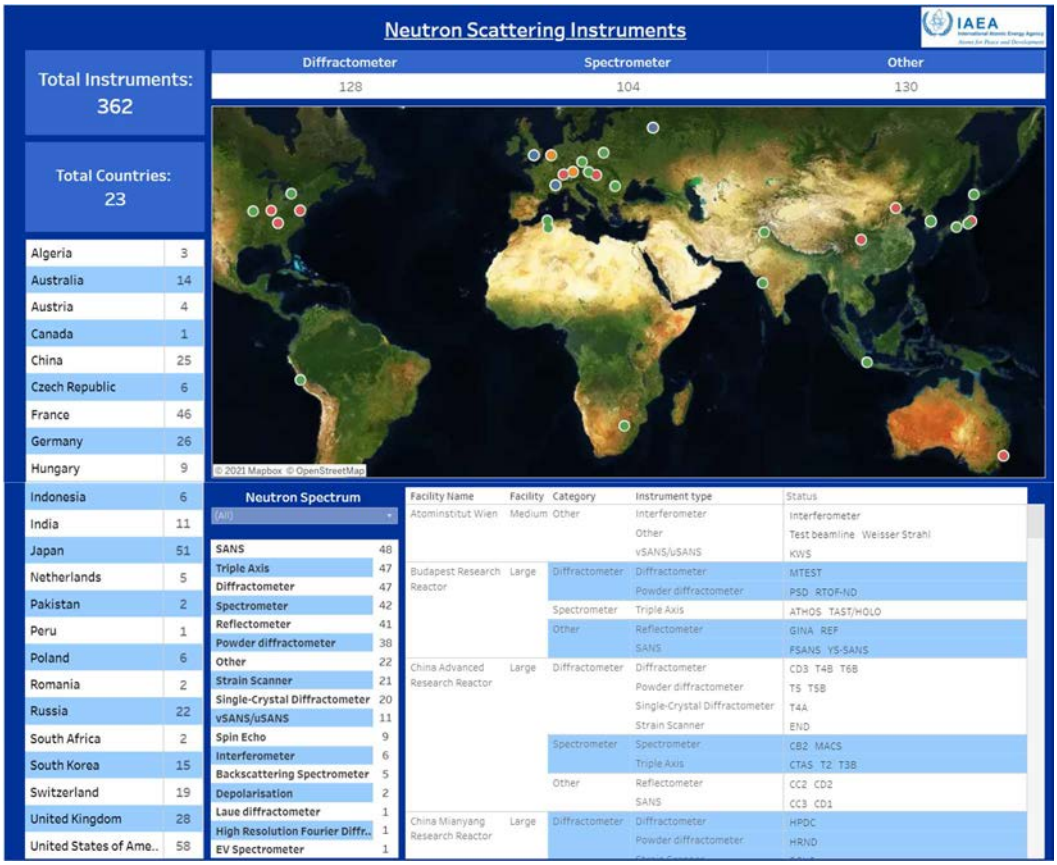

FIG. 2. Visualization map of the known neutron scattering instruments from Ref. [11].

2.1.1. Elastic neutron scattering

Elastic neutron scattering is a reciprocal space method where energy is not transferred between the neutron and the sample. It is sensitive to structural and magnetic correlations in the range of the neutron's wavelength: powder diffraction and single crystal diffraction are common elastic neutron scattering techniques used to investigate the arrangement of atoms on the scale of atomic distances.

Neutron diffraction is complementary to X-ray diffraction. In contrast to X-rays, the neutron's nuclear interaction potential does not increase monotonically with the atomic number, so that light elements, e.g. lithium, nitrogen, oxygen, and most importantly hydrogen, can be investigated in an environment of much heavier atoms. Similarly, as the neutron is neutral and interaction with matter occurs via the strong nuclear force, it is not strongly scattered by the charges on electron clouds (unlike X-rays), which leads to neutrons being very penetrating. There is also a large magnetic interaction of neutrons with unpaired electrons in materials due to the quantum spin of the neutron.

Neutron powder diffraction instruments are workhorses in neutron diffraction. High resolution instruments are routinely used for structure determination and refinement, in particular for magnetic structures. High flux instruments are used to study phase transitions or determine stress distributions within materials.

Cold neutrons, due to their longer wavelengths, are better suited than thermal neutrons to study large scale structures in soft matter, biomaterials, and metallurgy. Small angle neutron scattering (SANS), used for direct measurement of large scale structures, and reflectometry, used for measuring interfaces and surfaces, are usually performed with cold neutrons.

In 2016, there were about 220 elastic neutron scattering instruments in the world [12] (among which half of them were in Europe). Further information can be found on various web sites[1] and in Refs [5, 10].

2.1.2. Low energy neutron spectroscopy

Inelastic scattering is one of the great strengths of neutron scattering thanks to the very low kinetic energy of thermal and cold neutrons (in the meV range). This permits the study of excitations in the low energy regime energies ranging from neV (with spin-echo techniques) up to 0.1 eV in the lower part of the epithermal range (Section 4.3.1). This can be performed with triple axis techniques on a continuous neutron source, or with chopper spectrometers and inverted geometry crystal spectrometers on a pulsed neutron source. Inelastic neutron scattering[2] provides unique information about the dynamic properties of condensed matter such as phonons, magnons, other exotic magnetic excitations, molecular excitations, diffusion constants and molecular motions.

Exchange constants and inter-atomic forces can be derived by modelling inelastic neutron scattering cross sections. These microscopic parameters allow the prediction of the response at

[1] https://www.e-neutrons.org/, https://neutronsources.org/

[2] Throughout this document, the term inelastic neutron scattering is generally used in the sense of exchange of energy between the neutron and the chemical or magnetic structure (via phonons and magnons etc.). However, the term has two common meanings, and in nuclear physics concerns a specific type of nuclear reaction (see Section 2.3.3)

a macroscopic level. Self-, pair-, and spin-correlation functions can be obtained in absolute units from low energy neutron spectroscopy and directly compared to ab initio computer models. This simple and direct comparison between the cross sections and computer modelling and theory is vital for many fields of research. Inelastic X-ray techniques are largely complementary to inelastic neutron scattering, but none of them provides the same direct and universal access to absolute scattering functions as does neutron spectroscopy. Besides, the energy resolution of X-ray spectroscopy is limited.

In 2016, there were about 150 low energy neutron spectroscopy instruments in the world [8] (among which half of them were in Europe). Further information can be found on various web sites[1] and in Refs [5, 10].

2.1.3. High energy neutron spectroscopy

Neutrons above about 0.1 eV in the epithermal regime (Section 4.3) are used to measure momentum distributions in quantum and molecular fluids and solids, hydrogen momentum distributions and single particle dynamics in amorphous materials, polymers, catalysts, and metal hydrides [13, 14]. This method was first applied to measure the condensate fraction in superfluid helium. Epithermal neutrons are more readily available at accelerator-driven neutron sources than from typical research reactors, since the moderators from accelerators produce an energy spectrum of $1/E$ in the neutron slowing down region. This technique is known as neutron Compton scattering. Energy analysis is performed by combining the time-of-flight method with a resonance energy of a metal foil energy selector such as Au. Vesuvio at the ISIS Facility is an example of such a spectrometer [14].

2.1.4. Multiple-scattering and absorption in massive samples

In addition to the laboratory based techniques described above which are typically conducted on well-controlled samples and conditions, there are neutron techniques that are applied in industry in field conditions. One of the commercially relevant applications of neutron scattering as well as absorption is in geophysics and, specifically, for the oil industry. In this context, neutron interrogation of soil is performed utilizing a probe moving along a borehole, which contains the neutron source and a series of detectors in different specific positions. The neutrons returning to the probe after a complex chain of multiple scattering processes (elastic and inelastic), and having surviving absorption, can be counted on each of the detectors considering a spectral analysis and, if a pulsed source is used, also arrival time analysis. This type of measurements allows for a multivariable characterization of the formation. Depending on the specific systems and methodologies (that can include other associated measurement techniques), estimates for parameters such as porosity, density, amounts of certain compounds, and geometry patterns can be assessed [15–20]. On the basis that it is a well-established technique for geophysics and conventional oil exploitation, it is finding further potential applications, e.g., where fracking is used in combination with smart proppants that might be rich in neutron reactive compounds like Gd or Sm [19].

2.2. NEUTRON IMAGING

Neutron imaging is a real-space technique. It resolves structures at length scales ranging from mm down to a few μm. The attenuation of the neutrons arises either by absorption or by scattering. The absorption contrast is important only for a few elements like B, Li, or Cd.

Coherent scattering on crystal lattices can occur when the neutron wavelength is smaller than or equal to a lattice plane spacing. If the wavelength is longer than the maximum lattice spacing, coherent scattering is no longer possible, and the transmission increases significantly. This discontinuity is the so-called 'Bragg edge'. A more exotic source of transmission contrast is due to SANS or refraction effects which can be measured using grating interferometry.

In the case of gamma rays, the mass coefficient becomes smaller with increasing energy and increases with mass number. On the other hand, the absorption coefficient of thermal neutrons is isotopically dependent. The absorption coefficient for fast neutrons smoothly decreases with atomic number, and for atomic number above around 40 this value is less than that for a 6 MeV gamma ray. Therefore, thick materials can be radiographed by fast neutrons. The major source of contrast in neutron imaging is, however, the contrast from incoherent scattering from H which can be used in all types of problems where a hydrogenous liquid (typically water) interacts with a porous medium (rock, soil, concrete, steel, fuel cell membrane, living organisms, etc.)

2.2.1. Cold and thermal neutron imaging

Cold and thermal neutron imaging is a very suitable technique to observe organic materials surrounded by metal, e.g. lubricants inside a motor, or water induced corrosion inside steel [21]. Science cases include a vast range of areas including geology [22, 23], construction materials [24, 25], porous materials, and plant sciences [26, 27]. A typical technological application is the observation of the behaviour of water in fuel cells (Fig. 3).

Jet turbine blades are examined routinely for quality issues using neutron imaging. Currently, these are transported to a research reactor for investigation. It has been suggested that a CANS system based on a Deuteron-Deuteron or Deuteron-Triton source with a gas target be used instead and could be situated directly in the turbine manufacturing facility [28].

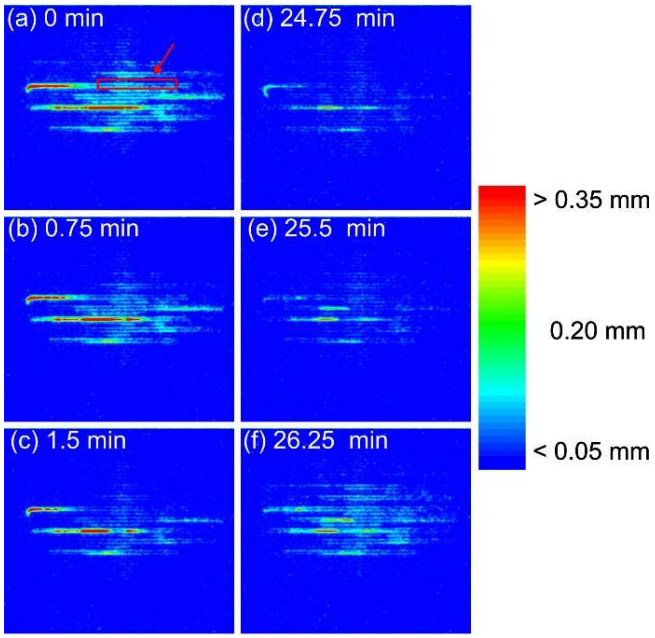

FIG. 3. Neutron radiographs of a proton exchange membrane fuel cell. The colour indicates thickness of water. After 24.75 min, deuterium gas replaces hydrogen gas and the contrast changes (Fig. 1 reproduced from Ref. [29] with permission courtesy of AIP Publishing).

Using polarized neutrons, magnetic field information can be reconstructed [30]. By using a pulsed neutron beam, the absolute value of the magnetic field is easily obtained. Figure 4 shows an example of the magnetic field distribution in a superconducting metal and Fig. 5 the spatial distribution of magnetic moments with a certain orientation within a soft magnetic foil.

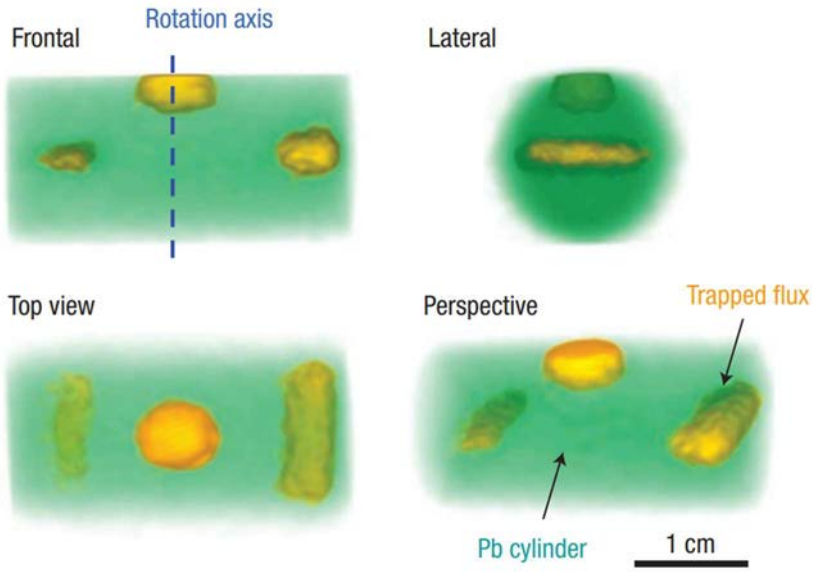

FIG. 4. Trapped flux in a polycrystalline lead cylinder at T = 7K revealed by neutron imaging (Fig. 3b in Ref. [26], courtesy of Nikolay Kardjilov, Helmholtz-Zentrum Berlin, Germany).

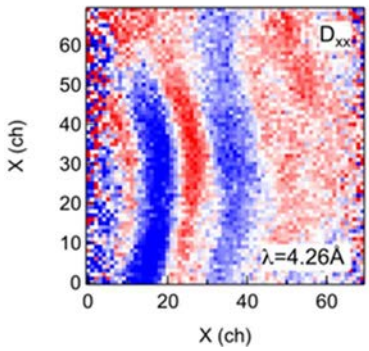

FIG. 5. Neutron polarization distribution associated with the magnetic field distribution in a soft magnet foil (Fig. 10 reproduced from Ref. [31] with permission. © IOP Publishing. All rights reserved. Licensed under CC BY).

2.2.2. Epithermal and fast neutron imaging

While neutron imaging is most often performed with a thermal or cold neutron beam, the penetration of thermal or cold neutrons is not always sufficient for thick samples. Therefore, epithermal neutrons can be used for more 'real world' applications, e.g. on machine parts or rock samples containing water in crystalline structures.

A 1–2 mm Cd filter effectively absorbs all neutrons with energies lower than 0.4 eV, but is relatively transparent for higher energies, including epithermal neutrons. Examples of epithermal neutron imaging measurements are given in Ref. [32]: it shows that image quality can be improved by increasing neutron penetration and by filtering out scattered and thermalized neutrons.

Fast neutron imaging is the only technique that can give a transmission image of high density and large volume objects with reasonable contrast [33, 34]. This is applicable, e.g., to homeland security to see hidden explosive materials, nuclear fuel, cultural heritage, inspection of infrastructure like bridges, and so on. A pulsed, high-current neutron generator has been proposed for fast neutron imaging in Russia [35].

2.2.3. Time resolved imaging

Thanks to the use of fast charge coupled device imagers, it is possible to perform neutron imaging measurements at very high speeds, down to 50 μs time frames in stroboscopic mode and a fraction of a second for single shots (Fig. 6, Ref. [36]).

Neutron cross sections of many elements (isotopes) have characteristic features depending on the neutron energy. These are discussed briefly below.

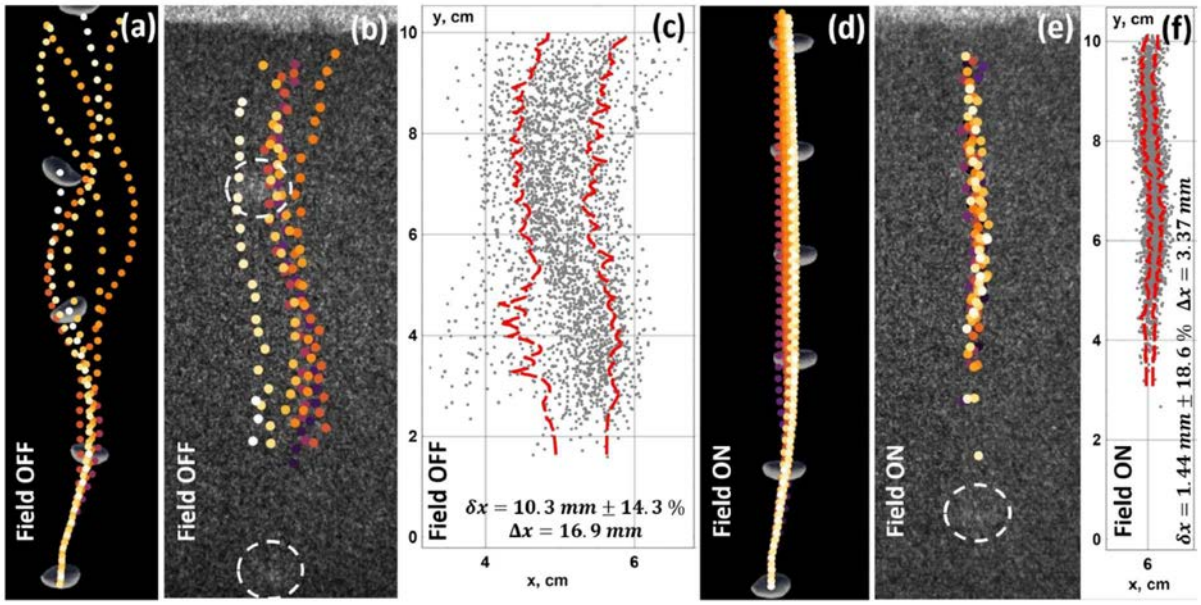

FIG. 6. Several bubble trajectories for a 100 cm^3/min flow rate derived from simulations (a,d) and experiments (b,e). In cases (a,b) there is no magnetic field, and in (d,e) the field (~0.3 T) is applied. Bubble detection points are colour coded by order or appearance, dark purple to white (Reprinted from Ref. [36] with permission from IOS Press. The publication is available at IOS Press through http://dx.doi.org/ 10.3233/JAE-209116).

2.2.3.1. Thermal and cold neutron regions

In the thermal and cold neutron regime, the measured cross section from a material is sensitive to its atomic structure. Bragg edge structures appear in this regime due to the onset of diffraction. Figure 7 shows the Bragg edge transmission spectrum of a steel. By using an analysis code (e.g. RITS [37]), one can obtain the lattice spacing from the edge position, the crystallite size from the transmission intensity, the texture from the shape around the Bragg edge and the strain from the shift of the Bragg edge positions [38].

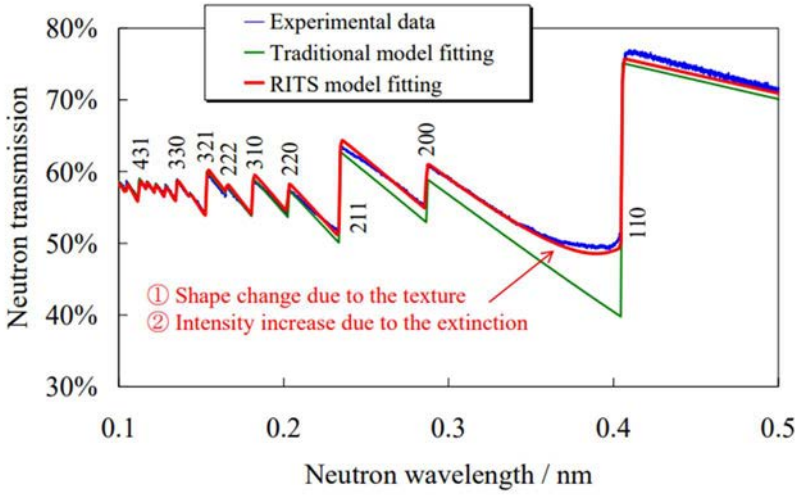

FIG. 7. Bragg edge experimental transmission spectrum, RITS simulation result and model transmission using a standard cross section (Fig. 1 from Ref. [31] reproduced with permission. © IOP Publishing. All rights reserved. Licensed under CC BY).

This is of interest, e.g., in steel production, where the mixture and order of martensitic and austenitic phases determines important mechanical properties of the material.

Energy selective neutron images can also be measured at different energies over the area of a welded region of a metal [38, 39]. Changes in the neutron cross section reflect the changes of crystallographic structure in the welded region. The measurements in Refs [38, 39] were done with a monochromated continuous neutron beam but are much easier to perform with a pulsed neutron beam with time-of-flight methods; as an example, quenched and unquenched regions have been identified as a function of depth in quenched ferritic steel samples by Bragg edge analysis and Vickers Hardness measurements [40]. Studies have been performed at large and medium scale neutron facilities, but also at CANS [38, 41, 42].

2.2.3.2. Epithermal and fast neutron regions

Epithermal neutron cross sections typically consist of a constant potential cross section and resonance absorption cross sections. If the resonance cross sections are large enough, isotope selective images can be obtained, or temperature can be measured [43–45]. These kinds of measurements are carried out using energy selective imaging at pulsed neutron sources. Figure 8 shows such element specific imaging using resonance absorption.

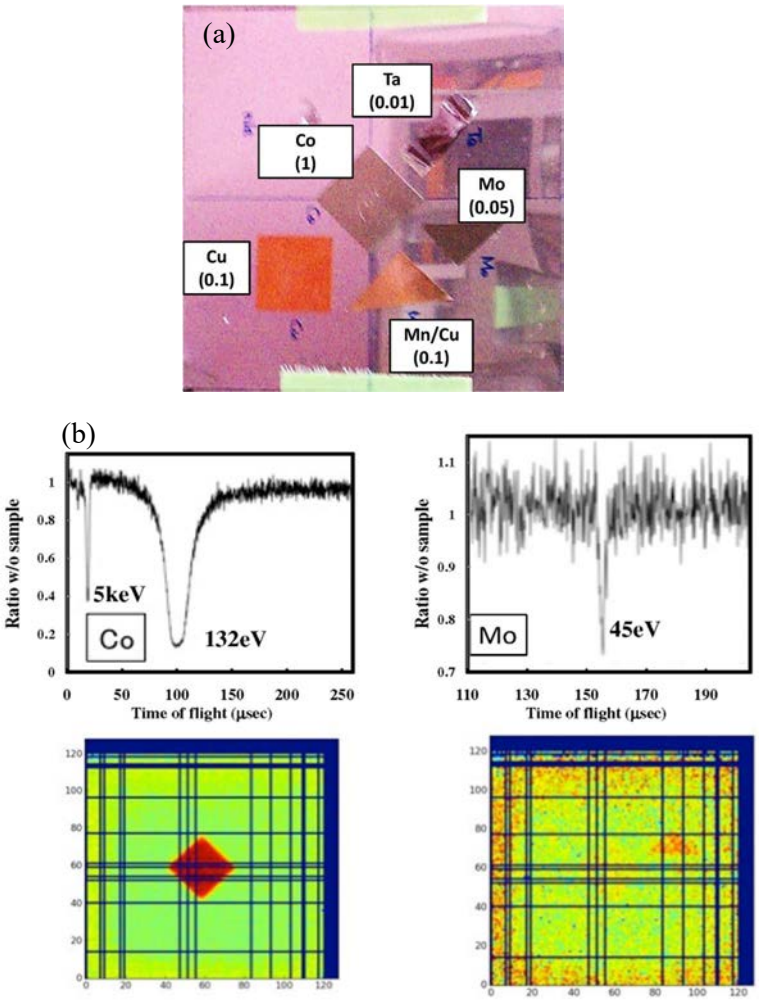

FIG. 8. Resonance absorption imaging of sample materials (a) Sample setting for resonance measurements (thickness in mm). (b) Transmission spectra around the resonance absorption energies of Co and Mo (upper), and their images (lower) (Reproduced by permission of IOP Publishing from Figs 9 and 10 of Ref. [45], doi:10.1088/1748-0221/9/07/C07012. © OP Publishing Ltd and SISSA Medialab Srl. All rights reserved.)

2.3. NUCLEAR PHYSICS

Neutron-induced nuclear reactions are of key importance for a variety of applications in fundamental science, from the origin of the elements to basic nuclear physics. Slow neutrons, which CANS can supply, play an important role as a tool that can address key questions of particle physics and cosmology at the low energy, high precision frontier, complementary to the high energy frontier probed directly at large particle accelerators.

2.3.1. Neutron cross section measurements

Apart from research reactors, accelerator based neutron sources play a major role in experimental studies for the determination of reaction cross sections over a wide energy range. The Working Party on International Nuclear Data Evaluation Co-operation [46] was established by the Nuclear Energy Agency of the Organisation for Economic Co-operation and Development to promote exchange of information on nuclear data activities by its members. One of the Working Party on International Nuclear Data Evaluation Co-operation's objectives is to assess needs for improvements in nuclear data and to stimulate initiatives to fulfil these. A

High Priority Request List[3] is updated periodically with the goal to identify accuracy targets for the improvement of nuclear data, primarily for application in the nuclear industry [47].

In the area of nuclear structure physics, information about nuclear reaction channels in the energy range from 5 to 10 MeV is crucial. Neutron cross sections are key parameters for the safety and criticality assessment in nuclear technology. Current nuclear data requests are concentrating on the determination of precise fast neutron cross sections of actinides for neutron energies up to 1 MeV, for the development of future Gen-IV reactors. Improved fast neutron cross sections are needed for structural materials, coolants, fuel, and fuel cladding, i.e., Na, Mg, Si, Fe, Mo, Zr, Pb, and Bi. A special report was prepared by the Working Party on International Nuclear Data Evaluation Co-operation to address the needs of advanced reactor concepts like the Very High Temperature Reactor and fast breeder reactors. Neutron cross section data are also needed for nuclear fusion facilities for materials used for breeders, neutron multipliers, coolants, shielding, magnets, and insulators. Radiation dosimetry requires nuclear reaction data to assess the safety hazards associated with the radiation fields.

In the nuclear fusion field, neutron cross section data are measured using D-T neutron sources (14 MeV neutrons). Dedicated experimental stations, such as Neutrons For Science [48] around the SPIRAL2 accelerator, have also been built to measure cross sections of fusion neutrons. Nuclear transmutation using an Accelerator Driven System and a fast breeder has been proposed. An Accelerator Driven System project named Multi-purpose hYbrid Research Reactor for High-tech Applications, better known by its abbreviation MYRRHA, [49] has just started. For such systems, precise cross sections of minor actinides are required to obtain total capture cross sections. This is not so easy since many actinides are radioactive, and some of them are very difficult and expensive to obtain. Thermal neutron cross sections of various compounds are required for some specific applications. As an example, the nELBE superconducting electron linac with a liquid Pb target is used extensively to improve nuclear data in the fast neutron regime including for fission cross sections [50].

In medical neutron therapy like BNCT (see Section 3.5), the determination of the optimum irradiation parameters (neutron energy and time) depends on the neutron cross sections data from nuclear physics. Various compounds existing within a human body may affect neutron slowing down and diffusion. Even in the case of neutron imaging, simulation is sometimes required for the precise analysis of a complicated object including several compounds.

2.3.2. Neutrons in nuclear astrophysics: (n,γ) reactions

Neutrons play a prominent role in nuclear astrophysics studies. Their ability to overcome any Coulomb barrier, as they are uncharged particles, permits the synthesis of elements heavier than Fe. This is achieved through a process where neutron capture reactions are accompanied by β^- decays. This capture process may evolve either slowly or rapidly. In the former case, one refers to the *s*-process [51], with *s* standing for 'slow', which corresponds to a time scale of several tens of thousands of years. Here, the neutron density is comparatively low, ranging from ~10^6 to ~10^{12} n/cm^3 and the stellar sites where the *s*-process takes place have $T \sim 10^8$ K. In the case of the rapidly evolving scenario, known as the *r*-process [52], nucleosynthesis takes place under explosive conditions lasting only a few seconds in a stellar environment with $T > 10^9$ K and neutron densities of at least 10^{20} n/cm^3.

[3] https://www.oecd-nea.org/jcms/pl_23118/wpec-expert-group-on-the-high-priority-request-list-eghprl-for-nuclear-data

In any case, the ratio of the β^- decay rate to the neutron capture rate together with the neutron density of the stellar environment define the nucleosynthesis pathway along the table of isotopes. Fig. 9 depicts the main stellar nucleosynthesis pathways across the table of isotopes. As shown therein, elements lighter than Ni are made by charged-particle-induced reactions forming chains or cycles, whereas the heavier ones are produced by the *s*- and *r*-processes.

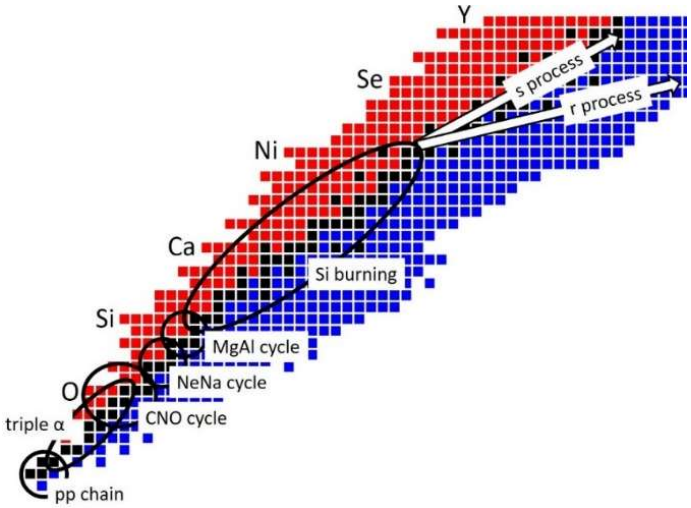

FIG. 9. The nucleosynthetic processes across the table of nuclides up to yttrium are shown in the panel. The black squares indicate stable nuclei, whereas the blue and red ones correspond to β^- and β^+ emitting unstable isotopes, respectively. Not shown are the two nucleosynthetic mechanisms termed p- and rp-processes which are responsible for the production of proton-rich nuclides heavier than Ni and lying 'northwest' of the stability line (black boxes). Details on these processes can be found in Refs [53] and [54], respectively. (Reprinted by permission from Springer Nature Customer Service Centre GmbH (Licence No. 5024750721867) for Springer Nature - The European Physical Journal Plus, from Ref. [55]. Copyright 2018.)

As shown in Fig. 9, the vast majority of the stable isotopes heavier than Fe are synthesized through the *s*-process. Isotopes produced via this process (*s*-process nuclei) provide the 'seed' nuclei for the synthesis of the so-called *p*-nuclei (grey squares of Fig. 10). Hence, studying the evolution in time of the *s*-process is crucial for understanding stellar nucleosynthesis. In this context, the creation and destruction of the *s*-process nuclei via (n,γ) reactions and β^- decays, respectively, is of paramount experimental interest.

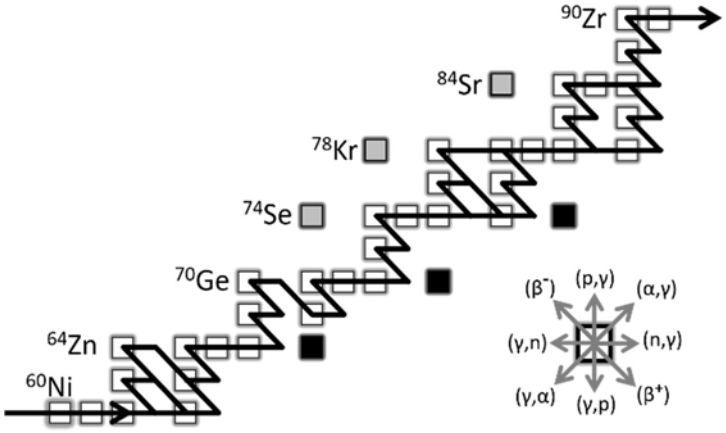

FIG. 10. The s-process path (zigzagged curve) between Ni and Zr. All squares plotted therein indicate stable isotopes. As shown, almost all stable isotopes are produced via the s process, apart from three black and three grey ones. The former ones are synthesized via the r-process, whereas the grey isotopes are created by means of the p-process. At some unstable nuclei, the reaction path splits into two branches due to competition between neutron capture and beta decay. (Reprinted by permission from Springer Nature Customer Service Centre GmbH (Licence No. 5024750721867) for Springer Nature - The European Physical Journal Plus, from Ref. [55]. Copyright 2018.)

In general, a nuclear reaction cross section is determined from the absolute number of the produced 'radiation' (particles or photons), which in the case of the (n,γ) reactions are the emitted γ rays. Capture reactions, like the (n,γ) ones relevant to the *s*-process, lead to the formation of a stable or an unstable compound nucleus. In the former case, the corresponding cross section can be determined by 'in-beam' methods, in which the emitted γ rays are detected during irradiation with neutrons. When an unstable nuclide is produced, then one can also employ the well-established 'activation' technique (see Section 2.4.1.2), provided the relevant half-life is neither 'very short' (less than a few seconds), nor 'very long' (greater than a few hundred days).

Following the *s*-process path (see Fig. 10), it can be concluded that the vast majority of the relevant (n,γ) reactions lead to the formation of stable nuclei and therefore 'in-beam' cross section measurements are mandatory. Under these conditions, the most consistent method to determine the cross section is by measuring the angular distributions of the γ transitions depopulating the excited levels of the produced compound nuclei. As shown in Ref. [55], this approach can be very time consuming due to the numerous γ transitions that have to be analysed at each energy and for every detection angle. In addition, when the level scheme of the resulting compound nucleus is not sufficiently well-known, various uncertainties may arise in the data analysis. As a result, one may derive significantly underestimated cross sections.

To avoid such problems, alternative methods were developed. They are all based on the idea of γ-summing, which is described in detail in Ref. [56] for the case of (p,γ) or (α,γ) reactions. In brief, this method takes advantage of the response function of scintillating detectors with 4π solid angle coverage. These two conditions enable the summing of all γ transitions forming cascades between the entry state of the produced compound nucleus and its ground state. As a result, instead of analyzing numerous γ lines, only a single 'sum' peak arises in the spectra. The cross section is derived from the efficiency-corrected area under the sum peak.

Compact accelerator based neutron sources are very suitable for such measurements. For example, using a pulsed proton beam from the 3.7 MV single-stage Van de Graaff accelerator of the Forschungszentrum Karlsruhe, neutrons were produced via the ^{7}Li(p,n)^{7}Be reaction. The energy of the proton beam was varied between 10 and 100 keV above the reaction threshold (1881 keV) with a repetition rate of 250 kHz, 0.7 ns pulse width, and an intensity of ~2 μA. The beam impinged on a ~1.8 mg/cm^2-thick metallic Li target on a water-cooled Cu or Ag backing. A neutron flux with a Maxwellian energy distribution around 30 keV and total number of ~5×10^6 neutrons per second over 4π was produced on average. As shown in Fig. 11, the neutrons were properly collimated and guided to the sample, which was positioned at the centre of a 4π BaF_2 spectrometer consisting of 42 crystals shaped as hexagonal and pentagonal truncated pyramids forming a spherical shell with 10 cm inner radius and 15 cm thickness. The detector registered capture cascades with 95% probability above a threshold energy of 2.5 MeV. The energy of captured neutrons was determined via time of flight for a flight path of 77 cm. The setup together with many other experimental details and typical spectra can be found in Ref. [57]

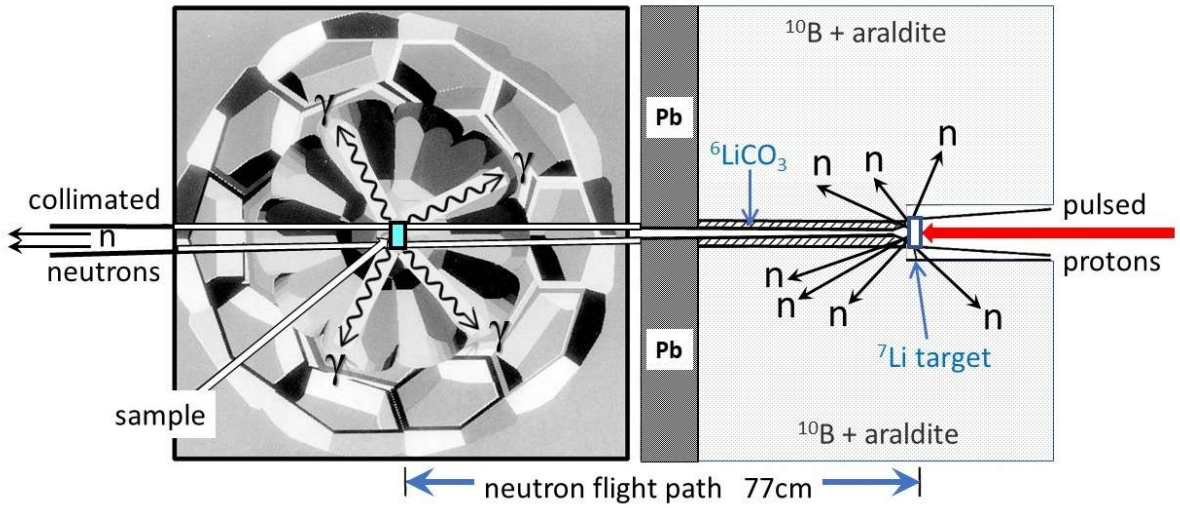

FIG. 11. The experimental setup of the Karlsruhe Van de Graaff used as a pulsed CANS with a ^{7}Li target and 4π spectrometer for (n,γ) cross section measurements. (Modified from Ref. [57] copyright (1990), with permission of Elsevier).

2.3.3. Neutrons in nuclear structure studies: (n,n′γ) reactions

For more than twenty years, γ rays produced by (n,n′γ) reactions, i.e., in inelastic neutron scattering (INS)[4] experiments, have been used to investigate the level scheme of, primarily, even-even nuclei, with the aim to understand collective or single-particle excitations of nucleons and test the corresponding predictions of various nuclear structure models. INS experiments can provide γ ray angular distributions and level lifetimes by avoiding the feeding from the above lying excited states.

INS experiments with γ ray detection are ideal to populate excited nuclear states that are inaccessible by other reactions. Moreover, at low incident neutron energies the (n,n′γ) reaction is a 'non-selective' one, i.e. it populates all states produced within the energy range and angular momentum limits introduced by fast neutrons with typical energies of a few MeV. As such, the (n,n′γ) reaction is best suited for the study of low spin (≤ 6) excited levels.

In INS experiments, monoenergetic neutrons are produced at accelerator laboratories, mainly by means of the ^{1}H+^{3}H→^{3}He+n and ^{2}H+^{2}H→^{3}He+n reactions, with Q values of ~ –764 and 3269 keV, respectively. Typically, the γ rays produced by the (n, n′γ) reaction are detected with high-purity germanium (HPGe) semiconductor detectors either in γ-singles or γ–γ coincidence mode. The latter case is almost exclusively applied when the main goal of the INS experiment is to investigate the level scheme of the target nucleus, whereas γ-singles spectra are mostly used to determine the mean lifetimes of its excited states by means of the Doppler Shift Attenuation Method [56, 58].

Knowledge of lifetimes is of key importance in nuclear structure studies as they provide the strengths of the γ transitions' depopulating excited states, which, in turn allow for a reliability test of the various nuclear structure models since they are related to the nuclear wavefunctions

[4] The term 'inelastic neutron scattering (INS)' is used in this section only in the common meaning used in nuclear physics to refer to reactions involving the formation of an excited compound nucleus and release of a γ ray from the excited state. In solid state physics and chemistry and the rest of this publication, the same term usually refers to the exchange of energy of a neutron with excitations of the chemical or magnetic structure; e.g., phonons and magnons (see Section 2.1).

describing the initial and final states of the γ decay. In Doppler Shift Attenuation Method measurements, one compares the lifetime of the level of interest with the slowing down time of a recoiling atom in a solid. Obviously, this time should either be known experimentally or else has to be calculated from indirect experimental data using a well-established theory.

Inelastic neutron scattering experiments for nuclear structure studies have been carried out by some CANS facilities across the globe. Among these, the Accelerator Laboratory of the University of Kentucky [59] continues to play a leading role and is henceforth presented as prominent example of a low-energy facility with a very successful research program in this field. The laboratory operates a 7-MV CN single-stage Van de Graaff vertical accelerator that delivers pulsed proton beams with ~1 ns pulse width and 2 mA current, which impinge on ^{3}H contained in a gas cell. This way, nearly monoenergetic neutrons with continuously variable energies between ~0.5 and 6 MeV are produced from the induced ^{3}H(p,n)^{3}He reaction. Under these conditions a fast neutron intensity of ~5×10^{7} n/s is achieved at the target position, typically located at a distance between 5 to 6 cm from the end of the gas cell at an angle of 0° with respect to the beam direction. The FWHM energy of the neutrons irradiating the target sample ranges typically between 50 and 100 keV. When the ^{2}H(d,n)^{3}He reaction is employed, the produced neutrons have energies ranging from 4.5 to ~10 MeV.

Depending on the type of experiment, γ rays produced by the (n, n′γ) reaction are detected either with one HPGe detector with a relative efficiency of at least 50% and surrounded by an annular bismuth germanium oxide scintillation detector for Compton background suppression or with an array of four HPGe detectors, when γ–γ coincidences are measured. For the reduction of extraneous background events, time-of-flight gating of events related to the beam pulse is also applied. The relevant experimental setups are shown in Fig. 12.

Nuclear structure studies with the (n,n′γ) reaction are generally limited to stable nuclei. Moreover, large amounts (> 10 g) of scattering samples are typically required, which makes the experiments with enriched isotopes of low natural abundances quite costly.

Among the different types of excited nuclear states, which have been extensively investigated in INS experiments with γ ray detection is a certain category of low-spin states termed mixed-symmetry (MS) states. Collective excitations of nucleus result from the motions of protons and neutrons. When these are not in phase, then MS states can occur. It is shown that in the case of rotational nuclei, the lowest in energy MS state lies at ~3 MeV with positive parity and spin = 1, i.e. it is a 1^{+} level. In contrast, the lowest lying MS state in vibrational and γ-soft nuclei is a 2^{+} level expected at ~2 MeV excitation energy.

Studying MS states allowed for testing the predictions of those nuclear structure models that distinguish between proton and neutron excitations, such as the well-known Interacting Boson Approximation model in its second version of formulation, i.e. IBA-2, which was proposed in the late 70's [60, 61]. Experimental investigations seeking MS states were underway for almost two decades and confirmed their existence in even–even nuclei across a wide mass range above $A \geq 50$. Typical experimental nuclear structure investigations carried out at the University Kentucky Accelerator Laboratory can be found in [62–65] and in references given therein.

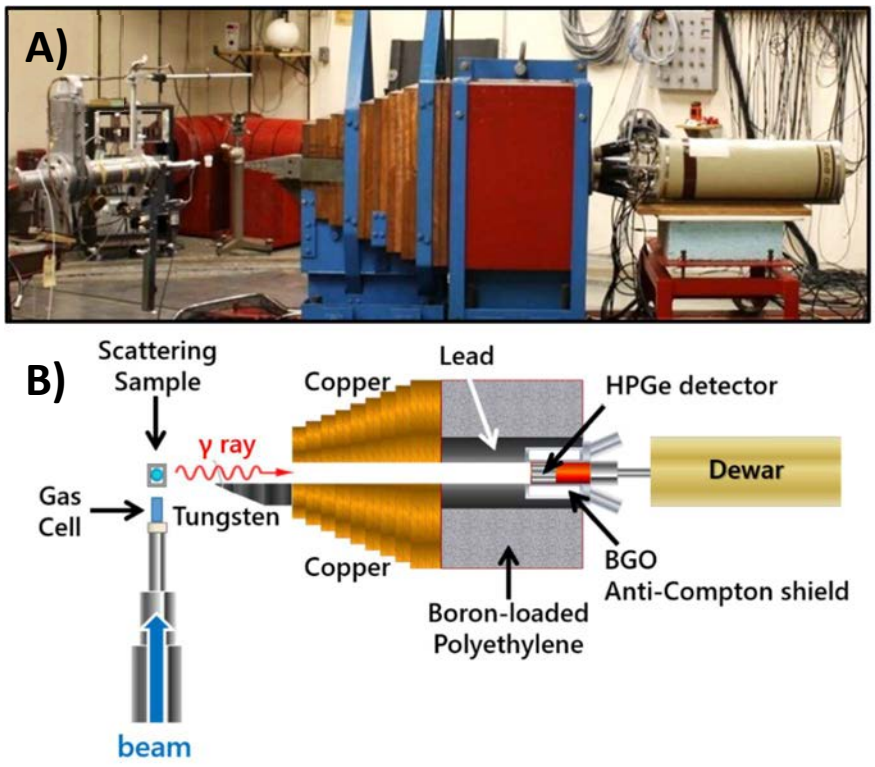

FIG. 12. A) Experimental setup used at the University of Kentucky Accelerator Laboratory for measuring γ-singles spectra. B) The setup including the detector and shielding that consists of a pyramid-shaped copper block followed by a lead cylinder surrounded by boron-loaded polyethylene is mounted on a goniometer such that the angle of the detector with respect to the beam direction can be varied. This allows for measuring angular distributions of the emitted γ rays and DSAM lifetime experiments. More details on the setups employed to measure γ-singles spectra as well as γ-γ coincidences can be found in Ref. [66] (courtesy of S. Yates, University of Kentucky).

2.3.4. Further nuclear physics experiments

Preliminary experiments for charge–parity violation search measurements at the Japan Proton Accelerator Research Complex are underway using CANS. Lanthanide compounds are candidates for spin-polarized nuclear targets for charge–parity violation search experiments. A single crystal is desirable as a spin polarization target, but such crystals are prone to twinning, which can be evaluated by the Bragg edge imaging method (Section 2.2.3.1) using a CANS.

Instrumentation development and characterization are also very important. For example, the development of spin filters for spin-polarized neutron beams in the energy region above 1 eV is underway. This technique is based on dynamic nuclear polarization using photo-excited triplet electron spins. Testing of such filters using epithermal neutron beams can be performed on CANS, and they can also be used in the development and manufacturing quality processes of self-powered flux detectors or fission chambers.

2.4. NEUTRON ACTIVATION

2.4.1. Activation analysis

Activation analysis, where samples are irradiated in neutron beams, is one of the most sensitive analytical methods with very wide applications in areas such as forensic science, art or archaeology, where it is a primary method of measurement for quantitative multi elemental analysis with excellent detection limits as low as μg/kg (one part in a billion sensitivity).

Depending on when the gamma radiation is measured, activation analysis falls into two types:

(a) Prompt Gamma Activation Analysis (PGAA), where the measurement of prompt gamma radiation emitted from nuclei in an excited state is performed during sample irradiation. PGAA relies on the same nuclear processes as used by 'in-beam' (n,γ) cross section measurements for nuclear physics (Section 2.3), but the term is usually reserved for simpler apparatus used for chemical or isotopic identification and quantification.
(b) Neutron Activation Analysis (NAA), where the measurement of gamma radiation emitted during the radioactive decay of activation products takes place sometime after sample irradiation [67].

2.4.1.1. Prompt gamma activation analysis

PGAA allows a panoramic analysis of samples, since all elements, except He, emit prompt gamma rays. It is particularly useful for the accurate detection of light elements for which not many non-destructive analytical techniques are available. Hence, PGAA is a unique method to determine the H content in any kind of samples with a detection limit at ppm level or below and at the same time to provide the elemental content (for example, pollutants) of the investigated sample [68]. In practice usually only a handful of elements are routinely detected. Sensitivity of PGAA using the relatively low fluxes from a neutron generator is limited, but it is highly sensitive for certain elements such as B, Cd, Hg and REEs which can be detected down to ppb level [69]. Deuteron-Deuteron (DD) generators have been developed for this capability [70, 71].

PGAA can be used as an inline analytical method for certain industrial processes, such as cement, coal and nuclear fuel assay during production [20, 72]. Mobile CANS are being developed in Japan to inspect bridges weakened by salt ingress with one of the methods of investigation being the profiling of chlorine content in concrete bridges and structures using PGAA [73]. Neutron generators can also be used to identify explosives [74], and for well profiling in the oil industry [16, 75].

2.4.1.2. Neutron activation analysis (NAA)

NAA requires a homogeneous, stable thermal neutron flux and is usually performed by irradiating samples within the core of a research reactor. Typically, a pneumatic transfer system is used to position the sample in the irradiation position for a fixed amount of time, before returning the irradiated sample for gamma spectroscopy. NAA is not practical for all elements and each has its own detection limit [76]. In practice, NAA is used for a lot more elements than PGAA: up to ~60 can be measured, and usually 30 can readily be measured. For conventional NAA, the total thermal flux is important, so for CANS systems, well thermalized CW systems would be ideal candidates. It is also possible to perform epithermal or fast NAA. To do this, a Cd wrapper is usually used in a research reactor sample to filter out the thermal neutrons. However, this epithermal method has not been as widely deployed as the thermal method. This could be due to the historical availability of thermalized research reactor spectra. Neutron generators have been utilized for certain specific NAA applications [77, 78].

The number of research reactors performing NAA has fallen, partly due to closure of ageing facilities, partly due to the rise of other elemental analytical techniques such as inductively coupled plasma optical emission spectroscopy, which makes analysing a wider range of multiple elements, including those not measurable by NAA, more practical and without the

overheads of operating a research reactor. Remaining advantages of NAA include that (i) it does not require destruction or dissolution of the sample: materials that cannot be readily dissolved (some silicates, phosphates); (ii) that it can measure samples that are volatile and may escape during sample preparation for inductively coupled plasma techniques (e.g., halogenated hydrocarbon pollution in soils); and (iii) that it can measure samples that are unique, or require further analysis by other techniques and are too valuable to be destroyed (forensics) can be analysed. NAA also enables first principles traceability without the need for sample matched certified reference materials (CRMs), so can be used as a primary technique, e.g., to certify CRMs. In some cases, relatively large objects (up to several kg) can be irradiated. One related technique is neutron activation autoradiography, which has been used for authenticating paintings [79].

A related technique is delayed neutron counting where, for instance, U-bearing samples can be bombarded with neutrons and the delayed fission neutrons counted rapidly with ^{3}He tubes to determine the U content and/or enrichment levels [80]. Again, the ability to measure U in whole rocks, refractory ores, or in different stages along the milling and refining pathway is an advantage. As with NAA, traditionally this was done by in-core irradiation and a rabbit transfer system. However, 'in-beam' delayed neutron counting has been developed and could be an opportunity for a CANS [81].

It seems unlikely NAA would be considered as a commercial venture for a CANS. For CANS for which education and training in nuclear techniques is important, however, the above techniques may be deployed at low cost [82].

2.4.2. Neutron depth profiling

Neutron depth profiling is a non-destructive analytical technique to determine the concentration of some isotopes as a function of the depth in the near-surface region (some μm) of a sample [83]. Neutron depth profiling is based on the detection of prompt energetic charged particles emitted during the absorption of cold or thermal neutrons by certain isotopes such as ^{3}He, ^{6}Li or ^{10}B. By using measurements with a calibrated sample, the concentration depth profile can be derived in absolute units. Recently, the intense interest in Li-ion batteries has created a new interest in the neutron depth profiling technique because of its sensitivity to the ^{6}Li isotope [84, 85].

3. NEUTRON APPLICATIONS TO OTHER FIELDS

Section 2 dealt with analytical methods that can be applied to condensed matter, nuclear and related areas of science, together with some typical examples. This section deals with potential applications of CANS to other fields. Table 1 gives some typical source strengths required for these applications.

3.1. NEUTRON IRRADIATION DAMAGE

The nuclear and electronics industry depend on irradiation experiments to understand the impact of high energy radiation on materials (e.g. mechanical stability, reliability in a high radiation environment) as well as on the human body to protect astronauts and nuclear energy workers. There is a drive to produce more radiation tolerant materials for future fast fission and fusion reactors (see Section 3.1.1). The study of radiation damage to electronic devices and systems is also an important field of scientific and technological research (see Section 3.1.2). Understanding the radiation damage to tissues is essential for providing appropriate radiation protection to the public, radiation therapy patients, and workers that might be exposed to neutron radiation fields (see Section 3.1.3).

3.1.1. Nuclear materials

For many countries, life extension of the current power reactor fleet is essential to satisfy their demand for electricity, because new reactors cannot be brought on-line in sufficient time. Therefore, there is a push to safely operate existing reactors for more than 80 years, which is much beyond the original target life of 40–60 years. The effect of radiation on materials has to be investigated carefully. New radiation-induced phenomena have been found as reactor conditions have been changed and operation time increased: e.g., radiation-induced hardening and swelling in fast reactors, and high-temperature embrittlement due to helium. The effects of irradiation on materials are major issues for the nuclear industry in several areas:

- *In-core components and reactor vessels:* irradiation changes the mechanical properties of materials leading to embrittlement and cracks;
- *Cables:* irradiation changes the elasticity of polymers used for insulation of metal wires;
- *Fuel:* irradiation experiments of fuel are needed to qualify new types of fuel for advanced reactors;
- *Concrete:* degradation of concrete structures due to irradiation needs to be investigated because all reactor containments are made of concrete;
- *Nuclear waste:* containers used to store nuclear waste have to withstand the radiation effects produced by the decaying nuclear waste.

Core components of today's power reactors consist mainly of austenitic stainless steels, nickel-based alloys, and zirconium alloys. Stress corrosion cracking has occurred in all water cooled reactors: in light water reactors, irradiation assisted stress corrosion cracking [86] is one of the most important effects. The threshold fluence for irradiation assisted stress corrosion cracking in control blade sheath of boiling water reactors is approximately 5×10^{20} fast n/cm^2 and cracking is observed at 2×10^{21} n/cm^2. This corresponds to about 25 days of continuous irradiation in the High-Flux Isotope Reactor at Oak Ridge, USA, which has a fast neutron flux of approximately 10^{15} n/s/cm^2 and a thermal neutron flux of 2.5×10^{15} n/s/cm^2. More challenging is the irradiation of in-core materials with their expected lifetime dose, e.g. 100 dpa (displacements per atom) in a PWR (Pressurized Water Reactor). To perform this type of

irradiation experiment at Oak Ridge's reactor on steel samples would take approximately 10 years.

Future nuclear energy systems will require structural materials and fuels that can operate in environments that are more aggressive and experience higher levels of radiation damage. Depending on the reactor concept the lifetime radiation damage requirements of in-core materials is between 10 and 200 dpa [86].

Many future power reactor designs have a much 'harder' neutron spectrum than today's moderated reactors. The fast neutron displacement rate for structural materials is much higher so new materials need to be developed. There are few fast irradiation facilities, e.g. the BOR-60 reactor, capable of testing such materials.

Similar problems exist with testing materials for future fusion reactors. The IFMIF DONES project (International Fusion Materials Irradiation Facility DEMO Oriented Neutron Source) aims at building a neutron radiation source of energy and fluence similar to DEMO, to study and select the materials that will be needed for that project and in future fusion power plants [87]. The facility aims to provide 30–40 dpa rapidly for accelerated testing of candidate materials.

Material irradiation testing often requires very large scale facilities. The International Fusion Materials Irradiation Facility (IFMIF, currently at the design stage) has been proposed for fusion reactor environment studies providing appropriate neutron energy and flux. The facility will consist of two 125 mA deuteron accelerators, a liquid Li target, and an irradiation test facility. Due to its scale, construction costs are expected to be 1.4 billion Euros, half-sized facilities that use one accelerator, including A-FNS and IFMIF-DONES neutron source programs [88], are currently proposed in Japan and the EU, respectively, for operation in 2030. These material irradiation test facilities can supply fast neutron fluxes sufficient to achieve 20 dpa per year, but the test volume is relatively small compared to the test volume of nuclear reactors. So, small specimen and test methods will have to be developed and applied and may need to be discussed with the regulatory body. Moreover, heavy ion irradiation facilities and fission research reactors can be used to support the development of fusion materials. Smaller CANS are being developed for fast neutron damage (e.g., the cyclotron facility at Řež described in Section 4.1.2.).

Steady state compact fusion neutron sources have been proposed in several options, for material irradiation tests, integral effect tests of fusion reactors, and especially for the breeding blanket development.

3.1.2. Radiation hardness of electronics

3.1.2.1. Hardware errors

Radiation effects on electronics is a very important field of scientific and technological research. Radiation tolerance is of prime importance for many applications of electronics: space applications, high energy physics, nuclear reactors, and nuclear medicine. Showers of cosmic neutron radiation are intense enough that they may disrupt the normal operation of electronic systems and represent a particular threat to aircraft avionics.

3.1.2.2. Software errors

Neutron induced Single Event Effects on electronics may result in recoverable soft errors such as a Single Event Upset, e.g., temporary memory data corruption or logic circuit status changes, as well as a permanent hard error. The main material used in semiconductors is Si, and Si has three naturally occurring isotopes: ^{28}Si (92.23%), ^{29}Si (4.67%), and ^{30}Si (3.1%). Soft errors are caused by charged particles produced by neutron reactions mainly with Si nuclei. For fast neutrons, spallation reactions occur and produce charged particles. On the other hand, for lower energy neutrons, the major reactions are Si(n,p) and Si(n,α) reactions (See Table 2). The threshold energies indicate that neutron energy above about 10 MeV is necessary for an effective acceleration test of the devices although the small soft error cross section remains low below a few MeV as shown in Ref. [89]. Some components contain boron, and the capture of thermal neutrons by ^{10}B is also a significant hazard that is receiving attention.

A list of facilities in the USA offering accelerators for Single Event Effects testing of space applications using protons or fast neutrons is given in Appendix B of Ref. [85]. Some of the larger neutron sources such as the ISIS spallation source, UK, offer Single Event Effects testing with a near atmospheric spectrum of neutrons for avionics with dedicated facilities such as ChipIR [90]. Some accelerators with lower energy proton beams such as NEPIR, a 30–70 MeV cyclotron in Italy, are developing facilities such as ANEM (Atmospheric Neutron Emulator) for this purpose [91].

Tests using a CANS based around an electron linac at Hokkaido University, HUNS, whose source intensity is ~10^{12} n/s at the target with an evaporation spectrum with high energy neutrons over about 10 MeV have been performed to test components at an accelerated rate. An error rate of about 1 million times larger than natural was observed at this CANS [92]. An international standard of soft error testing for telecommunication systems was approved at ITU-T (International Telecommunication Union Telecommunication Standardization Sector) in 2018, providing a guideline for use of CANS for such purposes [93].

TABLE 2. NEUTRON REACTIONS WITH Si

Reactions with Si	Threshold energy
$^{28}Si + n \rightarrow ^{28}Al + p$	3.999 MeV
$^{28}Si + n \rightarrow ^{25}Mg + \alpha$	2.749 MeV
$^{29}Si + n \rightarrow ^{29}Al + p$	3.009 MeV
$^{29}Si + n \rightarrow ^{26}Mg + \alpha$	35 keV
$^{30}Si + n \rightarrow ^{30}Al + p$	8.040 MeV
$^{30}Si + n \rightarrow ^{27}Mg + \alpha$	4.341 MeV

3.1.3. Radiobiology

Neutron sources are required in order to provide experimental data on radiation damage to human and animal tissues. Data on ‘non-traditional’ neutron fields (i.e. those not typical of fission) are required.

3.1.3.1. Radioprotection of humans

Ionizing radiation is present in a variety of environments and workplaces, e.g., at nuclear reactors, radiotherapy facilities, aircrafts at high altitude, and outer space. In all cases, there are undesired or natural radiation fields. In order to better assess the health effects and risks on the general public, nuclear energy workers, health system patients and workers, pilots, flight attendants, and astronauts, it is important to have the possibility to perform experimental studies on the impact of radiation on living organs, tissues and cells (e.g. chromosome aberrations in human blood lymphocytes) [94]. The biological effectiveness of radiation depends on its type (electron, proton, alpha, neutron, gamma, ion), its energy, its distribution in time and space, and on the characteristics of the biological target. Radioprotection protocols, which consider safety margins, make use of a dose equivalent (in Sieverts) taking into account the radiation type and energy. In radiation therapies a relative biological effectiveness factor that considers radiation type, energy and target tissue is typically used. There are also more advanced methodologies that try to make a more realistic bridge between radiation energy deposition and overall biological and clinical effects. All high energy particles interact with matter by creating various other secondary particles. As the cross sections of all these reactions are energy dependent, it would be advantageous to be able to modify the spectrum of the incoming neutron or gamma beams to mimic the true spectrum that humans are exposed to; e.g., astronauts at the International Space Station [95]. Some of the higher powered CANS may contribute to this area.

The advent of accelerator based BNCT is demanding more radiation biology studies to support its development (see Section 3.5).

3.1.3.2. Induced mutagenesis

Induced mutagenesis is an indispensable tool for the creation of new alleles which can be explored for crop improvement. It has great importance, particularly where natural sources for the genetic variations are limited. By means of inducing mutation using different mutagenesis approaches, evolution can be accelerated or directed to achieve the desired change in an organism. In plant breeding programs, physical and chemical mutagens are applied to develop new varieties with enhanced traits. Crop mutation breeding using gamma rays is a long-standing technique. Neutron radiation is a relatively new approach to induce mutagenesis in seeds for crop improvement [96]. CANS can provide a fast neutron spectrum for that purpose.

3.2. RADIOISOTOPE PRODUCTION

Radioisotope production may be considered as an additional revenue stream or justification for a CANS whose principal aim is research but has to be carefully examined as to its feasibility. Industrial use of radioisotopes covers applications in several industrial systems: physical measurement gauges, on-line analytics, pollution measurement, home-land security, smoke detectors (^{241}Am), tritium (or ^{3}H) used in emergency exit lights, laboratory or portable analytic systems, irradiation and radiation processing with ^{60}Co (sterilization of medical supplies, of pharmaceuticals or food packages, food irradiation, plastic curing), radioactive tracers (chemical reactions efficiency, mass transfer in industrial plants, behaviour of pollutants) and non-destructive testing (gamma radiography).

Radioisotopes are widely used in medicine for nuclear diagnostic imaging, positron emission tomography, bone density measurements and gastric ulcer detection, radioimmunoassay, therapeutic techniques and palliative care, radiotherapy with sealed sources and irradiation of blood for transfusion. Radioactive isotope production for nuclear medicine includes isotopes such as ^{99m}Tc for cardiological diagnosis and bone investigation; ^{177}Lu and ^{90}Sr are both used in immunotherapy; and ^{169}Yb is employed in the diagnostics of small joint injuries.

Most of the world's medical isotopes (~85%) are produced either in research reactors via neutron capture or fission. For diagnostic imaging, the dominant isotope is still ^{99}Mo (^{99m}Tc). The other route of medical isotope production is via accelerators. Two promising routes have been reported for the possible production of ^{99}Mo and ^{99m}Tc by accelerators that could be used as CANS: (i) ^{100}Mo(γ,n)^{99}Mo production using Bremsstrahlung produced by electron linacs and (ii) the ^{100}Mo(p,2n)^{99m}Tc reaction in a cyclotron [97, 98].

Cyclotron accelerators are widespread in medical facilities where neutrons are produced as an unwanted by-product of medical isotope production. The most common reaction is ^{18}O(p,n)^{18}F from a liquid-$H_2{}^{18}O$ target, which is most commonly processed to produce ^{18}F-fluorodeoxyglucose (^{18}F-FDG), the dominant radiopharmaceutical for PET-CT imaging [99]. A review of the principal manufacturers of cyclotrons is given by Schmor [100].

In principle, neutron capture or direct application of a proton beam on a target could be used to produce medical isotopes at a CANS whose principal aim is research and training, with the aim of making a revenue stream. The possible gains in revenue need to be offset against the demand for reliable isotope production schedules which may reduce flexibility of operations as a research facility: isotope production periods may require the beam current to be dedicated to isotope production targets. Furthermore, unprocessed radioisotopes are often low on the value chain in the production of radiopharmaceuticals and their final use in a clinical setting, so that the financial return to the CANS facility may be limited [101]. Safety considerations around possible targets failures etc. would need to be considered during design.

The energy of the accelerated beam needs to be considered with respect to the excitation function for the isotope that is to be produced. Careful attention to the thresholds for production of a given isotope and the yield at saturation are required in order to calculate the likely scale of production. The channels for the production of unwanted radionuclides also need to be considered as radionuclidic purity is important in radiopharmaceuticals. A close partnership with a radiopharmacy operating under Good Manufacturing Practice to manufacture the final radiopharmaceuticals would be required to ensure viability of any business plan involving medical isotope production, as the capital and operating expenses of such a facility are considerable [102, 103].

3.3. SILICON DOPING

A specific transmutation reaction can be used to dope silicon for the semiconductor industry, using the following reaction:

$$^{30}\mathrm{Si}(n,\gamma)^{31}\mathrm{Si} \rightarrow {}^{31}\mathrm{P} + \beta^{-}$$

where Si atoms are transmuted into P atoms leading to n-doping. The key advantage of the neutron transmutation doping method is that, due to the very low neutron absorption by Si, the

doping is very homogeneous compared to classical diffusion or ion implantation methods. Hence, these methods provide doped Si for high-power semiconductor components.

This method is used in the pool of research reactors, close to the core where a high thermal neutron flux is available; e.g., Orphée at Saclay, France and Forschungsreaktor München II (better known as FRM II at Garching, Germany, or in irradiation tubes [104].

Production volumes are small, so that this activity is only performed around research reactors. The facilities typically handle crystals that are 50 cm long and 20 cm in diameter (8 inches). For example, the FRM II reactor in Garching produces about 15 tons of n-doped Si per year [105]. A dedicated IAEA publication is available on this topic [106]. As a relatively large irradiation area is required to irradiate significant quantities of large boules of Si, this will probably limit the use of CANS in this application.

3.4. REACTOR PHYSICS

Accelerator driven sub-critical systems (ADS) are currently under development. An ADS can be used for various applications:

- Power source (fission of fissile and fissionable isotopes);
- Breeding of fissile fuel (e.g., ^{233}U bred from ^{232}Th by neutron capture or ^{239}Pu and ^{241}Pu bred from neutron capture in ^{238}U);
- Transmutation of minor actinides by fast fission of e.g., ^{232}U, ^{234}U, ^{236}U, ^{236}Np, ^{237}Np, ^{238}Pu, ^{240}Pu, ^{241}Am, ^{243}Am or by neutron capture and subsequent fission of transmuted isotopes;
- Transmutation of long-lived fission products such as, e.g., ^{90}Sr, ^{137}Cs,^{129}I, ^{93}Z, ^{99}Tc.

Experimental studies with an ADS using the Kyoto University Critical Assembly are performed with a 100 MeV proton beam at the Kyoto University [107]. The MYRRHA project (Multipurpose hYbrid Research Reactor for High-tech Applications) uses a 100 MeV proton beam in combination with a lead-bismuth cooled fast reactor [49]. However, the Kharkov Institute of Physics and Technology of Ukraine in collaboration with the Los Alamos National Laboratory are developing an ADS that will be powered by a 100 MeV electron beam [108].

3.5. BORON NEUTRON CAPTURE THERAPY (BNCT)

3.5.1. Principle of the technique

Locher proposed the Boron Neutron Capture Therapy (BNCT) concept in 1936, very shortly after Chadwick's discovery of the neutron and Taylor and Goldhaber's discovery of the ^{10}B(n,α)^{7}Li reaction. BNCT is a binary form of radiation therapy that uses nonradioactive ^{10}B to capture thermal neutrons [109] and generate alpha particles. The capture of a neutron by a ^{10}B nucleus is highly probable via the ^{10}B(n,α)^{7}Li reaction, with a cross section of 3837 barns for thermal neutrons, and releases 2.79 MeV. In 6.1% of cases, the energy is shared between the Li nucleus and α-particle, while in the remaining 93.9%, the Li nucleus remains in an excited state, and emits a 0.48 MeV γ ray (Fig. 13). The ^{7}Li nucleus with energy of 0.84 MeV and α-particle with 1.47 MeV have high mean stopping power (162 and 196 keV μm^{-1}, respectively), with correspondingly small ranges in water or tissue: 5.2 and 7.5 μm, comparable to the typical size of mammalian cells. The stopping power of the γ quantum is significantly lower: 0.3 keV μm^{-1}.

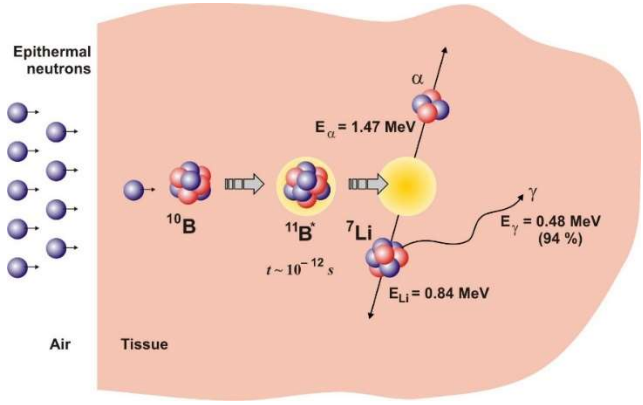

FIG. 13. Schematic representation of the BNCT principle (courtesy of Sergei Taskaev, Budker Institute of Nuclear Physics).

Therefore, the main part of the energy release in the nuclear reaction $^{10}B(n,\alpha)^{7}Li$, namely 84%, occurs within a single cell. If a sufficient amount of ^{10}B can be delivered and concentrated on the surface, or preferably in the interior, of cancerous tumour cells, neutron irradiation of the cancer will generate a Compound Biological Effectiveness factor (CBE) sufficient to kill tumour cells while preserving normal tissue to a greater extent.

3.5.2. Technical realization and developments

BNCT was pioneered at a variety of research reactor sites around the world. However, numbers of patients in standardized clinical trials were insufficient to demonstrate efficacy. Furthermore, the location and environment of a typical research reactor is often not optimal for treatment of cancer patients. The advent of CANS optimized solely for BNCT which can be installed at a clinical facility may change the availability of BNCT and test its efficacy in a statistically and clinically meaningful manner. A number of different CANS technologies and targets are being developed for this purpose, with at least three companies supplying equipment dedicated for this purpose to date. Attention has been focused on the following four reactions [110]: $^{7}Li(p,n)^{7}Be$, $^{9}Be(p,n)^{9}B$, $^{9}Be(d,n)^{10}B$, $^{13}C(d,n)^{14}N$. The main requirement for a therapeutic neutron beam is set by the need for an epithermal neutron flux $>10^{9}$ cm^{-2} s^{-1} so that the duration of the treatment is shorter than 1 hour. This sets a minimum neutron yield and power for CANS dedicated to BNCT.

The $^{7}Li(p,n)^{7}Be$ reaction is advantageous when the projectile energy is just above the threshold energy of the reaction (~2.5 MeV) so that a maximum number of 'soft' epithermal neutrons are produced in the forward direction (in the laboratory frame of reference) with minimum γ-radiation, fast neutrons, and daughter nuclei. The flammable and low melting-point of Li targets present a number of technical challenges, such as heat removal and target protection against radiation damage by the proton beam. Furthermore, production of radioactive ^{7}Be makes target handling and storage complicated.

The $^{9}Be(p,n)^{9}B$ reaction is also being evaluated because handling and manufacturing of such a target is easier. However, this reaction requires a higher proton energy (E_p), typically above 5 MeV, to get sufficient neutron production, and thus results in the production of higher energy neutrons, E_n, where typically $E_n < E_p - 2$ MeV, well above the epithermal spectrum.

In the case of both Li and Be targets, the energy of the produced neutrons is higher than that required for therapy and, therefore, the neutrons require moderation. However, the smaller the

initial neutron energy the easier is the moderation process to achieve a suitable energy spectrum (see Section 4.3.1). Some of the current projects and technologies are outlined below.

The most advanced project is the project of the Japanese company Sumitomo Heavy Industries, Ltd. (SHI), which has built and commissioned a neutron source based on a 30 MeV, 1 mA cyclotron with a Be target for the clinic in South Tohoku in Fukushima Prefecture. SHI has performed a clinical trial of the BNCT system targeting carcinoma of the head and neck region in collaboration with Stella Pharma Corporation. In March 2020, SHI obtained approval of the system as a medical device permitting it to manufacture and sell its system of accelerator based BNCT system for clinical use.

The University of Tsukuba together with Mitsubishi Heavy Industry Co. and KEK and JAERI have produced an 8-MeV 5-mA linac with a Be target for BNCT purposes. To date, a proton beam with a current of 2.8 mA has been obtained.

The project being developed by the Cancer Intelligence Care Systems for the National Cancer Center in Tokyo is potentially attractive. AccSys Technology, Inc. (California, United States), manufactured a 2.5 MeV linac with a current of 20 mA. To generate neutrons, it is proposed to use a target with a thin Li layer on a Pd substrate. To date, a proton beam with a current of 11 mA has been obtained.

Neutron Therapeutics (United States) has supplied a 2.6 MeV 30 mA single ended electrostatic accelerator for the clinic of the University of Helsinki (Finland) with a rotating Li target. As of late 2020, the facility is being commissioned.

Another project developing in parallel is that of TAE Life Sciences (California, USA), which is supplying a 2.5 MeV 10 mA VITA and a Li target for the Hospital in Xiamen, Fujian, P.R. China. The accelerator and target prototypes were proposed and developed at the Budker Institute of Nuclear Physics, Novosibirsk, Russia (see Section 4.1.4.2 for more details).

The Atomic Energy Commission of Argentina, CNEA, is also developing a single-ended electrostatic quadrupole, ESQ, accelerator of 1.44 MV and 30 mA designed to work with the deuteron induced reactions $^{9}Be(d,n)^{10}B$ and $^{13}C(d,n)^{14}N$. CNEA has signed a collaborative agreement with the Korea Institute of Radiological and Medical Sciences, KIRAMS, to work jointly on the development of BNCT based on that ESQ.

An interactive map of current BNCT facilities, both reactor and accelerator based, is one component of the interactive maps in Ref. [7]

3.5.3. Cancer treatment

Boronophenylalanine (BPA), which is phenylalanine synthesized with a ^{10}B atom, is being used in clinical trials. The ratio of boron concentration between tumour and normal tissue is approximately 3. Currently, clinical trials using accelerator-based neutron source and BPA have been conducted for recurrent brain cancer, head and neck cancer, and superficial cancer.

Throughput of patients is limited by the neutron flux and the time to fix the patient in the treatment position. In Kyoto, four treatments a day are foreseen, and it is estimated that 800 patients could be treated each year.

At Tohoku, Japan, a switching magnet can be used to steer the beam to treat one patient in one location while setting up the other room for the next treatment. The facility currently being built

in Xiamen, China aims at eventually treating 2500 patients per year with three rooms. While technical improvements on the accelerator and targets could increase throughput, in practice, staff numbers are also a strong limitation on patient throughput.

3.6. METROLOGY

Neutrons can span many orders of magnitude (from GeV in a spallation source down to ultracold neutrons with a few tens of μeV kinetic energy). Metrology is essential for the calibration of area and personnel monitoring. Ultimately, detectors for metrology and monitors need to be traceable to a primary standards laboratory. The various types of reactions available to produce monoenergetic neutrons are described in Ref. [111].

For example, in France, the IRSN's CEZANE and AMANDE facilities at Cadarache produce all the reference neutron field types recommended by international standards (ISO 8529 and ISO 12789) for calibrating neutron measuring instruments. The CEZANE facility uses an accelerator to generate a fission neutron spectrum moderated using elements representative of the shielding used in the nuclear industry. The AMANDE facility produces monoenergetic neutron beams with an energy of between 2 keV and 20 MeV which allow determining how instrument response varies as a function of neutron energy.

Typically, the primary standards laboratories only have access to neutron fluxes in the range of 10^6–10^7 n/cm^2/s. Access by such laboratories to higher flux sources, especially ones with 'non-traditional' neutron spectra are quired to support calibration and development of standards in this fields. In this area, CANS serve both as a supplier and a customer to the metrology laboratories.

4. COMPONENTS OF A CANS SYSTEM

The principal components within a CANS facility, include the accelerator systems, target technologies, and the moderators and reflectors that surround them. Some of the most common choices are outlined below.

4.1. ACCELERATORS

The most common accelerator types either in use of being developed as CANS are described in the following subsections

Some accelerator types that could be used as the basis of CANS systems have been in existence for several decades; e.g., neutron generators, cyclotrons, electron linacs. Each of these types has several manufacturers, that enables typical values for sizes and costs to be given, together with some practical information such as neutron yield and challenges that may be particular to their design.

Towards the end of the section are types of accelerators for which less general guidance can be given. There is a new generation of high current, low energy electrostatic accelerator designs dedicated to neutron production which are either still under development or undergoing their first sales, driven largely by the interest in accelerator based BNCT. Two examples are given of these technologies. Similarly, proton/deuteron linacs are typically custom designed and built. Some of the main design parameters are discussed, but it is difficult to give generic values for costs and size as they are so variable. Finally, laser driven neutron sources are undergoing rapid development at big laboratories. They represent a possible future source for certain applications, but widespread deployment is not yet near at hand.

4.1.1. Neutron generators

Neutron generators (NGs) are some of the smallest and simplest accelerator based neutron production devices [20, 113–116]. NGs provide a large degree of versatility and, accordingly, can be utilized in a wide variety of applications, going from basic science to industry [20, 112, 116, 117]. However, the mentioned simplicity is reduced when it is desired to scale up performance. Neutron generators are probably the most commonly used neutron sources in industry, with several companies devoted to their manufacturing and sale.

There are many different types of NGs. In this section, two of them are going to be considered. They are some of the most typical in this scale of device and share many important features. These two types are: *ultra-compact accelerator* based NGs (UCANGs) [20, 112, 113] and *inertial electrostatic confinement fusion* based NGs (IECF-NGs) [112, 117, 118]. These classes of NGs are mostly based on *deuteron-deuteron* (DD, ^{2}H–^{2}H) and/or *deuteron-triton* (DT, ^{2}H–^{3}H) nuclear fusion reactions (when tritons are present there might also be a minor contribution from triton-triton, TT, reactions and when both, triton and deuteron, are in the target triton–helion, T–^{3}He, reactions might appear and contribute neutrons) [118, 119]. Fusion neutrons are emitted nearly isotropically for DT and with moderate angular bias for DD. The main advantage of these reactions is that they can occur with particle accelerations as low as a few keV. Particles are accelerated by electric fields, from an anode (ion source region) to a target region that functions as a cathode. In some cases, radio frequency guiding is used. Applied voltages typically range from 50 to 100 kV (although lower voltages can be used in low yield applications and up to 300 kV can be used). The process happens inside a sealed chamber

containing deuterium and/or tritium gas. The gas is typically delivered by a getter (able to store, absorb, and emit the gas according to requirement) to the ion source region and/or to the acceleration chamber itself. Some devices do not have getters but only gas in the chamber (e.g. the 'neutron tubes').

Typical UCANGs are cylindrical and the anode/ion source and target/cathode are placed at opposite ends. Other designs have the anode in an external cylindrical sheath and the target/cathode in an inner cylindrical sheath. In some cases, the gas in the chamber may work as a secondary target. The energy required for the reactions is provided by an externally powered electric field. Primary fusion products other than neutrons are absorbed in the target and in the chamber walls. Two of the main limitations for this type of NG, with respect to overall durability and the ability to scale up neutron yield are the heat load and ion bombardment erosion of the target.

The main differences between UCANGs and IECF-NGs are found in the target configuration and consequent particle–target interaction, in how energetic ions are used, and in electrical properties.

IECF based devices are often called *fusors* and their relative simplicity at low intensities allows for many types of implementations. In IECF-NGs, the target is a deuterium and/or tritium gas-plasma distributed inside the chamber. The device can be operated under various regimes according to the amount of gas-plasma and the configuration of the electric fields. The most typical geometry for IECF-NGs is spherical: an external spherical anode that can be a metal grid inside the chamber or directly the chamber wall; and an internal grid-type, spherical and more or less concentric cathode. Similarly, another often used geometry is cylindrical: an external anode and an internal cathode. The main idea in this type of generator is to accelerate the ions radially so that they interact in the centre of the chamber, with themselves and/or with the gas. Those that do not initially fuse bounce back and forth through the cavity marked by the cathode (that shows levels of radial transparency above 90% for accelerated ions) until they fuse, are lost to the cathode, or recombine/neutralize and heat the gas-plasma. The energy required for the reactions is provided by the externally powered electric field; however, some concepts additionally consider the effective utilization of all of the particles and energy in the chamber, including part of the energy provided by the fusion reaction. Primary fusion products other than neutrons, after interacting with the gas-plasma, are mainly absorbed in the cathode and in the walls of the chamber. The main limitations for this type of NG with respect to the overall durability and scaling up the neutron yield are heat load, ion bombardment erosion in the cathode grid, and spurious currents due to high voltages.

Target designs for IECF-NGs and UCANGS are discussed in Section 4.2.2.1.

4.1.1.1. Challenges

a) *Moderation and collimation.* Neutron generators provide fast neutrons that are emitted isotropically in a 4π solid angle. A moderator and collimator assembly need to be considered if neutrons are not going to be used as they are produced from the source. The type of the assembly is directly dependent on the end-use of the facility: in some cases, it might be very simple but, many times, acquiring the appropriate assembly means a research and development project *per se*, with significant demands on human and material resources.

b) *Heat load.* Operation produces a heat load in the components of the NGs and, given the motivation of simplicity and compactness inherent in their design, providing cooling systems is not a trivial task. According to the cooling strategy, power and durability of the device can be strongly affected. For UCANGs, the critical piece is the solid target while for IECF-NGs the cathode grid is critical.

c) *Scaling up the yield and energy efficiency*. There would be a very interesting niche of applications of NGs due to their compactness and versatility if their neutron yield could be increased by 1–2 orders of magnitude. However, the simplicity and compactness motivation together with heat load, bombardment erosion and some physics of fusion reaction in solid and gas-plasma targets are limiting factors. Another factor might be the difficulty in applying very high voltages in small devices. This currently limits NGs to low neutron yield applications. Nevertheless, important efforts are being made to overcome these limitations.

4.1.1.2. Cost per facility

Neutron generators are commercially available and market prices can go from some US $80 000 to 300 000, according to the type of device, neutron yield, durability, end-use and manufacturer. Typical neutron yields for that range of prices goes from around 10^6 to 10^{10} n/s, respectively. The cost of the facility is related to the end-use of the system. NGs can be classified as bench-top devices; most of the cost of a facility is often related to moderation, collimation, and shielding assemblies as well as to other systems associated to the end-use.

4.1.1.3. Operational costs

Since NGs are small devices, energy consumption is usually limited below 1 kW, and typically below 500 W. Except for the largest devices, they do not require complex cooling systems that can add significant consumption. Depending on the device, neutron production per unit power ranges from ~7×10^3 to ~3×10^7 n/s-W (or ~3×10^{10} to ~1×10^{14} n/kWh) for DT reaction based NGs. Note from Fig. 14 that the maximum theoretical output without using energy feedback from fusion products would be in the range of ~4×10^8 to ~4×10^9 n/s-W (or ~1×10^{15} to ~1×10^{16} n/kWh), for voltages between 50 and 300 kV. DD based NGs are expected to have production rates between 1% to 10% of that obtained with DT.

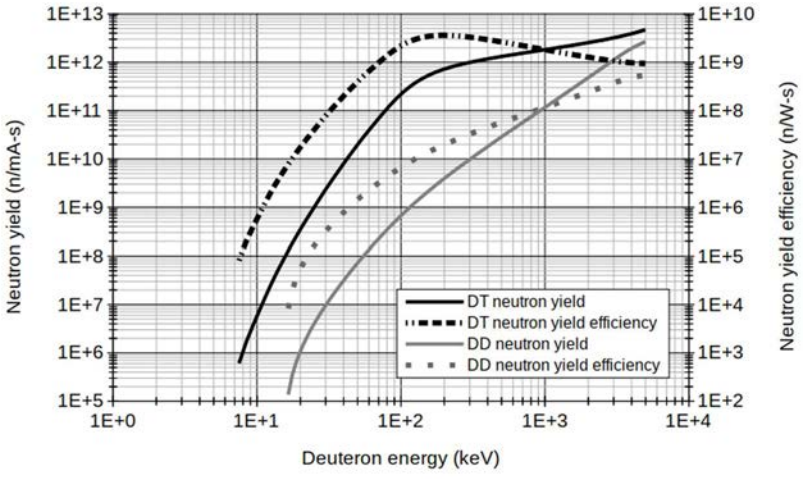

FIG. 14. Estimated neutron yield and neutron yield energy efficiency for deuterons impinging on a 100% tritium target (DT) and on a 100% deuterium target (DD) (courtesy of Manuel Sztejnberg, CNEA).

4.1.1.4. Footprint

NGs have characteristic sizes that can be far below 1 m^3. UCANGs are typically smaller than 0.5×0.5×0.5 m^3. Some devices can even be a few cm in diameter and around ten cm long. IECF-NGs can also be on the order of tens of cm size and go up to 1 m. Typically the required power supply systems are also below 1 m^3 size and can be located remotely, outside the experimental area. The required size of the experimental area depends on the purpose of the facility.

4.1.1.5. Neutron yield

Typical devices can offer a wide range of outputs ranging from around 10^6 to 10^{11} n/s for DD and DT generators. Figure 14 shows the estimated neutron yields as a function of the particle energy, in terms of neutron generation rate per unit particle current and per unit power, for deuterons impinging on a 100% tritium target (DT) and on a 100% deuterium target (DD). The curves represent the ideal neutron yield for devices consisting of a beam and a static target (which consider neither hot plasma interactions nor energy feedback from fusion products). Current NGs do not reach these levels but are typically ~1% of the curve values, and for some cases ~10%. (Larger, more complex accelerators with gas targets can get very close to these curves.) The main reason for the losses is due to interactions of the accelerated ions with the non-hydrogenous atoms of the target and to other interactions that do not end in fusion process but in energy and ion loss. Substantial improvements in performance in NGs could come from the following areas: improvement of solid targets and/or use of optimized gas-plasma targets, minimizing or overcoming the amount of interactions other than fusion, maximizing the population of ions and the amount of collisions between accelerated ions, and taking advantage of fusion product energy. In this frame, IECF-NGs show important potential for improvement which, it is worth noting, would imply progressing on the very complex and specific gas-plasma dynamics of these devices.

4.1.1.6. Energy, spectrum, and current

DD reactions produce, almost with the same probability, a 2.45 MeV neutron and a 0.82 MeV helion particle, or a 3.03 MeV proton and a 1.01 MeV triton (for total energy releases of 3.27 and 4.04 MeV, respectively). DT reactions produce a 14.06 MeV neutron and a 3.52 MeV alpha particle (for total energy release of 17.58 MeV). Appearance of the much less probable TT reactions would imply the production of an alpha particle and two neutrons sharing an energy release of 11.32 MeV. For several applications, neutrons can be used directly with the energy with which they are emitted from the devices. However, there are many applications where other neutron spectral distributions are required. Many times, thermal or epithermal neutron beams are needed, and moderator assemblies need to be considered to shape the energy spectrum. Unfortunately, moderation comes with the cost of decreasing neutron fluxes (as measured in $n/cm^2/s$).

Ion current is one of the key factors related to NGs output and to the overall reactions of ions with the target. Consequently, it is intimately associated to heat load. Ion currents are typically ~1 mA, although a wide range of currents going from 0.1 to 50 mA can be found among the variety of NGs.

4.1.1.7. Reliability

Neutron generators are well established in industry and there are several providers that offer reliable systems. Users need to be aware that, in spite of the relative simplicity for building NGs, obtaining reliable and high performance devices requires substantial research and development. One of the critical concerns on operation is the target or the cathode grid integrity, for UCANGs or IECF-NGs, respectively. Operations for long periods and at high outputs may limit device performance and lifetime. Another potential limitation is tritium depletion, whose management needs to be seriously considered. Typical UCANG lifetimes can be in the thousands of hours, although some may reach ~10 000 hours. IECF-NGs can have lifetimes reaching 20 000 hours.

4.1.1.8. Efficiency

Efficiency is related to the overall process of neutron generation. It might be expressed in terms of particles, i.e., the ratio between the number of emitted neutrons to the number of accelerated ions. Under this definition, current NGs efficiency would be below or around 0.0001%. Another definition of efficiency could be the ratio between kinetic energy of the emitted neutrons to the injected energy. In this case, efficiency would be found below or around 0.01%. The neutron generation rate per unit power is also a measure of the efficiency of the system.

4.1.1.9. Continuous wave (CW)/Pulsed

NGs exist with CW and/or pulsed working cycles. There is a large variety of offers that can include different combinations of pulse width and frequency. Pulse widths from around 1 μs to 1 ms are available. Pulse frequencies can range from a single shot to 200 kHz.

4.1.1.10. Particular radiation protection and regulatory issues

In general terms, NGs are devices with few radiation issues: they have low intensity, they are switch-on/off devices, the most intense radiation fields are confined to small areas and those areas are inside a sealed container. However, when NGs are operating, radiation is emitted all around them, and the whole device becomes a hot spot. Soft X-ray radiation and neutron interaction products need to be considered in addition to the desired neutrons. Activation of NGs needs to be checked after switching them off, since some materials or undesired impurities within them might become radioactive during operation. This concern is especially important in large devices and if the device or surrounding equipment are to be handled shortly after operation. Another point to consider is the content of tritium, especially in DT based NGs: the chamber needs to be routinely checked for leakage. If tritium remains in the chamber, as designed, NGs can be typically considered as 'UN2911 Class 7 Radioactive material, excepted package-instruments or articles' given the load is below 400 GBq (see IAEA's Regulations for the Safe Transport of Radioactive Material [120]), even for those with the largest outputs. DT sources may be subject to stricter regulatory requirements than DD sources in some countries. DD based NGs suffer some tritium build up, but the amount is much lower than in DT based NGs.

4.1.2. Cyclotrons

In a cyclotron, charged particles enter the centre from the ion source and they are accelerated particles using an RF modulated electric field while being held within a static magnetic field.

The gap between the 'D'-shaped electrodes ('dees') is where the charge particles experience acceleration. With each traverse of the dees the energy of the charged particles increases and the radius of their path increases, resulting in a spiral trajectory within the cyclotron. For cyclotrons which accelerate positive ions such as protons, the extraction of the beam of charged particles is typically with an electrostatic deflector. For cyclotrons which accelerate negative species (such as H^- ions), they are extracted by stripping the charge, usually with a conductive foil.

Cyclotrons are well established in the medical community, and available commercially with energies of up to 30 MeV to produce radiopharmaceuticals for nuclear medicine diagnostics and treatment. Treatment uses with neutrons include BNCT (Section 3.5) and fast neutron therapy [121].

Another use of cyclotrons specifically for neutron production that has recently been pursued is that of a fast neutron source for radiation damage studies of fusion related materials. A 24 MeV, 300 μA cyclotron supplied by Advanced Cyclotron Systems, Inc has been used as the basis of a materials test facility using a Be target to yield 5×10^{12} n/s/sr as a point like source with neutrons up to 22 MeV. The system is under development at the Nuclear Physics Institute, Center of Accelerators and Nuclear Analytical Methods, Řež, Czech Republic [122].

4.1.2.1. Challenges

Cyclotrons are typically limited to currents of the order of 1 mA. This and their maximum accelerating energy dictate the maximum neutron source strength from a given target, typically Be. Cyclotrons that accelerate positive species tend to experience more activation than those that accelerate negative species. Two recent technologies have been identified that make cyclotrons more attractive as efficient accelerators for neutron production:

(a) *Superconducting electromagnet technology* can reduce the existing magnet size. In the case of a conventional normally conducting electromagnet cyclotron, the magnet weighs about 40 tons for a 30 MeV cyclotron. Superconducting electromagnet cyclotrons can greatly reduce the size and weight of cyclotrons to less than half, and the power consumption of the electromagnet can also be greatly reduced. Unlike the normal conducting cyclotrons, superconducting cyclotrons need to use RF cavity devices with a very high RF resonance Q value. If a Dee voltage of more than 200 kV is used in a superconducting RF cavity, the acceleration turn number can be drastically reduced and the turn gap can be broadened. The current of the accelerated ion beam can be greatly increased as well.
(b) *High current cyclotron technology* is required. A high current cyclotron requires a high current ion source, RF power, high quality factor RF resonator and high vacuum technology. The ion source can increase the cyclotron beam current intensity from some hundreds of μA up to 2 mA when using external ion sources, such as multi-cusp and electron cyclotron resonance (ECR). However, the cyclotron system becomes more complicated. Recently, the development of Penning Ionization Gauge (PIG) ion source technology and advances in vacuum technology have enabled a beam current intensity of 300 μA for an internal ion source cyclotron. With an internal ion source technology such as a PIG ion source, cyclotrons have the potential to become more widespread as small neutron sources.

Currently, innovative improvement methods are being planned to increase the beam current. For example, ions can be drawn out from two or three ion sources inside the cyclotron, to control the phase and accelerate at the same time, thereby increasing the current by two to three times. A second approach involves a multi-beam being accelerated by stacking multiple Dee cavities between cyclotron electromagnet pole gaps. In this case, the current of the ion beam can be increased in proportion to the number of RF cavity layers.

4.1.2.2. Cost per facility

As cyclotrons are available as commercial products, cyclotrons are among the most cost effective ion beam accelerators to own and operate. Currently, the price of a cyclotron per unit energy is about US $80 000/MeV, comparable to an electron accelerator. Cyclotrons under 20 MeV can be equipped with a self-shielding system, so do not necessarily require a shielded bunker. Self-shielding requires about US $20 000/MeV of energy. Typical costs of a 30 MeV cyclotron when equipped with beamlines and targets are in the range of 3.5–6 million US dollars, depending on specifications [123].

4.1.2.3. Operational cost

One of the reasons for the increase in accelerator production costs is the high production cost of RF systems. A cyclotron has a relatively low production cost compared to others because the proportion of the RF system in overall cost is less than that of linear accelerators, and other parts do not require very high specifications. The advantages of cyclotrons are low failure rate and high stability of the acceleration beam together with their lower production cost. Therefore, a cyclotron is simple to maintain with low maintenance costs.

Given the requirement for 50 kW of electric power cost, and assuming a cost ~US $0.1/kW.hr, the yield of the ~1×10^{13} n/s would result in ~7×10^{15} n/US dollar in direct electrical operating cost of neutron production.

4.1.2.4. Footprint

For a 30 MeV cyclotron, for example, the accelerating sections occupy a floor area of about 8.6 m long, 7.5 m wide, and 7.2 m high and are located in a room with minimal shielding. The target room footprint depends on the end-use of the facility.

4.1.2.5. Neutron yield

The beam operation of a cyclotron is generally continuous (CW) and the neutron yield from an energetic proton beam on a Be target is roughly proportional to ~$(E_p(\text{MeV}) - 2)^2$. The cooling limit under nominal conditions on the Be target could be 0.5–1 kW/cm^2. The Target-Moderator-Reflector (TMR) structure of a CANS is usually compact, i.e., small in area and volume, so the target area will be around 10–20 cm^2. The neutron yield from the target is then ~1×10^{13} n/s for a proton beam of a 30 MeV/300 μA cyclotron. Although a higher yield could be achieved with a higher proton energy, the shielding requirements would be heavier around the TMR assembly. A lower energy accelerator is cheaper and easier to build. In the case of CANS applications, the appropriate type and accelerator energy need to be considered depending on the intended application.

4.1.2.6. Energy, spectrum and current

Cyclotrons are ion beam accelerators that are widely used in hospitals and laboratories for various medical purposes and can be divided broadly into two classes:

(a) *Low energy cyclotrons* of 30 MeV or less are used for radioisotope production for nuclear medicine diagnosis.
(b) *High energy cyclotrons* of 50 MeV or more are used for radiation treatment; high speed neutron treatment can be performed with cyclotrons with a proton energy range of 50–70 MeV. Proton therapy using cyclotrons has been also implemented with high energy cyclotrons of 200 MeV or more. 70 MeV cyclotrons are used only for eye cancer treatment. Recently, the establishment of superconducting electromagnet cyclotron technology (Section 4.1.2.1) has led to cost reduction and is becoming more popular in proton treatment. Table 3 provides a summary of typical applications of cyclotrons of different accelerating energies.

Cyclotrons producing isotopes intended for nuclear medicine diagnosis can be divided into the production of positron emitting and gamma emitting nuclides. Most positron emitting nuclides require a cyclotron with a proton energy less than 20 MeV. The target material of the positron emitter is generally in gaseous or liquid form, so it is necessary to use beam currents of about 100 μA due to cooling limits of the target. Gamma emitting nuclides are mainly solid targets, depending on the melting temperature of the target material, but by using the most commonly used nuclides such as ^{201}Tl, ^{67}Ga, and ^{111}In, the beam current can be 200 μA higher than that of a liquid or gas target. For the specific case of gamma emitting ^{123}I, a Xe gas target is used, so sufficient production can be achieved even with 50 μA.

For BNCT (see Section 3.5), Sumitomo Heavy Industries have gained approval for the use of their 30 MeV azimuthally variable field cyclotron design as part of a medically approved BNCT system in conjunction with a boron containing pharmaceutical [124]. This is the world's first approved accelerator based BNCT treatment system. A flux of a little in excess of 10^9 n/cm^2/s/mA is generated.

TABLE 3. CYCLOTRON ENERGY RANGES AND THEIR TYPICAL APPLICATIONS AND RESEARCH AREAS

Cyclotron energy	Applications and research areas
8–20 MeV	Medical positron emitter production
	Fast neutron production
20–70 MeV	Medical gamma emitter production
	Medical positron emitter production
	Proton therapy and neutron therapy
	Fast neutron production
70–250 MeV	Proton therapy
	Development of new radioisotope candidates for medical use

The neutron spectrum from a cyclotron depends on the target used. The most common is Be, which produces a neutron spectrum with maximum energy that is 2 MeV lower than the incident proton beam.

As outlined in the Section (4.1.2.1), Cyclotrons are typically limited to current of about 1 mA. This limits the ultimate neutron yield for a given particle energy.

4.1.2.7. Reliability

The cyclotron is a very reliable ion beam accelerator, and thus used routinely in hospitals around the world; e.g. in the production of ^{18}F for positron emission tomography scans, which must be made reliably every day.

4.1.2.8. Efficiency

The beam efficiency of cyclotrons may reach 30% so that 10 kW power deposition into the target to produce ~1×10^{13} n/s requires about 30 kW power consumption of the cyclotron. With cooling power requirements of ~20 kW, a total of roughly 50 kW electric power would be used to produce ~1×10^{13} n/s.

4.1.2.9. Continuous Wave (CW)/pulsed

Cyclotrons have the highest beam stability among neutron-generating accelerators. Cyclotrons can accelerate from MeV to GeV proton beams and can also accelerate metal ions, typically as CW beams, but pulse modulation of the proton beams can be used to produce a pulsed neutron beam.

4.1.3. Electron linear accelerators

Today, utilization of RF based linacs is the most prevalent and efficient technique for the acceleration of electrons to high energies (typically ranging from 4 MeV to 30 MeV) by subjecting them to a series of oscillating electric fields along the beam line under high vacuum conditions. The high power non-conservative RF fields used for electron acceleration are produced through the process of decelerating electrons in retarding potentials in special evacuated devices like magnetrons and klystrons that typically run at about 2856 MHz (S-band) [125]. While other electron accelerators could be used (microtrons, rhodotrons) this section deals only with the most common accelerating structure: the electron linac.

An electron linac was used very productively as a CANS at Bariloche, Argentina for many years for pulsed diffraction experiments, nuclear cross sections, moderator development, and Deep Inelastic Scattering [126]. The HUNS [127] and KURRI-LINAC [128] are long-standing examples of electron linacs in use in Japan for research with neutron beams. Gelina[5] (Belgium) and nELBE[6] are examples of electron linacs used extensively for fast neutron cross section measurements (Section 2.3.1, Ref. [50]).

[5] https://ec.europa.eu/jrc/en/research-facility/open-access/relevance-driven/2019-1-rd-eufrat-gelina
[6] https://www.hzdr.de/db/Cms?pOid=12048&pNid=35

The major hardware constituents of an electron linac are:

(a) *Electron gun*. Electrons are thermionically emitted from a heated cathode, focused into a pencil beam by a curved focusing electrode and accelerated towards a perforated anode through which they drift to enter the accelerating waveguide. The electrostatic fields used to accelerate the electrons in the diode gun are supplied directly from the pulsed electron gun modulator power supply in the form of a negative pulse delivered to the cathode of the gun [125].

(b) *Radiofrequency (RF) power source*. The microwave radiation required for accelerating electrons to the desired kinetic energy is typically sourced by a magnetron or a klystron. Both devices use electron acceleration and deceleration in a vacuum for the production of high power RF fields; however, it may be noted that the magnetron itself is a high power RF source, whereas the klystron is an RF power amplifier that amplifies the low power RF generated by an RF oscillator, commonly called the RF driver. Tuned frequency is fed to the RF driver from a low power external signal generator [125].

(c) *Waveguides for radiofrequency power transmission.* The microwave power produced by the RF sources is transported to the accelerating structure through rectangular waveguides of matched impedance that are either evacuated or, more commonly, pressurized with a dielectric gas (such as Freon or SF_6) to twice atmospheric pressure. A 'circulator' (sometimes referred to as an isolator) is inserted in between the RF source and the accelerating waveguide to protect the RF source from reflected power [125].

(d) *Accelerating structure*. In the accelerating structure, a high vacuum, typically in the order of 10^{-7} Torr or better, is maintained to allow free propagation of electrons. The electrons are accelerated by means of energy transfer from the high power RF fields that are set up in the accelerating structure by the RF sources. The simplest accelerating structure is obtained from a cylindrical uniform waveguide by adding a series of discs (irises) with circular holes at the centre, placed at equal distances along the tube. These discs divide the waveguide into a series of cylindrical cavities that form the accelerating structure. The cavities of the accelerating waveguide serve two purposes: (i) to couple and distribute microwave power between adjacent cavities and (ii) to provide a suitable electric field pattern for the acceleration of electrons [125].

For electron acceleration, the following acceleration structures are used: (i) travelling wave, in which the microwaves enter the waveguide on the side with the gun and propagate to the high energy side – there, they are either absorbed without reflection or leave the waveguide where they are either absorbed or fed back into the accelerating structure; (ii) standing wave, where both ends of the accelerating structure have conductive discs that are present to reflect the microwave power, causing standing waves to be created with the waveguide. These cavities therefore serve only as coupling cavities [125].

(e) Beamline. In low energy linacs (<6 MeV), the target is usually embedded in the accelerating waveguide and no beam transport between the accelerating waveguide and target is required. In medium and high energy (>15 MeV) linacs, an electron beam line (i.e. evacuated drift tube) is used for transporting the electron beam from the accelerating structure to the X-ray target. In large setups, steering and focusing coils are used over beam line for collimation purposes [125].

(f) *Auxiliary systems.* There are several systems that enable proper functioning of the aforementioned main hardware such as: (i) Vacuum pumping systems, (ii) Water cooling systems, (iii) Pneumatics for controlling high gas pressures, (iv) Radiation shielding etc.

In a linear accelerator, electrons are accelerated to an energy of several MeV and are directed into a high-*Z* target to produce X-rays by the Bremsstrahlung interaction. Recent studies have examined the spectra of photoneutrons produced by linacs with electron energies of 5 MeV [129], 15 MeV [130, 131], 18 MeV [132], 25 MeV [133] and 18, 28, and 38 MeV [134], and have potential for application in nuclear physics, polymer science, radioisotope production, materials science, condensed matter physics, etc [136–138].

Electron accelerators generate Bremsstrahlung photons through the interaction of an electron beam impinging on a heavy metal target of optimum thickness for which, at the defined energy, the photon flux is maximum. This interaction produces a cascade of photons whose spectrum has an endpoint energy value that is equal to that of the maximum accelerating potential. Photons produced in this way are then redirected towards a suitable photoneutron (γ–n) target. The absorption of a photon in the γ–n target leads to the formation of a compound nucleus which decays by the emission of one or more neutrons if the excitation energy is larger than the binding energy of the last neutron in the compound nucleus [135]. This threshold depends on the *Z* and is lowest for D (2.23 MeV) and Be (1.67 MeV) [135, 138]. Some of the nuclides with low and high photodisintegration energy thresholds are listed in Tables 4 and 5, respectively.

TABLE 4. TARGETS OF LOW PHOTODISINTEGRATION ENERGY THRESHOLD

Nuclide	Threshold (MeV)	Reaction
^{2}D	2.225	^{2}H(γ,n)^{1}H
^{6}Li	3.697	^{6}Li(γ,n+p)^{4}He
^{6}Li	5.67	^{6}Li(γ,n)^{5}Li
^{7}Li	7.251	^{7}Li(γ,n)^{6}Li
^{9}Be	1.667	^{9}Be(γ,n)^{8}Be
^{13}C	4.9	^{13}C(γ,n)^{12}C

TABLE 5. TARGETS OF HIGH PHOTODISINTEGRATION ENERGY THRESHOLD

Nuclide	Threshold (MeV)	Isotope Abundance (%)
^{206}Pb	8.09	24.10
^{207}Pb	6.74	22.10
^{208}Pb	7.37	52.40
^{181}Ta	7.58	99.99
^{180}W	8.41	0.12
^{182}W	8.07	26.30
^{183}W	6.19	14.28
^{184}W	7.41	30.70
^{186}W	7.19	28.60

For maximum production of epithermal neutron fluxes from a photonuclear reaction, the appropriate choice of the photoneutron target materials (on the basis of its photodisintegration threshold), its photoneutron cross section, geometry and physical dimensions are of significant

importance [138]. A larger photonuclear cross section means there is a greater probability for the interaction to occur. The cross section of the photonuclear effect is characterized by a Giant Dipole Resonance (GDR) and it is most pronounced in materials with high-*Z*, as shown in Fig. 15. An exception to this rule is found in the γ–n cross section of ^{13}C. Its cross section increases almost linearly from 0.01 mb at 5 MeV to 8 mb at 25 MeV [139]. The γ–n cross sections for Be and D are on the order of few mbarn in the 0–5 MeV energy range [129].

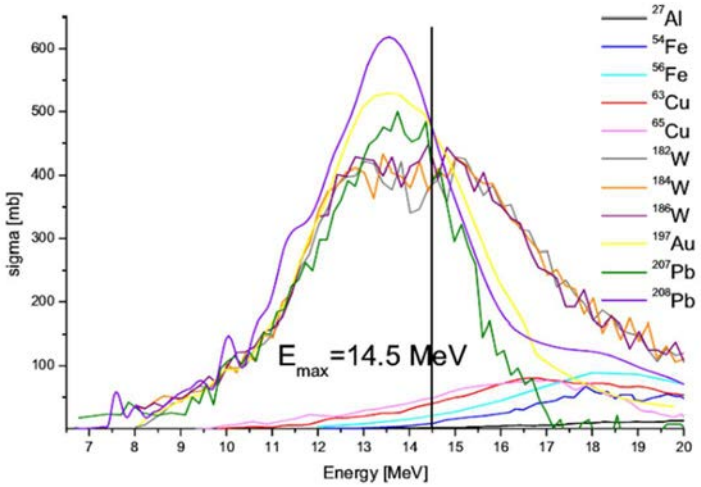

FIG. 15. Photoneutron interaction cross sections for high-Z materials (reproduced from Ref. [139] with permission).

In the category of high-*Z* photoneutron targets, U possesses the highest photoneutron cross section; however, its neutron energy spectrum is higher than others, and the average energies of neutrons released are fast neutrons. After U, W has the highest photoneutron cross section with advantages such as easy access, reasonable price, and non-toxicity [139].

For measuring photoneutron flux in a high gamma environment, neutron activation analysis is used (see also Section 2.4). Activation occurs when a stable isotope is converted into an excited radioisotope by the absorption of a neutron. The radioisotope de-excites through the release of radiation to a more stable form according to its half-life decay time. This de-excitation energy is often released in the form of a gamma ray and may be detected through conventional spectroscopy [138]. Because of its large thermal cross section (~98.65 barn) and insensitivity to gamma, Au foil is the most preferred choice in such setups and its activation by the photoneutrons results in the production of excited ^{198}Au nuclei. ^{198}Au has a very convenient half-life of 2.7 days and its de-excitation occurs by the emission of a 411.8 keV gamma ray which is measured by a gamma detector with good energy resolution (for e.g. HPGe/BGO/$LaBr_3$). A variety of activation foils suitable for neutron detection from fusion energies downwards are discussed in Ref. [140].

4.1.3.1. Challenges

As with most other accelerator types, for neutron production there are no significant challenges with the accelerator equipment itself if purchased from reputable, commercial suppliers.

There are, however, some challenges with their application

- Tailoring the effective particle range for the desired effect;
- Coping with extraneous unwanted reactions due to the above;

- Coping with heat dissipation;
- Design and practical limits on using the available beam power efficiently;
- Effectiveness of beam conversion (beam power) to neutron production rate.

These challenges affect all accelerators used as a neutron source but some such as the first three items are less difficult for electron accelerators than for ion accelerators. See Section 4.1.3.5 below describing the two-step process unique to photoneutron production.

4.1.3.2. Cost per facility

Electron accelerators suitable for application as a CANS are available from at least two reputable commercial suppliers. The price for 40 MeV, 100 kW average power electron linac is in the range of 5–7 million US Dollars.

4.1.3.3. Operational cost

During full power operation a 40 MeV 100 kW electron linac requires about 400 kW of electrical power for the linac itself, and about 100 kW of electrical power to remove excess heat (using refrigeration equipment) for a total of about 500 kW. The heat removal cost may be reduced somewhat by using ambient air or water as the heat sink.

As a conservative basis for a cost estimate, one may start with the calculation of neutron yield per electron. Using data from Table 6, at 40 MeV, neutron yield is about 4.5×10^{-3} n/e which, for 100 kW average beam power (2.5 mA average beam current) would produce about 7.0×10^{13} n/s. So, operating energy cost for an hour at 500 kW and US \$0.1/kW-hr would be about US \$50 and during that time, gross neutron production would have been 2.5×10^{17} neutrons. Direct electrical cost of production per neutron then is US $\$2\times10^{-17}$/n or 5×10^{16} n/US Dollar.

TABLE 6. CALCULATION OF TOTAL NEUTRON YIELDS (SOURCE STRENGTHS)

Electron Energy (eV)	Neutron Yields (n/e) FLUKA	Neutron Source Strength at the target (n/s) MCNP[a]	FLUKA
20	1.205×10^{-3}	7.9×10^{12}	7.52×10^{12}
30	3.108×10^{-3}	1.9×10^{12}	1.94×10^{13}
40	4.51×10^{-3}	2.7×10^{13}	2.81×10^{13}
50	5.67×10^{-3}		3.54×10^{13}

Note: FLUKA statistical accuracy < 1%. Agreement exists in the yield calculation to within a few percent between MCNP and FLUKA calculations. Hypothetically, a 1 mA electron current generates 6.24×10^{15} e/s.

[a] nELBE published results: Ann. Nucl. Eng. **34** (2007) 36–50.

4.1.3.4. Footprint

The accelerating sections occupy a floor area of about 4 m length, 1 m width, and 1.3 m height and are located in a room with some minimal shielding. The power supply cabinets can be located elsewhere with a total footprint area of about 10 m^2 and height 2.1 m. Experimental areas will depend on the overall facility intent.

4.1.3.5. Neutron yield

Yield can be expressed in several ways. For simplicity, neutron yield will be described as n/sec-kW of electron beam power incident on a Bremsstrahlung converter, which could also be the Bremsstrahlung to neutron converter. This is a useful way of describing the overall effect but oversimplifies the actual process and does not highlight the significance of particle interactions (neutrons produced per incident particle of a given energy). The conversion process of electron beam power to neutron intensity occurs in two steps: (i) Beam power (kW) to Bremsstrahlung (photons/s) and (ii) Bremsstrahlung to neutron intensity (n/s). These two steps can be achieved in physically separate devices or integrated into a single device. And, if physically separated, heat dissipation can be better managed than if integrated, as is always the case in proton or deuteron targets. The electron and Bremsstrahlung beams can also be separated for other purposes.

Photoneutron emission occurs if the photon energy exceeds the nuclear binding energy of the most loosely bound neutron. The energy of the ejected neutron is [141, 142]:

$$E_{pn} \sim \frac{A-1}{A}\left(E_\gamma - Q - \frac{E_\gamma^2}{2m_n c^2(A-1)} + \frac{E_\gamma}{A}\sqrt{\frac{2(A-1)}{(m_n c^2 A)(E_\gamma - Q)}}\cos\theta\right) \quad (1)$$

where A is the mass of the target nucleus, E_γ is the energy of the photon, E_{pn} is the energy of the photoneutron, Q is the threshold energy, m_n is the neutron mass, c is the velocity of light, and θ is the angle between photon and neutron flight direction. Due to collisions in the target area, the energy of any individual photoneutron may be reduced. The average energies of the primary neutrons do not vary much with peak photon energies, as can be seen from Table 7 and Ref. [143].

Photoneutron yields depend on the target material and on the photoneutron source: its spectrum, strength and geometry. The spectrum of the photon source determines the photoneutron yield by the photodisintegration cross section, which is dependent on the photon energy [141]. The photoneutron yield, Y_n, is given by:

$$Y_n = \int_{E_{\text{th}}}^{E} \sigma(E_\gamma) W(E, E_\gamma) dE_\gamma \quad (2)$$

where W is the Bremsstrahlung photon spectrum, σ the photonuclear cross section that depends on the photon energy E_γ, E the electron energy and E_{th} the threshold energy.

TABLE 7. AVERAGE NEUTRON ENERGIES PRODUCED IN LINEAR ACCELERATORS

Photon Energy (MeV)	Average Neutron Energy (MeV)
15	1.8
20	2.1
25	2.2
30	2.4

Note: Data are taken from Ref. [143].

4.1.3.6. Energy, spectrum and current

The kinetic energy of an electron beam is a significant factor contributing to the photoneutron yield but is not the whole story. Once the energy has exceeded about 40 MeV, there is little increase in yield (as expressed in n/s-kW).

The energy spectrum of photons incident on the photoneutron target significantly affects the neutron flux output: emitted photons can never have energy greater than the maximum kinetic energy of the incoming electron, and the amount of kinetic energy lost by the electron is mainly determined by the distance to the attracting nucleus. This leads to the characteristic Bremsstrahlung spectrum, where the mean energy of the photons is approximately 1/4 of the kinetic energy of the incoming electrons (assuming interaction with monoenergetic electrons). The normalized photon spectrum for primary electrons accelerated to an energy of about 14.5 MeV is shown in Fig. 16. The mean energy of photons is ~4.2 MeV, with maximum intensity ~2 MeV [139].

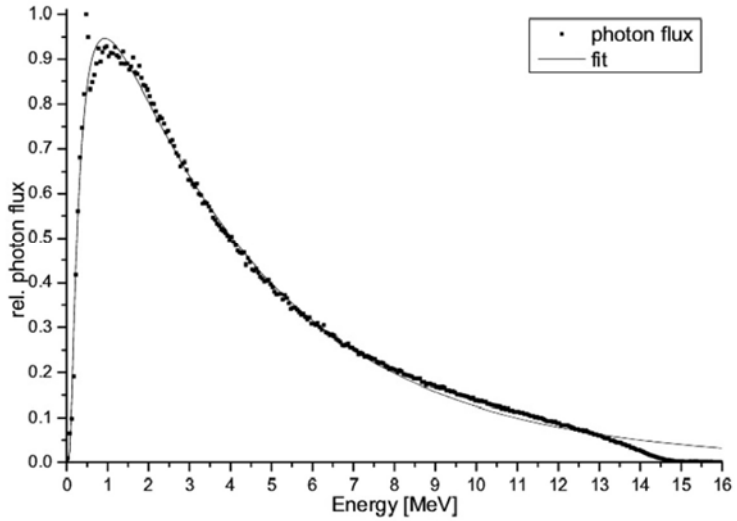

FIG. 16. Normalized photon spectrum for electron acceleration up 14.5 MeV (reproduced from Ref. [139] with permission).

The photonuclear reaction produces neutron intensities that resemble a fission spectrum and are nearly isotropic.

Electron beam current, whether peak or average, is a contributing factor to neutron yield; it is also the main factor in heat dissipation problems.

4.1.3.7. Reliability

As with most complex commercially available systems, electron accelerators in general are highly reliable and are easy for ordinary operations people to use. Like all equipment, failures occur but can be anticipated due to the nature of the control system and remedied in a scheduled fashion.

4.1.3.8. Efficiency

Electrical efficiency for electron accelerators ranges from about 20–50%, defined as electron beam power to electrical power input: there is significant heat to be dissipated, which increases

as beam power increases. Balancing this is the possibility, described above in Section 4.1.3.5, to separate the two conversion steps and manage their heat loads independently. An example of this balance is that for a 35 MeV beam impinging on a Bremsstrahlung converter, roughly half the beam power is converted to Bremsstrahlung and the remainder is waste heat. Following that, the Bremsstrahlung will enter the neutron converter target and by virtue of its low linear energy transfer, will distribute the Bremsstrahlung throughout the converter material. Not only that, but the Bremsstrahlung produced is very forward directed.

4.1.3.9. Continuous Wave (CW)/Pulsed

CW electron accelerators are usually longer than pulsed machines for a given energy, and a CW machine can be characterized by its beam energy and current. For CW machines, the average beam current *is* the beam current, and beam power is the product of energy and current.

A pulsed electron accelerator on the other hand is shorter than a CW unit for a given energy and is described as having a beam energy and an average beam current, whose product defines the beam power.

In both cases above, the overall effect on neutron production, *on average*, is the same for a given average beam power. But the difference arises when examining time structure. CW machines have only one component of time structure: that of the RF source powering the accelerating device. Whereas the pulsed type of accelerator delivers the beam in pulses (several μs long) at pulse repetition rates of 0–600 Hz. And within each pulse the inherent time structure of the RF source powering the accelerating device is superimposed. So, timing information is available from both types but opportunities for intentional experimental control over stimulation and relaxation times are only available in pulsed electron accelerators.

4.1.3.10. Particular radiation protection issues

Although very intense Bremsstrahlung is produced, the design intent is to use as much as possible to produce neutrons. Unused Bremsstrahlung, however, will cause at least three issues:

- Need for biological protection;
- Interference with experimental instrumentation;
- Activation of accelerator components beyond that normally caused by the intended neutron production.

Unintended activation of accelerator and beam line components can be significantly reduced by choice of accelerator operating frequency and diameter of beam line components thereby reducing unwanted beam impingement.

4.1.4. Electrostatic accelerators

Conceptually, the simplest charged particle accelerator is electrostatic; this uses static electric fields to accelerate ions. An important advantage of an electrostatic accelerator compared to an electrodynamic accelerator is the ability to obtain a tight distribution in the energy of particles accelerated. The technology is relatively simple and accessible compared to electrodynamic and radiofrequency technologies. The most common types of electrostatic accelerators generate high voltages based around the principles of the Cockcroft–Walton voltage multiplier or Van

de Graaff generators. The limits on voltage include 'sagging' at high voltages and the requirement to insulate the instruments with gases such as SF_6 or Freon to eliminate discharges.

So-called single-ended machines accelerate positive ions. An example of a single-ended electrostatic CANS used for BNCT is the device supplied by Neutron Therapeutics (see Section 3.5), and another used for nuclear cross section measurements is the Van de Graaff in Karlsruhe (see Section 2.3.2, Ref. [57]).

A separate class of electrostatic accelerator is the tandem accelerator. In a tandem accelerator, negative ions are accelerated first, and then stripped inside the high-voltage terminal to be reaccelerated as positive ions. The name 'tandem' originates from this dual use of the same high voltage. The direct advantage of tandem acceleration is the requirement of only half the potential to produce ions of the required energy. Also, the ion source is located outside the terminal, which makes accessing the ion source while the terminal is at high voltage significantly easier, especially if the terminal is inside a gas tank. The disadvantages of tandems include a more complex design for the required negative ion sources than that for positive ion sources, and the need to use a stripping target (either foil or gas). Commercial versions of these are sold for ion beam damage or ion beam analysis studies. An example of a commercial tandem electrostatic accelerator used as a CANS is the Nagoya University Accelerator Neutron Source (NUANS), which utilizes a 2.8 MeV, 15 mA proton beam from a Dynamitron™ dedicated to BNCT development [144].

The acceleration of ions in electrostatic accelerators is typically carried out in accelerator tubes consisting of a set of electrodes of increasing potential with insulators between them. Two new designs dedicated to neutron production are being developed and are described below: the Tandem-ElectroStatic-Quadrupole (TESQ) which has electrostatic quadrupoles inside the tubes to produce strong transverse fields, and the vacuum insulated tandem accelerator (VITA).

4.1.4.1. Tandem-Electrostatic-Quadrupole accelerator

A Tandem-ElectroStatic-Quadrupole (TESQ) accelerator is being developed at the National Atomic Energy Commission (CNEA) in Buenos Aires, Argentina [146–148]. The project's final goal is a machine capable of producing a 30 mA, 2.5 MeV proton beam which is coupled with a neutron producing Li target using the ^{7}Li(p,n) reaction. Initially, a single-ended accelerator was developed that could produce p and d beams of ca. 1.44 MeV, below the 1.88 MeV threshold of the ^{7}Li(p,n)^{7}Be reaction. The ^{9}Be(d,n) and ^{13}C(d,n) reactions appear as attractive alternatives [148, 149]. A smaller machine of 200 kV has already been completely developed. Fig. 17 shows the accelerators being developed:

- The initial prototype, single ended 200 kV machine;
- The 720 kV TESQ using the ^{9}Be(d,n) reaction for neutron production;
- The 1.44 MV TESQ that can use ^{7}Li(p,n) for neutron production, or alternatively a single ended variety could be used with the ^{9}Be(d,n) and ^{13}C(d,n) reactions.

The final voltage on the dome of an TESQ is generated by a series of alternators that float at high voltage, and which in turn are fed by a chain of insulating, rotating shafts, driven by a motor [150]. The motor and negative ion source are both at ground potential. The dome of the TESQ houses a bending magnet and a gas stripper for charge exchange with the accelerated particle. As an alternative, single ended ESQs can be manufactured with positive ion sources installed at the respective terminals.

Figure 18 shows a photo of the 0.72 MeV single-ended, in-air electrostatic quadrupole accelerator that is in operation. An image of a 10 mA beam propagating through the accelerator is shown in Fig. 19. The cost of the single-ended, in-air Electrostatic Quadrupole accelerator for a 1.44 MeV, 30 mA deuteron beam is in the range of 3-4 million USD. Electrical power is about 200 kW, including air conditioning. For a thick Be target, the neutron yield is 0.9×10^{13} n/s and the direct electrical operational cost of neutron generation is 1.62×10^{15} neutrons/US Dollar. For a thick ^{13}C target [149], the neutron yield is 0.6×10^{13} n/s.

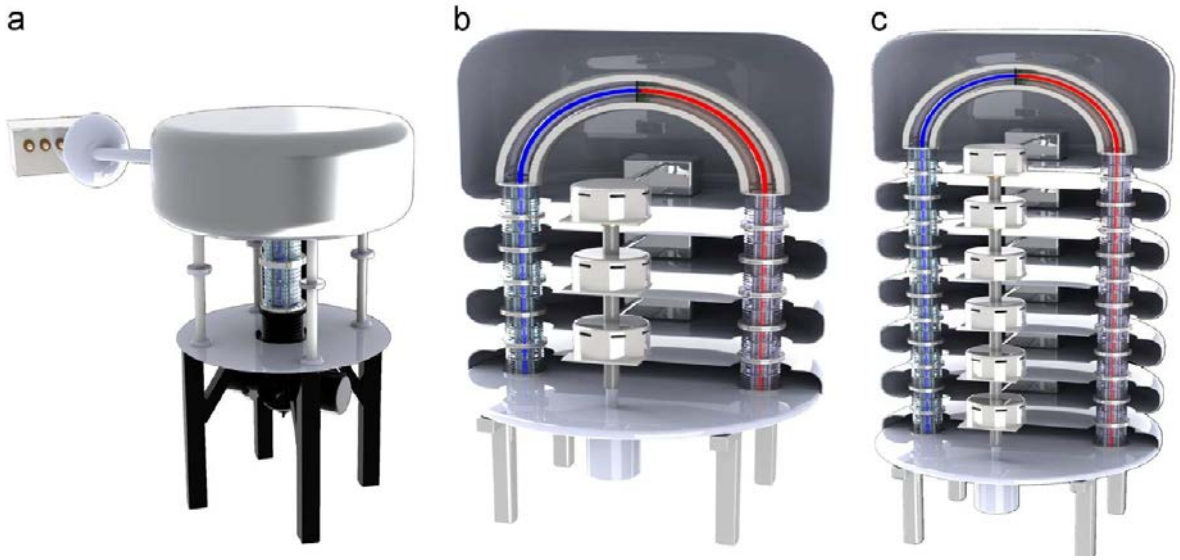

FIG. 17. Different types of accelerators being developed: (a) single ended 200 kV electrostatic machine; (b) 720 kV TESQ;(c) 1.44 MV TESQ for the $^{7}Li(p,n)$ reaction or in a single ended version also for the $^{9}Be(d,n)$ reaction operating with a positive source in the terminal (reprinted from Fig. 1 of Ref. [145] Copyright (2014) with permission from Elsevier).

FIG. 18. Photograph of 0.72 MV Electrostatic Quadrupole (ESQ) accelerator completed (reprinted from Fig. 1 of Ref. [146] Copyright (2020) with permission from Elsevier).

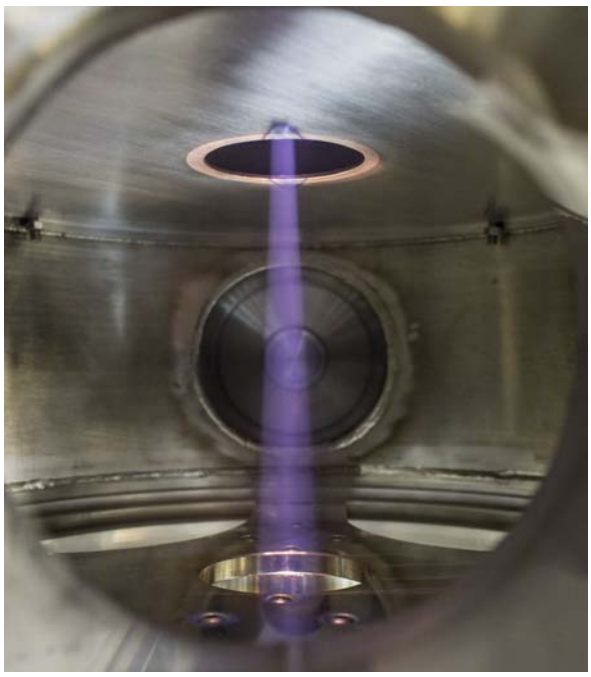

FIG. 19. Image of 10 mA beam propagating through the accelerator revealed through the induced fluorescence in the residual gas (courtesy of Andres Kreiner, CNEA).

4.1.4.2. Vacuum insulated tandem accelerator

The vacuum insulated tandem accelerator (VITA) [151, 152] is unlike conventional tandem accelerators, as accelerator tubes are absent: the intermediate electrodes *(5)* are fixed on the single feedthrough insulator *(8)* as shown in Fig. 20. This design places the insulator as far as possible from the accelerating channel and reduces the impact of secondary charged particles and ultraviolet radiation on the insulator, which arise in the interaction of the ion beam with residual and stripping gas; these enable the maximum proton beam current to be increased.

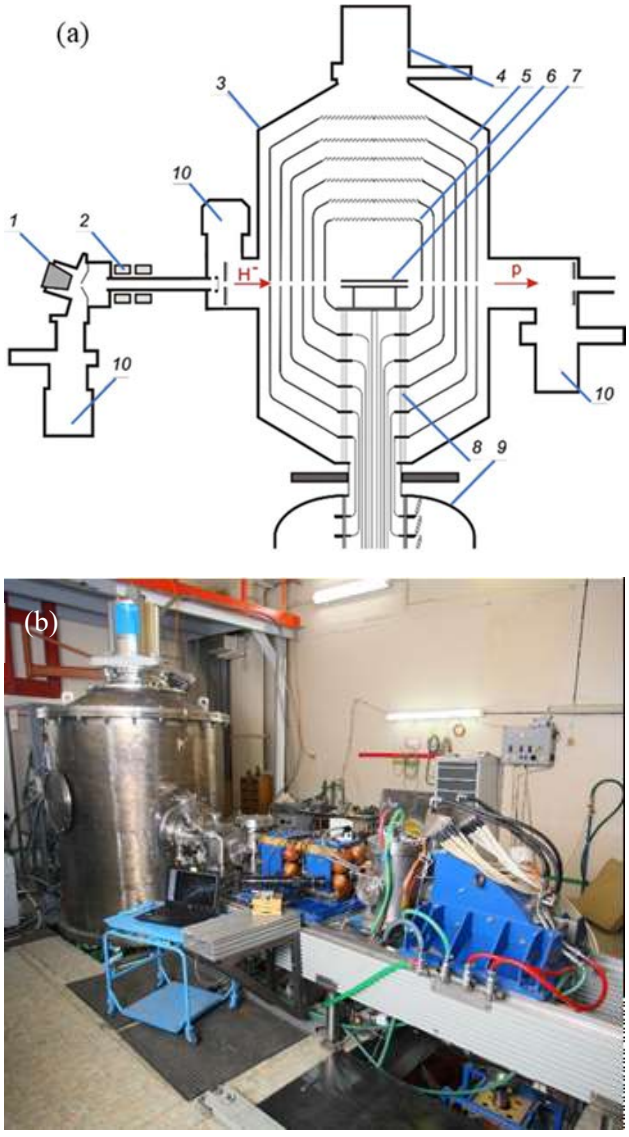

FIG. 20 (a) Vacuum insulated tandem accelerator: scheme (b) photo of set-up: 1 – H^- source, 2 – magnetic lenses, 3 – accelerator, 4 – cryogenic pump, 5 – intermediate electrodes, 6 – high-voltage electrode, 7 – gas stripper, 8 – feedthrough insulator, 9 – high-voltage power supply, 10 – turbomolecular pumps. Arrows show the direction of propagation of negative hydrogen ions (H^-) and protons (p). (Reproduced by permission of IOP Publishing from Fig. 1 of Ref. [156], doi:10.1088/1748-0221/11/04/P04018. © OP Publishing Ltd and SISSA Medialab Srl. All rights reserved.) (b) Photograph of an installed VITA with focussing and bending magnets on the high energy side. (courtesy of Sergey Taskaev, Budker Institute for Nuclear Physics).

Protons are obtained in a VITA as follows: a low-energy beam of negative hydrogen ions generated by the source *(1)* is focused by the magnetic lenses *(2)* to the accelerator input port *(3)* and is accelerated to an energy of 1.15 MeV. In the gas stripper *(7)* installed inside the high-voltage electrode *(6)*, negative hydrogen ions turn into protons that are accelerated to an energy

of 2.3 MeV by the same high-voltage potential and are transported to the neutron producing target. The potential on the high-voltage electrode *(6)* and five intermediate electrodes *(5)* is fed from the high-voltage power supply *(9)* (the larger part is not shown) through the feedthrough insulator *(8)* with a resistive divider. Gas is evacuated by turbomolecular pumps *(10)* placed near the ion source, at the accelerator input and output ports and by the cryogenic pump *(4)* through electrode blinds.

The accelerator features a high rate of charged particle acceleration of 25 kV/cm. Because of this, the input electrostatic accelerator lens is powerful. It refocuses the injected negative hydrogen ion beam in front of the accelerator's entrance lens. Using an OWS-30 wire scanner (D-Pace, Canada), installed in front of the accelerator entrance diaphragm, the dependencies of the profile and current of the H^- ion beam on the residual gas pressure are measured; the beam phase portrait is measured by an additional movable diaphragm in front of the scanner [153, 154]. The effect of the space charge and spherical aberration of focusing magnetic lenses on the ion beam is measured. The beam profile has a shape close to that of a ring, and the maximum beam density is found at intermediate residual gas pressure in the transport channel. To improve the quality of the injected beam, the original magnetic focusing lens made of two counter lenses was replaced by a lens in the form of a solenoid.

Secondary charged particle fluxes were detected, identified and measured in the accelerator [155]. They are due to the ionization of the residual and stripping gas by the ion beam, penetration of electrons from the transportation path into accelerating gaps, and electron emission from the walls of the vacuum tank during their irradiation with positive secondary ions. An almost 10-fold suppression of the secondary charged particle current in the accelerator gaps has been achieved: from an initial 60% of the ion beam current to less than 8% [156]. This was achieved after several modifications: the installation of a cooled diaphragm at the accelerator input port, a ring under negative potential to lock electrons in the transportation path, the placement of an additional vacuum pump close to the start of the ion acceleration position, and coating of a part of the walls of the vacuum tank with a metal mesh under negative potential to suppress secondary electron emission.

The application of two pairs of video cameras monitoring the input and output diaphragms of the first accelerating electrode permits monitoring and controlling the position of the ion beam in the accelerator by recording visible radiation from the interaction of ions with the residual and stripping gas (Fig. 21) [157].

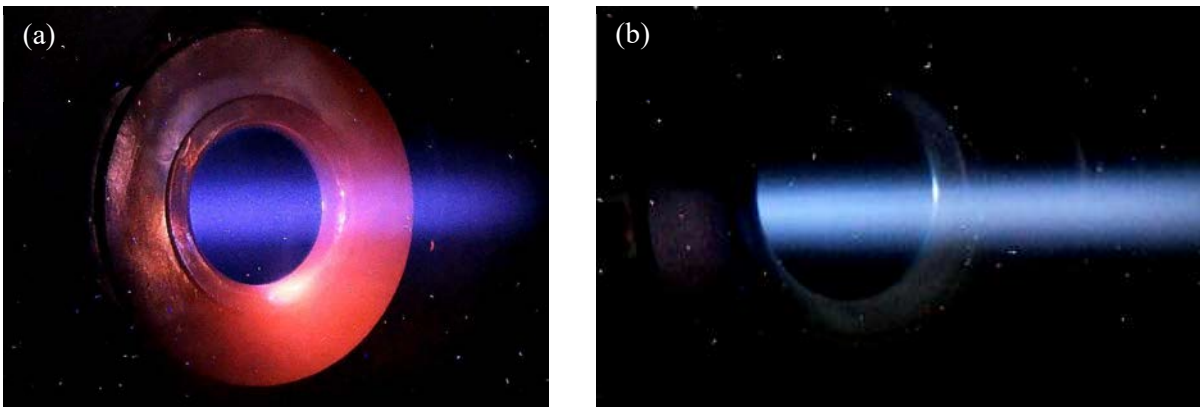

FIG. 21. Example of video camera images. (a) the ion beam is visible in blue; the heated diaphragm is visible in red; (b) the image at a proton current of 9 mA (courtesy of Sergey Taskaev, Budker Institute of Nuclear Physics).

Improvements in the VITA design enabled increases in proton beam current from the initial 100 μA [158], to 1.6 mA, after the optimization of the ion beam injection into the accelerator and the gas stripper [159], to 5 mA, after the suppression of the secondary charged particle flux [160], and then to 9 mA after establishing control over the ion beam position and size at and inside the accelerator input port. At present, the proton beam current is limited by the injected negative hydrogen ion beam current.

In the vacuum part of the feedthrough insulator, glass ring insulators were replaced by ceramic rings of double height, which made the placement of a resistive divider, which often burns out, inside the feedthrough insulator unnecessary [161]. Via video cameras, breakdowns in the accelerating gaps and on the surface of insulators can be monitored; breakdowns on the external vacuum surface of ceramic insulator rings cause the appearance of visible traces, but do not decrease the high-voltage strength of the feedthrough insulator. The modernization of the feedthrough insulator led to the elimination of high-voltage breakdowns in the accelerator and to a fundamental change in the operation of the facility: since September 2019, the facility has provided stable continuous generation of neutrons without any breakdowns [162].

Tests were performed in which one of the accelerating gaps was deliberately short-circuited: it was determined that the critical voltage is limited by the voltage in the accelerating gap rather than the total voltage. This result extends VITA for applications where a larger proton energy is required, as the energy can be increased by adding accelerating gaps into the accelerator design.

The path of the proton beam from the accelerator to the neutron producing target is equipped with correctors, inserted Faraday cups, cooled copper diaphragms, a DC non-destructive Bergoz current transformer, bending magnet, gas stripper efficiency sensor [163], video camera for monitoring the position of the proton beam on the target by Li luminescence and the scanner. The proton beam at the accelerator output has a diameter of about 1 cm [164] and 3 cm on the target located at a distance of 5 m from the VITA. The proton beam diameter on the target does not depend on the beam current, which indicates the absence of space charge effects during its transportation. The proton beam diameter on the target is increased to 10 cm by the scanner.

Since 2017, the TAE Life Science company (California, USA) together with the Budker Institute of Nuclear Physics (Novosibirsk, Russian Federation) have been engaged in the construction of an epithermal neutron source for the hospital in Xiamen (Fujian, China), commissioned by the Neuboron Medtech Ltd. company (Nanjing, China). The neutron source consists of a 2.5 MeV 10 mA VITA and a Li target. The neutron yield from a thick Li target is 8.8×10^{12} n/s, and the average neutron energy is 320 keV, well suited for the production of an epithermal neutron flux for BNCT (see Section 3.5).

The neutron source in the Budker Institute of Nuclear Physics is planned to be used for radiation tests of fibres of the laser calorimeter calibration system of the Compact Muon Source electromagnetic detector to work on the High-Luminosity Large Hadron Collider in CERN [165]. To generate fast neutrons, hydrogen was replaced by deuterium, a deuteron beam with an energy of 2 MeV and a current of 1.1 mA was obtained and 5.7 MeV neutrons emitted from a Li target. The neutron yield was 1.4×10^{12} n/s [166].

In summary, VITA is a compact tandem accelerator for producing a stationary proton or deuteron beam with an energy of 0.6 to 2.5 MeV with a current of 0.5 to 10 mA. Monochromaticity and stability of ion energy are 0.1%, current stability is 1%. The accelerator is simple and reliable. The cost of the accelerator is several million dollars. Due to the high efficiency, operational cost

is low: direct electrical operating cost for neutron generation is ca. 5×10^{15} epithermal neutrons/US Dollar and 10^{16} fast neutrons/US Dollar. VITA occupies a floor area of about 10 m length, 6 m width, and 5 m height and can be placed in a room with minimal shielding.

4.1.5. Proton and deuteron radiofrequency quadrupoles and linacs

Compact linacs for high ion (proton or deuteron) currents combine a Radio Frequency Quadrupole (RFQ) injector coupled to a Drift Tube (DTL) or a SuperConducting (SCL) linac.

The advantages of using ion linacs come from their ability to:

- Enable optimization for and operation at Continuous Wave (CW), pulse mode, or both;
- Enable high beam current with low beam loss. Compared to a typical cyclotron, similar beam losses in a linac occur at about one order of magnitude higher current under CW operation and about two orders of magnitude in pulse mode;
- Enable neutron production in a single (nuclear) interaction, which makes the neutron production scheme, for many applications, efficient and less complex than in electron accelerators;
- Operate at different beam energies which can be optimized to the required neutron source.

The operating cost per neutron can be cheaper when using an ion linac as a CANS, although the capital cost for the accelerator and the lack of commercial manufacturers might be a drawback. Proton linacs are likely to be the backbone of a national CANS for a major country (e.g. see the conceptual design report for the 70 MeV linac proposed for a High Brilliance Source designed in Germany [6]). The upper limit in current for a proton or deuteron linac is likely ca. 100 mA [5, 6]. At this time, this is near the limit of what has been reliably achieved, although the IFMIF-DONES facility in Spain has a target of 120 mA [87, 88].

The theory and practice of RFQ and linacs are well covered in textbooks such as Refs [167, 168].

4.1.5.1. Radiofrequency Quadrupoles

RFQs are used as ion injectors to linear accelerators. The RFQ connects the ion source to the RF linac, provides preliminary acceleration of ions from tens keV/u to one or few MeV/u for injecting to the linac, and can bunch a DC beam. The main advantage of the RFQ over earlier electrostatic injectors is its high stability in terms of low electrical sparking rate. An RFQ is characterized by its high transverse focusing and longitudinal bunching strength. It is therefore a key technology for injectors for high current ion accelerators.

There are mainly two types of RFQ, 4-vane and 4-rod, which are different in their RF cavity shape (Fig. 22, Ref. [169]). The 4-vane has a higher acceleration efficiency (higher shunt impedance) and so is also more stable than the 4-rod RFQ. In general, the 4-vane RFQ has better physical parameters performances. The advantages of the 4-rod structure lie in its low cost and maintainability.

The transverse size of the 4-vane RFQ increases with the decrease of the RF frequency, while the 4-rod size does not depend on the frequency. Typically, 4-rod RFQs are optimized for low RF frequency (< 200 MHz where 4-vane RFQs become too large) and 4-vane RFQs at high

frequencies [169]. Therefore, it is a challenge to design and build a low frequency 4-vane RFQ, although examples exist.

RFQ linacs used as CANS include the Low Energy Neutron Source (LENS) at the University of Indiana, which has developed a diverse neutron research program with cold, epithermal, and fast beams based on a 13 MeV DTL. The epithermal and fast neutrons were developed with an interest in electronics effects and imaging, and cold fluxes used for SANS, spin echo measurements, and the development of cold moderators [170]. The RIKEN Accelerator Neutron Source (RANS) is another example, in Japan, of a proton linac used for such purposes [171].

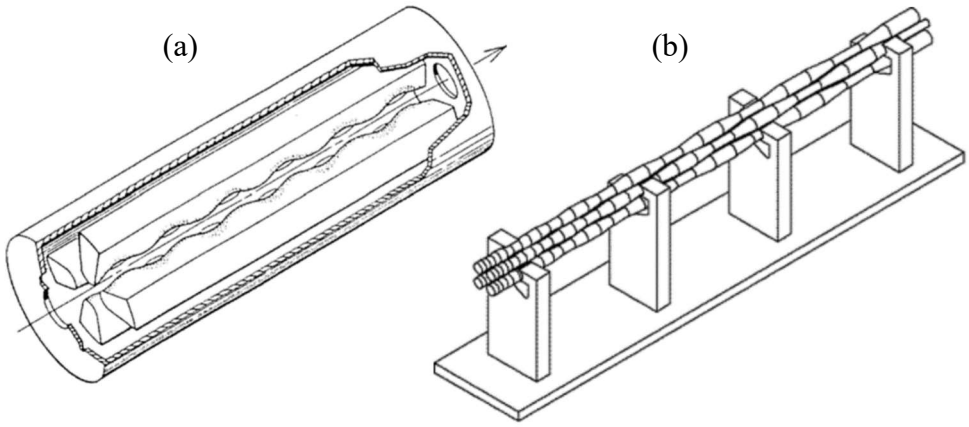

FIG. 22. Diagrams of (a) 4-vane and (b) 4-rod RFQs are licensed by A. Schempp under CC BY-3.0.

4.1.5.2. Drift Tube (DTL) versus Superconducting (SCL) Linac

In general, DTL accelerating cavities are cheaper and less complex than SCL cavities; however, DTLs are limited by cavity wall power dissipation and associated heat removal challenges, which limit the:

(a) *Beam current or the pulse length*. For beam pulses shorter than 10 μs DTLs are more efficient, and for pulses longer than 1 ms SCLs may be required [172]. Long neutron pulses make cold neutron time-of-flight (TOF) applications more efficient without spoiling the neutron energy resolution measurements. CW operation reduces the heat load along the linac [173] and the heat load and thermal shocks on the neutron production target.
(b) *Accelerating efficiency* to one ion velocity profile all along the linac, which practically limits the efficiency to one ion species. On the other hand, SC technology permits independently phased accelerating cavities that can optimize the ion velocity profile and maintain a high accelerating efficiency for different ions species and energies. This can be useful for certain applications; e.g., a tuneable ion energy at the linac exit enables shaping the neutron energy spectrum in order to perform integral measurements [174].
(c) *Size of the radius of the beam vacuum*, which increases the beam loss with a consequent increase in component activation that, by itself, is the basic limit of high intensity accelerators due to the requirement of hands-on maintenance.

4.1.5.3. Commercial availability

While RFQ or linac components are available separately from several commercial companies (see for example in the international linac conference series exhibitors list and Refs [176–179]), an integrated ion linac that includes the ion source, the RFQ and a SCL or DTL are rarely available commercially. Ref. [5] gives a rule-of-thumb for a price of a proton linac of

1-1.5 million Euros/MeV. A detailed cost estimate of a normal conducting or superconducting linac of high intensity (5 mA and 125 mA) CW 40 MeV deuteron, is found in Ref. [179].

4.1.5.4. Choosing the parameters for a compact accelerator based neutron source based on a radiofrequency quadrupole and linac

The parameters of the RFQ and the linac need to be optimized together with the intended neutron utilization. The RFQ+linac alternative may be selected when a CW proton beam current higher than 1 mA is required, when specific pulse shapes are required and when residual activity estimation, based on the facility operating program, limits the possibility for hands-on-maintenance. Some of the main choices include:

(a) *Protons or deuterons.* For applications using fast neutrons in the range of 5–25 MeV, nuclear reactions involving deuterons on light elements (Be, Li, C) is the optimal scheme and much more efficient than the alternative (Fig. 23 and Ref. [180]). This is the reason why fast neutrons projects, such as IFMIF [181], SPIRAL2 [182], SARAF [164] and BISOL-IDD [183], are based on deuteron accelerators. For these projects, an SCL structure begins just after the RFQ to reduce beam loss, since low energy deuterons that hit structural materials might create residual activity and prevent hands-on-maintenance.
Acceleration of deuterons enables the production of neutron rich isotopes via the direct surrogate reactions (d,p). This is the case for example for the radiopharmaceutical production scheme of ^{176}Yb(d,p)^{177}Yb $t_{1/2}$=1.9h → ^{177}Lu and ^{98}Mo(d,p)^{99}Mo.

(b) *Ion energy transition between the radiofrequency quadrupole (RFQ) and linac.* The RFQ acceleration structure is more expensive to build than the linac structure. Therefore, RFQs are used up to an ion energy where the linac structure can take over acceleration. Due to mechanical fabrication constraints in the linac structure, the linac acceleration gap length (g) cannot be smaller than a few cm. In RFQ and RF linacs the longitudinal distance between two acceleration gaps is equal to about one $\beta\lambda$, where β is the ion velocity relative to the speed of light and λ is the RF wavelength. In low energy ion linacs, $\beta\lambda \gg g$. This sets a minimal ion energy (i.e. β) for the transition between the RFQ and the linac.
On the other hand, since the nuclear reaction of protons on copper, which generates long-lived ^{65}Zn residual activity, opens at about 2.1 MeV, it is recommended that the RFQ proton exit energy not exceed this energy. Deuteron nuclear reaction channels on copper open at lower energy, so it is recommended that the deuteron RFQ exit energy not exceed 1.5 MeV/u [184].

(c) RF frequency. Historically, the leading basic RF frequency in the large proton accelerators in Europe is 352 MHz (CERN-Linac4, ESS, GSI-proton) and in the US is 402 MHz (LANSCE, SNS). CANS can save costs in the accelerator design and life cost by adopting the front-end of a spallation neutron source. However, the front-end of a high-energy proton machine may not be optimal for low-energy CANS requirements. If this is the case then usually the optimal RF frequency of the low-energy proton accelerator is a harmonic of these leading frequencies (i.e. 352/2, 352/4).

At low RF frequency, when the magnitude of $\beta\lambda$ does not limit the linac cavity fabrication, 1 MeV/u would be a practical value for the RFQ exit ion energy.

The choice of frequency may affect fast neutron (MeV) TOF measurements, if required. For good energy resolution, in fast neutron TOF measurements, sub-ns pulses are required. Such short pulses may be possible by single bunch transmission. The RFQ bunches the ion bunches

to a sub-ns length. Single bunch chopping is easier when the RF period is larger because the time difference between two bunches is larger. Traveling wave fast choppers, downstream of the RFQ, have been designed for several RFQ+linac projects. A very simple low-cost single bunch fast chopper upstream of the RFQ was built and tested for RF frequencies of 176 MHz at SARAF [185].

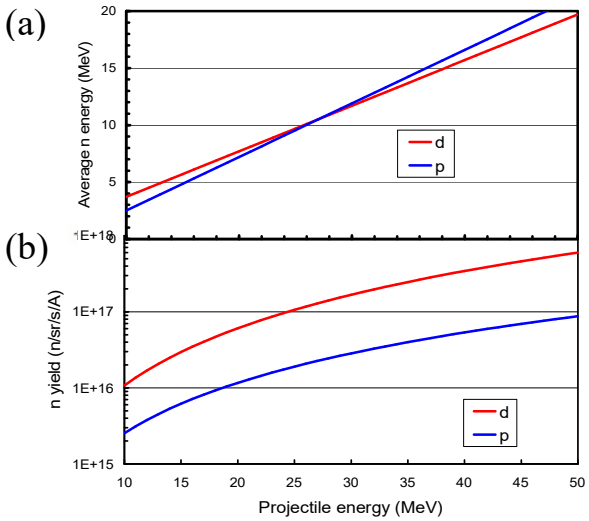

FIG. 23. Neutrons (with E > 2 MeV) from the reaction of deuterons and protons with a thick Be target, at forward direction showing (a) average neutron energy and (b) neutron yield versus projectile energy. Data taken from Ref. [180] (courtesy of Dan Berkovits, Soreq).

4.1.6. Laser driven neutron sources

Laser driven neutron sources are undergoing rapid developments in dedicated laboratories and in the future may become more widespread in applications laboratories. Ultra-intense lasers have demonstrated the capability of accelerating short and intense bursts of ions [186, 187]. These ion bunches have been used to generate short bursts of neutrons by irradiating a converter in close proximity to the source, making this scheme a very compact and bright source of neutrons of up to more than 100 MeV in energy [188]. Using novel laser ion acceleration, mechanisms with directed bunches of neutrons can be generated, which increases the brightness of these sources when compared to earlier versions. Recently, research using a mechanism based on relativistic transparency has been able to drive the most intense laser-driven neutron sources to develop initial applications.

The promise of future ultra-intense lasers as drivers for brilliant, compact, and highly efficient particle accelerators for electrons and ions (potentially replacing in some cases much larger conventional accelerators) also ushers in the prospects for driving next generation neutron sources.

In the following, we do not address the production of neutrons by thermonuclear fusion reactions, as this usually requires MJ (megajoule) laser systems the size of a ‘football stadium’ (NIF is roughly 100×170 m [189]). Instead we will focus on neutron production using compact, high-powered short pulse lasers.

Early experiments used excitation of giant resonances in nuclei to determine laser on-target intensities [190, 191]. This research was motivated by the ultimate question, “How much laser intensity actually reaches the critical target surface?” The interaction of the laser drives hot electrons into the target due to the ponderomotive force. The hot electron energy distribution

function can be estimated according to Wilks [192] to scale with the laser strength parameter $a_0 = eE_L/m_e\omega_L c$, resulting in a temperature equivalent of $k_B T_h = m_e c^2((1 + a_0^2)^{1/2} - 1$. The laser strength parameter is linked to the laser intensity by

$$a_0 \cong 0.85 \times 10^{-9}\, \lambda_L[\mu m](I_L[\mathrm{W/cm^2}])^{1/2} \quad (3)$$

and becomes of order of one at high intensities near 10^{18} W/cm^2. E_L hereby is the electric field of the laser, e and m_e the electron charge and mass, ω_L the laser angular frequency, c the speed of light, $k_B T_h$ the hot electron thermal energy and I_L the laser intensity. The Bremsstrahlung photons from this high-energy (i.e. hot) electron component therefore directly scales with the laser intensity: the higher the intensity, the hotter the electron component. The range of the Bremsstrahlung spectrum thereby can exceed the threshold of photon-induced nuclear reactions. Diagnostics based on photoneutron disintegration reactions have been used to determine the laser intensity, and reactions up to (γ,7n) in gold have been observed indicating the presence of 'hard' photons above 60 MeV [190].

Recently, photo-induced neutrons have gained new attention as new short pulse lasers have produced very short neutron bursts using low density targets in a pitcher–catcher geometry [193].

Cluster fusion – In the late 1990s, the production of neutrons from short pulse lasers reached a new level using cluster targets. The interaction of a short, intense laser pulse with deuteron clusters of an optimum size of around 50 μm resulted in cluster Coulomb explosion and the subsequent generation of D-D fusion neutrons from a compact source. In the early experiments in 1999, about 10^5 n per shot were produced [194]. This method has been improved, resulting in a yield of 10^7 n/shot at the Texas Petawatt Laser [195] that can deliver 120 J in a 170 fs pulse duration. The source size in these experiments is of order only a few tens of microns (which is the focal region in the cluster volume).

Ion beam driven fusion – Due to the large cross section of neutron producing reactions, ion-induced neutron sources have been widely used with conventional accelerators. The advent of laser-driven ion bunches spurred the idea of compact neutron sources. The first experiments in 2000 resulted in 4×10^8 n/shot using 15 J laser pulses provided by the laser system at LULI (Laboratoire pour l'Utilisation des Lasers Intenses). In these first experiments that used a deuterated plastic target (the 'pitcher') and a titanium 'catcher' highly doped with deuterons, the 2.45 MeV neutron signal from D-D fusion reactions was observed [196].

During the following years, neutrons have been produced by laser-driven ion bunches using the Target Normal Sheath Acceleration mechanism [197], which typically results in energetic proton bunches, as this mechanism preferentially accelerates surface contaminants according to their charge-to-mass ratio. The first experiments explored the possible neutron yield for applications. These experiments did not address applications directly, but rather tried to optimize the neutron conversion efficiency in order to demonstrate the principle concept of laser-driven neutrons. In 2004, Lancaster et al. used the ^{7}Li(p,n)^{7}Be reaction for fast neutron imaging applications [198]; and in 2010, Higginson et al. increased the neutron yield to 2×10^9 n/shot using the Titan laser at LLNL [199]. The result indicates the prospect for neutron resonance spectroscopy. A year later, using short laser pulses of 360 J energy, the neutron yield was further increased, and the maximum neutron energy was increased to 18 MeV [200]. This time not only was the yield increased to 8×10^9 n/shot, but also a pronounced directed neutron emission was observed. The basic reaction in all the above cases used the pitcher–catcher

configuration and the conversion of proton bunches into neutrons using light catcher elements (Li, Be) (see Fig. 24).

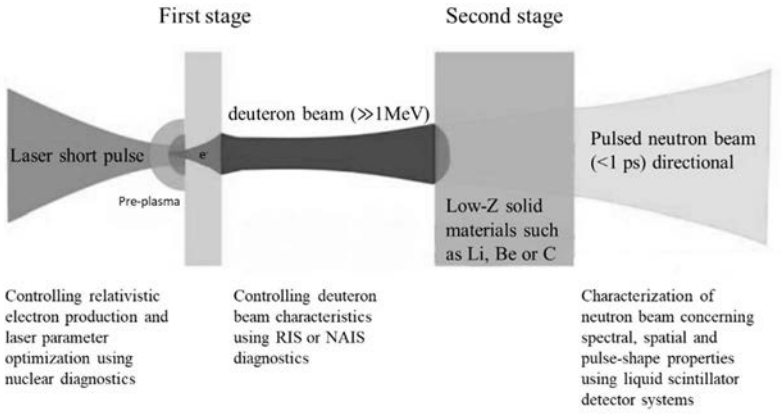

FIG. 24. Typical pitcher–catcher geometry for laser-driven neutron production using ion bunches (courtesy of Markus Roth, Institut für Kernphysik).

Relativistic transparency – The fundamental problem of the prior experiments was the limit in ion energy as the cross sections, and therefore the yield for neutron production, strongly increased with energy. Moreover, accelerating ions other than protons requires special target treatment or the controlled application of the ion species of interest as the rear side surface contaminant [201].

In recent years, the contrast of high energy short laser pulses has largely improved, allowing the irradiation of solid targets with thicknesses well below 1 μm [202]. At the same time, the laser intensity at the target surface has increased to above 10^{20} W/cm^2. In 2007, a new ion acceleration regime was found in first 3D Particle In Cell simulations, opening the onset of relativistic transparency of solids with a large impact on laser-driven ion beams [203, 204]. In this regime, the foil thickness is small, and during the rise time of the short laser pulse, the electrons in the target start to deplete. At the same time, the increasing intensity causes the quiver motion (i.e. mean oscillation velocity) of the electrons to become relativistic. The relativistic mass increase results in an increase of the critical electron density and a commensurate reduction of the plasma frequency to levels below the laser frequency, thus allowing the laser pulse to penetrate through the otherwise sub-relativistically overdense target. The experimental confirmation of this theoretical prediction is known as the Breakout Afterburner mechanism [204, 205] and leads to ion energies in excess of 100 MeV for the first time, as well as the predicted change from surface acceleration to acceleration of the bulk foil material.

4.1.6.1. Neutron production

Ion induced neutron production can be separated by ion kinetic energy: a high energy regime with ion (mostly proton) energies from hundreds of MeV up to several GeV, and a low energy regime starting at a few MeV. For the high energy regime, neutron spallation is favoured by the use of heavy nuclei allowing for multiple neutron emissions per ion impact. The low energy regime can be addressed with CANS (e.g. cyclotrons) and, most recently, short pulse laser systems. For this regime, low *Z* converter materials offer the best ion-to-neutron conversion efficiency.

As efficient acceleration of the bulk material allows for the use of more efficient reaction channels for neutron production, the focus has changed from a proton induced reaction for neutron production to deuteron driven neutron production. The acceleration of deuterium offers two important advantages: First, every accelerated deuteron carries a neutron, which is loosely bound with a separation energy of only a few MeV; and second, following separation, the remaining proton can still evaporate a further neutron on impact with the converter material. Assuming a purely Coulomb breakup, the deuteron with initial energy E_D decelerates as it approaches the target nucleus. At a certain point R_s (the distance from the target nucleus) the deuteron breaks up, with the proton and neutron each emerging with half of the initially available energy, E_D. On leaving the target nucleus, the proton gets re-accelerated in the Coulomb field but the neutron keeps its given energy, E_n, where $E_n = ½ (E_D - Ze^2/R_s - Q)$ MeV, where $Q = 2.22$ MeV [206].

As a further benefit, because neutrons from the deuteron breakup follow the initial deuteron trajectory, the neutron angular distribution becomes anisotropic, acquiring a distinct forward directionality. This results in higher neutron flux density and reduced shielding requirements compared to the more isotropic thermal sources.

4.1.6.2. Recent experimental results

With the use of solid target foils of submicron thickness and high contrast laser systems, recently the neutron yield has increased by orders of magnitude compared to the earlier Target Normal Sheath Acceleration based attempts. The parameters of the recently developed neutron source are summarized in Table 8.

In 2012, experiments at the Trident laser at Los Alamos National Laboratory resulted in a yield of 10^{10} n/shot (i.e. per laser pulse) and a neutron energy in excess of 100 MeV using 80 J pulses of a 600 fs duration incident on a 3 μm diameter spot [196, 207]. The neutron distribution also revealed a clear directionality. This was accomplished using a thin, deuterated plastic target (pitcher) and a sealed Be catcher. This was the first time that static single bunch neutron radiographs with fast neutrons were performed. In 2013, the anisotropic forward yield was further optimized with a cylindrical W reflector around the Be converter. In 2015, experiments at the PHELIX laser system at the Helmholtzzentrum für Schwerionenforschung – GSI in Darmstadt lead to a neutron yield of 2×10^{11} n/shot with incident laser pulses of 80 J energy of 450 fs duration. In both cases, the neutron emission was strongly peaked in the forward direction. The catcher material and geometry had been improved to match the several centimetre range of the ion bunch. Consistent with the predictions from relativistic transparency, there was a strong dependence on the target thickness with a distinct optimum. The neutron pulse duration is basically determined by the time the ion bunch needs to pass the moderator. Given the fact that the ion bunch has an initial duration of only a few ps and taking into account the temporal dispersion and increasing bunch duration commensurate with its energy spread (i.e. ion debunching), the neutron bunch can be of sub-nanosecond or nanosecond duration. This novel, short bunch capability enables various applications.

TABLE 8. PARAMETERS OF THE RECENTLY DEVELOPED NEUTRON SOURCE.

Parameter / Item	Parameter Range / Comment
Spectrum	Energy range from thermal to >100 MeV Energy spread 100%
Neutrons per bunch	$>10^{10}$/sr (up to 2×10^{11} in 4π)
Spatial distribution	Isotropic component and fourfold enhanced forward beam
Opening angle	Around 90°
Forward neutrons	2×10^{10}/sr
Temporal structure	Bunch duration initially sub-nanosecond Repetition rate: equals the laser driver rate
Neutron generation scheme	Pitcher (deuterated plastic) + catcher (Be) + W reflector Deuteron-to-neutron conversion efficiency: $>10^{-2}$ Co-moving particles: e^- (MeV), Gamma (MeV) Ions (depending on thickness of the converter) Target: thin, deuterated foil (200–800 nm)
Laser parameter	
Energy	0.1–500 J
Pulse duration	Picosecond

4.1.6.3. Summary

Lasers have been used to produce neutron beams for many decades. Apart from those experiments aimed at pursuing thermonuclear fusion, it has become clear that the development of modern short pulse lasers has been a breakthrough in this endeavour. First using cluster targets, then intense electron beams and after the discovery of laser-driven ion beams, the use of (p, n) reactions demonstrate that short pulse lasers have become an ever more efficient tool to produce neutron bunches. With the enhancement of the laser contrast and the exploration of the relativistic transparency regime, laser-driven sources now have entered a per-pulse yield level that is already suitable for real-world applications. The recent jump in neutron numbers mark only the beginning of what laser-driven sources might be able to do in the near future. Higher laser pulse energy, paired with higher wall plug efficiency (due to diode pumping) and a higher repetition rate, can at least add an order of magnitude to the average neutron flux. The very short initial neutron bunch length allows for very precise energy resolution. Based on the current experimental findings alone, a 200 J/10 Hz laser with high contrast could already provide around 10^{13} n/s. Due to the compact size of the system, the neutron flux density close to the converter already now exceeds 10^{20} n/s/cm^2.

With the commissioning of the most modern systems, such as BELLA, ELI or Apollon [208] for neutron experiments, new research can be envisioned that makes use of the excellent beam properties. As can be seen in Fig. 25, the yield of laser driven neutrons per pulse has been increasing over the last few years and with the upcoming facilities can close the gap to large scale spallation sources. Finally, as smaller systems can be fielded at universities, laser-driven

neutron sources can serve as a breeding ground for the next generation of young scientists in neutron science.

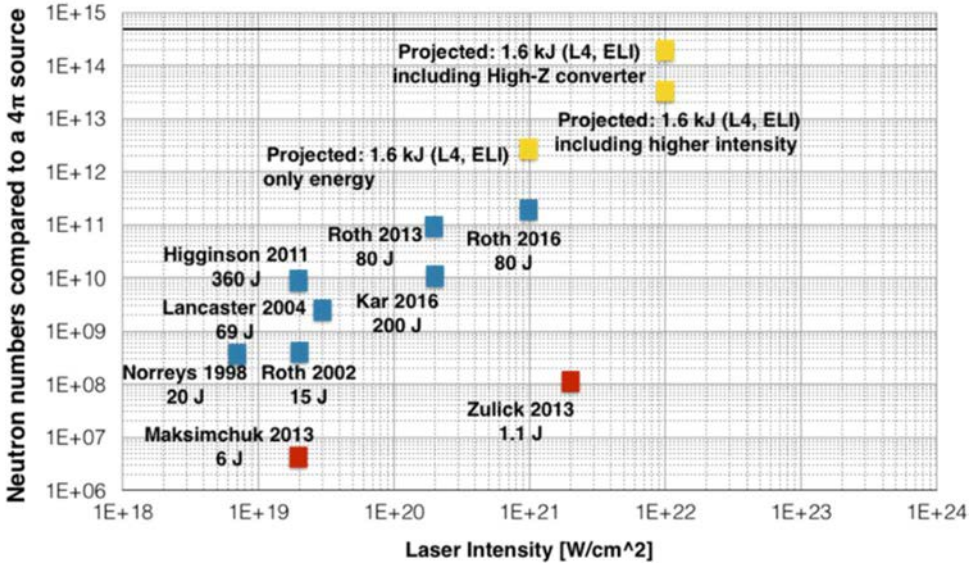

FIG. 25. Laser-driven neutron numbers versus laser intensity. The neutron numbers of the directed neutron beam per laser pulse are compared to a conventional isotropic (into 4π) neutron source. Results in red indicate short pulse lasers below 100 fs, blue are high energy lasers with around 0.5 ps pulse duration and the yellow marks indicate the prospect for upcoming systems currently under construction. The top black line indicates the single, 250 ns pulse and neutron yield at the converter target, produced at the LANL LANSCE facility spallation source (courtesy of Markus Roth, Institut für Kernphysik).

4.2. NEUTRON PRODUCTION TARGETS

The neutron production targets and the reactions that underlie their performance are a key component of a CANS system. The reactions most commonly used for neutron production in accelerators are outlined below together with some discussion on some specific target forms.

4.2.1. Neutron production reactions

The materials used in targets depend on the nuclear reactions used for the production of neutrons which can be fusion, low energy nuclear reactions, stripping reactions, and fission. The different nuclear reactions producing neutrons are shown below [209].

Fusion

$$^{2}\mathrm{H} + {}^{3}\mathrm{H} \rightarrow {}^{4}\mathrm{He} + n + 17.59\ \mathrm{MeV}$$

$$^{2}\mathrm{H} + {}^{2}\mathrm{H} \rightarrow {}^{3}\mathrm{He} + n + 3.27\ \mathrm{MeV}$$

as well as

$$^{3}\mathrm{H} + {}^{3}\mathrm{H} \rightarrow {}^{4}\mathrm{He} + 2n + 11.32\ \mathrm{MeV}$$

$$^{3}\mathrm{H} + {}^{3}\mathrm{He} \rightarrow {}^{4}\mathrm{He} + \mathrm{p} + n + 12.1\ \mathrm{MeV}$$

Low energy nuclear reactions with protons or deuterons

$$^{7}\mathrm{Li} + \mathrm{p} \rightarrow {}^{7}\mathrm{Be} + n + 1.65\ \mathrm{MeV}$$
(Threshold energy 1.88MeV)

$$^{9}\mathrm{Be} + \mathrm{p} \rightarrow {}^{9}\mathrm{B} + n + 1.85\ \mathrm{MeV}$$
(Threshold energy 2.06 MeV)

$$^{9}\mathrm{Be} + \mathrm{d} \rightarrow {}^{10}\mathrm{B} + n + 4.36\ \mathrm{MeV}$$

$$^{7}\mathrm{Li} + \mathrm{d} \rightarrow {}^{8}\mathrm{Be} + n + 15.03\ \mathrm{MeV}$$

$$^{7}\mathrm{Li} + \mathrm{d} \rightarrow 2\ {}^{4}\mathrm{He} + n + 15.12\ \mathrm{MeV}$$

$$^{7}\mathrm{Li} + \mathrm{d} \rightarrow {}^{5}\mathrm{He} + {}^{4}\mathrm{He} + 14.17\ \mathrm{MeV}: \quad {}^{5}\mathrm{He} \rightarrow {}^{4}\mathrm{He} \rightarrow n + 0.96\ \mathrm{MeV}$$

Figures 26 and 27 show examples of calculation results of angle dependent energy spectra produced by Li with 2.8 MeV protons and Be with 30 MeV protons. The energy spectra change as a function of the proton energy. Neutron production efficiency is much higher for Li than Be targets at low proton energy. Conversely, a Be target is used at larger proton energy. As a consequence, the neutron energy from a Li target is smaller than that of Be target since the threshold energies are almost the same. Figure 28 shows the neutron energy spectrum obtained by the d-Be reaction at 1.4 MeV. The energy at highest intensity is rather low but the spectra have a tail at higher energy.

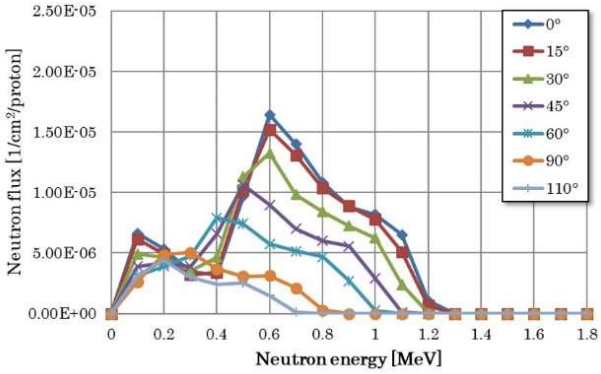

FIG. 26. Angle dependent neutron energy spectra of a p-Li reaction with 2.8 MeV proton. (Reproduced from Ref. [209] copyright (2018) with permission courtesy of Elsevier).

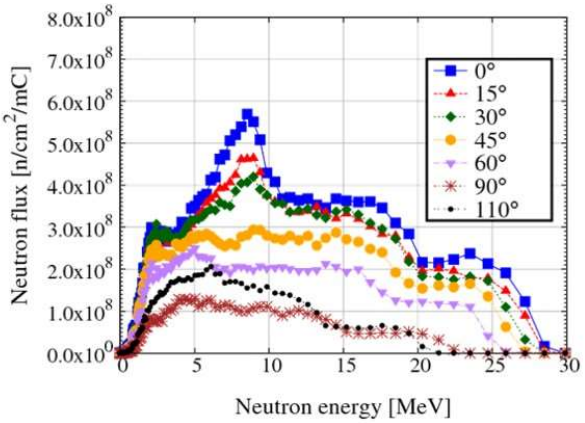

FIG. 27. Angle dependent neutron energy spectra of a p-Be reaction with 30 MeV proton. (Reproduced from Ref. [209] copyright (2018) with permission courtesy of Elsevier).

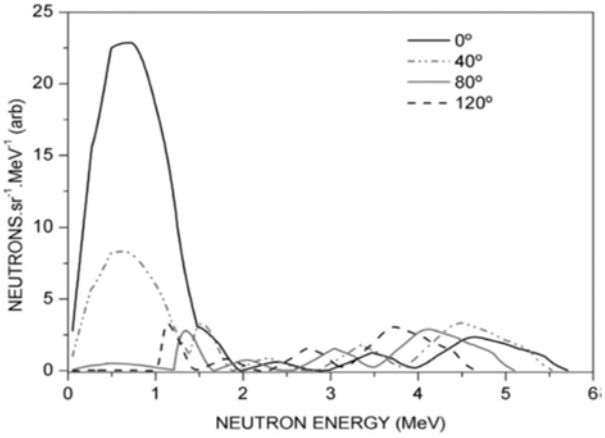

FIG. 28. Neutron energy spectra of d-Be reaction with 1.4 MeV deuterons (Fig. 1 reproduced from Ref. [210] Copyright (2014), with permission from Elsevier).

Photonuclear reactions. X-rays are produced from Bremsstrahlung which then proceed to generate neutrons predominantly via (X, n) reactions, although other reactions such as (X, 2n) and (X, fission) can contribute. Figure 29 shows the energy spectrum of Ta and Pb targets [211]. Figure 29 shows the neutron energy spectrum obtained by the d-Be reaction at 1.4 MeV. The energy at highest intensity is rather low but the spectra have a tail at higher energy.

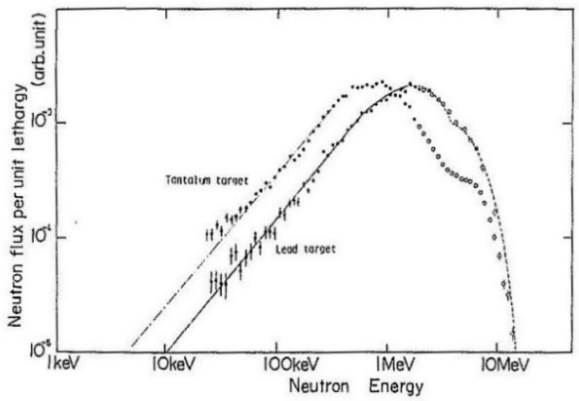

FIG. 29. Neutron energy spectra of photoneutron source with 35 MeV electrons (reproduced from Ref. [211] with permission courtesy of University of Kyoto).

Fission. Binary fission by a thermal neutron of a ^{235}U nucleus predominates in virtually all reactors.

$$^{235}\mathrm{U} + n_{\mathrm{thermal}} \rightarrow 2\ \mathrm{fragments} + 2.3\ n_{\mathrm{fast}}$$

Fission neutrons are produced in the fast spectrum in an energy distribution known as the Watt spectrum, and require a thermalizing moderator to be brought to the energy range in which the fission cross section for ^{235}U has a sufficiently high probability of fission that at least one of the generated neutrons will succeed in a further fission event in order to maintain a chain reaction.

In addition to the fission fragments (e.g., ^{90}Sr and ^{137}Cs), longer term radioactive waste is generated from actinides that are produced in the fuel materials in the intense gamma and neutron fields. Fission, other than photofission, is not a widely used process at CANS sources.

4.2.2. Target technologies

A wide variety of target materials and designs that utilize the above nuclear reactions to produce neutrons are used. Some of the most common are described below.

4.2.2.1. Targets for DD and DT sources

Devices that use DD or DT fusion reactions for producing neutrons are typically the smallest in the CANS family, in size and yield, since these reactions allow for accelerations with energies below 1 MeV and, consequently, reduced electric potentials (see Section 4.1.1). However, they need to deal with target nuclei that are not found in solid substances in a convenient fashion and, consequently, need to count on (a) target assemblies made of other materials within which D or T atoms are implanted or (b) the utilization of gas, or gas-plasma targets. In addition, utilizing D and T makes the situation more complex. Deuterium comprises only 0.0115% of natural hydrogen and needs to be obtained from some hydrogen enrichment process (including neutron capture). The T nucleus is not stable and emits β radiation with half-life of 12.32 years and end-point energy of 18.521 keV (a concern from the radioprotection standpoint). It needs to be obtained from some type of radioisotope production (e.g. neutron capture in ^{6}Li, ^{7}Li, or ^{2}H; DD fusion reaction). Nevertheless, both D and T are commercially available. They can be divided into two general types:

(a) *Solid targets.* In UCANGs the target system is based on a solid metal thin foil that has implanted atoms of deuterium and/or tritium. Given their affinity to hydrides, Ti, Sc, or Zr might be some of the materials of choice. This foil is placed over a metal substrate for mechanical and thermal robustness and, in some cases, electrical conductivity. Copper might be used for that role. In some devices, the implantation of D and/or T is done during manufacturing, while in others the implantation is a dynamical process that happens during operation of the NG. The size of the overall target is typically around a few cm but can reach tens of cm in some devices. The scale of these NGs allows operation without active cooling in most of the cases. However, scaling up neutron yield is limited in simple target systems especially when ion implantation does not fully cover the beam interaction surface and depth (something that is typical), and when heat load and ion bombardment is increased.

(b) *Gas or gas-plasma targets.* A natural, but not trivial, option to overcome target heating and erosion problems, and to improve DD- or DT-fusion generating ion interaction is the utilization of gas or gas-plasma targets. This means a target completely made of deuterium and/or tritium and, accordingly, a significant amount of their ions. In gas-plasma targets, having an important population of ions is desired since they are to contribute to fusion reaction rate. In gas targets, ions (other than primary beam particles) appear because of the several particle–target interactions but do not play a key role as for the gas-plasma case.

Some UCANGs use some amount of gas in the acceleration chamber with a combination of purposes: as reservoir, ion source, and/or as secondary target (in addition to the solid one). Some larger CANSs, such as small tandetrons also utilize DD and/or DT reactions. In this case, the voltage is scaled up to around 200 to 300 kV to accelerate deuterons and a deuterium and/or tritium gas target is placed in a chamber at the end of the acceleration path. There is no material window between the two regions and a differential pumping system maintains appropriate gas pressure in the target while keeping high vacuum in the acceleration tube. The gas target

chamber is large enough for the deuterons to stop completely inside the chamber. This strategy allows the device to perform close to the theoretical neutron yield curve (Fig. 14).

Gas-plasma targets can be found in IECF-NGs where deuterium and/or tritium and their ions are distributed inside the chamber. Gas pressure and ion population are fundamental for determining operational modes and performance. Initially, the target is typically a neutral gas but under operation certain levels of ionization are reached. Ion concentration increases towards the cathode and, consequently, the plasma is not homogeneous along the whole chamber. Since plasma is composed of energetic ions it can be considered relatively hot, at least in certain regions, a fact that favours fusion. Typical gas pressures are around 2 mTorr. Much larger pressures, or poorly tuned pressures, would result in gas electric breakdown at lower voltages preventing ions from accelerating at higher energies and, accordingly, limiting IECF-NG performance.

4.2.2.2. Liquid targets

A liquid target is used to reduce heat density load in a high power beam. A liquid Li target has been used at SARAF in Israel [254], which is used for neutron physics and also has a plan to be used for BNCT [212]. The target was tested at a power of 1.91 MeV and 1.5 mA. Liquid Ga has also been developed at SARAF both as beam dumps and neutron targets. Another liquid Li target is planned to be used at the IFMIF neutron source to simulate the fusion neutron spectrum by using the d-Li reaction. In this case, studies of the effects of neutron irradiation of fusion materials is the major objective. The accelerator is a 40 MeV / 250 mA deuteron linac. The liquid Li loop is completed and ready for neutron production. Other liquid targets have been used at spallation neutron sources. A mercury target is used at the spallation neutron sources SNS in the USA and JSNS in Japan. The accelerator power for these sources is in the range of 1 MW for both neutron sources. A lead-bismuth target is a candidate for accelerator-driven systems like MYRRHA.

4.2.2.3. Solid targets

Solid Li targets have been used at low power proton accelerators to produce quasi-monoenergetic neutrons for neutron cross section measurements. They are also used at high power accelerators (a few 10s kW) used for BNCT. Three types of targets are proposed: a rotating target at Helsinki University Hospital in Finland, a cone shape at the National Cancer Center in Japan and a sealed target to confine Li at Nagoya University in Japan [209, 213].

Be targets are used at various proton accelerators since it is easy to manufacture and handle Be targets. A Be target with a thickness of few mm is used as a target for protons above about 20 MeV and it works as a structural material of the target system. The protons sink in a water-cooling channel behind Be, and consequently blistering of the Be is much reduced. In the case of low proton energy, thinner Be is used as a target and a three-layered structure is adopted to avoid the blistering, namely, (Be / anti-blistering material / Cu cooling part) [214].

Photoneutron sources as well as a spallation neutron sources use heavy metal targets such as Pb, Ta and W. Depleted U can be used as a target since it produces about 1.5 times higher intensity of neutrons, but its handling and maintenance is very laborious and difficult. The Gelina facility in Belgium uses a U target cooled by Hg.

4.3. MODERATORS

In nuclear reactions, neutrons are usually produced as fast neutrons with energies in the MeV range. In a few specific cases (deuterons or protons on Li with energies close to the threshold of neutrons production), epithermal neutrons with a few tens of keV energies can be produced.

For some applications, the fast neutron spectrum is adapted to study specific nuclear physics reactions or to mimic fast neutron spectra generated in fusion reactors or in fast breeder reactors (see for example 'Neutrons for Science' at Ganil, France [215]). Fast neutrons may also be used to perform fast neutron imaging or soft error tests in electronic devices (Section 3.1.2).

However, in most cases, the neutron energy spectrum needs to be modified to suit the targeted application:

Table 9 gives a list of common definitions of neutron energies and in the following sections, a brief description of common moderator choices is given.

TABLE 9. TYPICAL DENOMINATIONS OF NEUTRON ENERGY RANGES

Neutron energy	Energy range
<300 neV	Ultracold
1–10 μeV	Very cold
<0.025 eV	Cold
0.025 eV	Thermal
0.025 eV–10 keV	Epithermal
0.1–20 MeV	Fast

Note: there is no agreed definition of the terms in the second column; e.g., when speaking of BNCT, the epithermal range is typically taken to be from 0.5 eV to 10 keV, and fast neutrons are used for all energies above that [216]. Ref. [217] provides an even finer division of terms.

4.3.1. Epithermal moderators

Neutron moderating systems for BNCT were initially designed for reactor sources and are now being designed for CANS to produce epithermal neutrons in an energy range from 0.5 eV to 10 keV. They are incorporated in a structure called the Beam Shaping Assembly (BSA). When the BSA is placed at a CANS, the term is equivalent to a shielded TMR with beam port (See Section 7.1.2) for BNCT: i.e. it moderates, reflects and directs neutron beams of appropriate energy. The epithermal moderator has to be optimized for the energy of the accelerated particle and the neutron emitting target. For a BNCT facility, the BSA also needs to filter gamma rays to reduce non-therapeutic dose to patients [219–221].

The energy of the neutrons emitted from the nuclear reactions at the target is higher than this energy range and needs to be moderated, however, not down to the region typical of thermal neutron moderators. Highly efficient moderators use elements with an atomic mass close to that of a neutron. However, epithermal moderators need to be less effective for slowing down than hydrogen while also emitting a smaller number of γ-rays by neutron absorption. Therefore, elements with moderate atomic mass are used.

Fluorine in the form of solid fluorides has been used as a key element of such epithermal moderators. MgF_2, CaF_2, and AlF_3 are major candidate materials. Fluorides are preferred to

oxides because the elastic cross section of ^{19}F has resonances in the fast range that boost performance as an epithermal moderator (Fig. 30). Fig. 31 shows the required accelerator power for MgF_2, CaF_2 and AlF_3 to attain a 1.5 times greater epithermal neutron intensity than the minimum recommended in the IAEA-TECDOC-1223 [216]. This indicates that MgF_2 is effective at energies less than about 20 MeV and above this energy the three materials have almost the same performance.

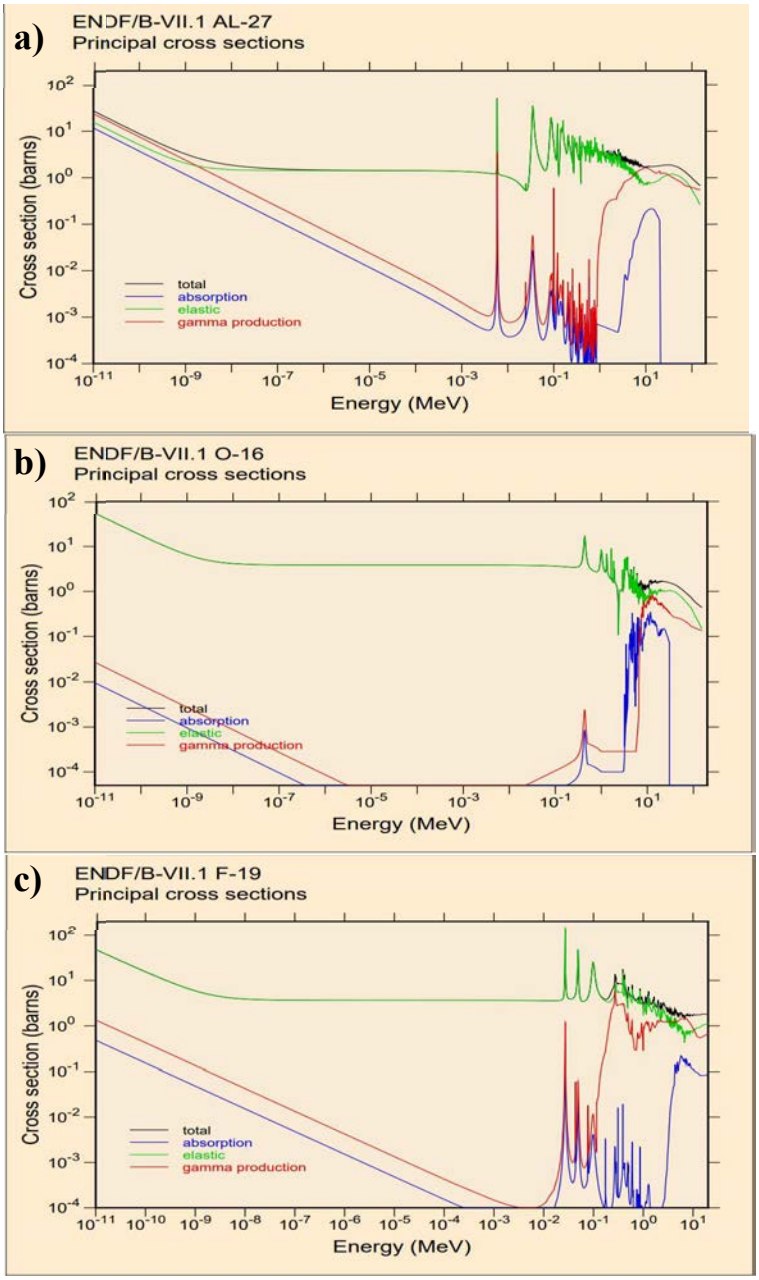

FIG. 30. Comparison of the principal cross sections of (a) ^{27}Al, (b) ^{16}O, and (c) ^{19}F. Although the elastic cross sections of ^{16}O and ^{19}F are similar over a wide energy range, in the range E >10 keV, the nuclear resonances give ^{19}F a significantly greater value. Similarly, ^{27}Al has several strong resonances that are beneficial in this range. Data are from the IAEA Evaluated Nuclear Data File.

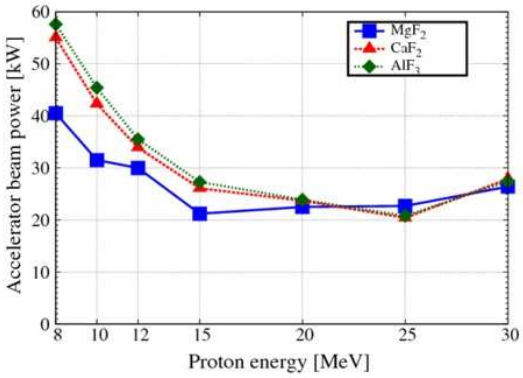

FIG. 31. Accelerator beam power required to fulfil a criterion for BNCT. (Reproduced from Ref. [221] copyright (2015) with permission courtesy of Elsevier).

4.3.2. Thermal moderators

Hydrogenous materials are the most effective moderators, as the hydrogen nucleus has the highest scattering cross section, a mass very close to a neutron. These characteristics lead to higher intensity and shorter emission times. As a thermal neutron moderator, water and polyethylene can be used. Metal hydrides may be considered as a candidate, but their dynamic spectra have no effective slowing down modes at thermal energy region, and the neutron spectrum forms a Maxwellian distribution with a much higher peak energy than the moderator temperature. Hydrogen number density, operation temperature, melting point, and boiling point are summarized in Table 10 for thermal and cold moderator materials. Polyethylene has a higher hydrogen number density than water and the neutron intensity from a polyethylene moderator is a little bit higher than water. However, polyethylene is less resistant to radiation damage. Therefore, a polyethylene moderator needs to be changed periodically.

TABLE 10. CHARACTERISTICS OF COLD AND THERMAL MODERATOR MATERIALS

Material	H/cm^3	Operational T	Melting point (K)	Boiling point (K)
H_2O	6.7×10^{22}	Ambient	273	373
$(CH_2)_n$	8.2×10^{22}	Ambient		
CH_4	7.8×10^{22}	20 K, 105 K	99.6	112
H_2	4.5×10^{22}	~15 K	20.4	14.7
C_9H_{12}	5.2×10^{22}	Ambient ~ 20 K	229	437

Maximizing the neutron intensity from the moderator is an important factor at low power sources such as CANS. One of the methods is to enlarge the emission surface of the moderator [222, 223]. Another method is to optimize the geometry of the target and the moderator. There are two geometries. One puts the target behind the moderator, namely, at the opposite side of a neutron emission surface of the moderator, which is called slab geometry. The other puts the target on the surface of one side of the moderator, which is called wing geometry. Slab geometry gives higher intensities than wing geometry, but the fast neutron component increases. Wing geometry can provide neutron beam extraction ports on both sides of the moderator. Many high intensity neutron sources use wing geometry moderators.

4.3.3. Cold moderators

In addition to the characteristics required for thermal moderators, cold moderator materials need to have a high number of low frequency excitations to slow down neutrons. In this energy range, the inelastic vibrational or rotational levels of the moderating compound are extremely important in determining moderator efficiency (unlike in the epithermal range where the neutron energy far exceeds the energies of the excitation spectra of the moderator and only kinetic effects play a role). Candidate materials listed in Table 10 are solid methane (CH_4), liquid hydrogen (H_2) and mesitylene [1,3,5-trimethylbenzene] (C_9H_{12}). A solid methane cold moderator was developed at the Hokkaido University Neutron Source (HUNS) [224, 225]. Methane has a very high hydrogen number density and a low energy rotation level (~1.3 meV). This low energy level very effectively reduces the neutron energy, and the high density of hydrogen nuclei contributes to the overall increase in neutron intensity. Figure 32 shows energy spectra from methane, hydrogen, ice and ethane moderators [230]: methane gives the highest intensity in the cold neutron region (few meV region). The cold neutron intensity from a hydrogen moderator is not as high. A similar trend is observed in ethane and ice moderators. Ice has the additional problem of expansion during solidification, which may destroy its vessel.

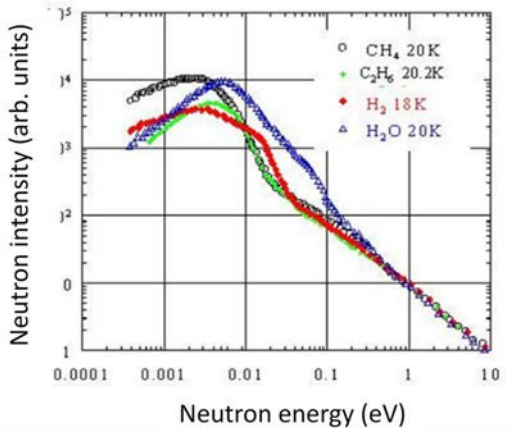

FIG. 32. Neutron energy spectra from various cold moderators. (Modified from Ref. [226] with permission courtesy of the Atomic Energy Commission of Japan.)

Cold moderators may be described as ‘coupled’ or ‘decoupled’: the latter type incorporate an absorbing element (such as Gd or Cd). Coupled moderators will provide more flux at the cost of an extended pulse. Decoupled moderators will provide shorter neutron pulses suitable for high resolution neutron scattering experiments at the cost of a significantly flux penalty (factor of 5 to 10) [227].

Methane has low radiation resistance, and it is necessary, even at low power sources, to exchange the methane gas after some irradiation time period, for example, about half a year at a 10^{12} n/s class photoneutron source. Coupled hydrogen moderators were originally developed to increase cold neutron beam intensity at spallation sources, since at high power neutron sources a solid methane moderator cannot be used, and coupled solid methane moderators have also been studied [228]. The energy spectrum of coupled moderators of both liquid hydrogen and solid methane are shown in Fig. 33. Each includes a pre-moderator of polyethylene (PE). The cold neutron intensity from the coupled methane moderator is almost the same as from the coupled liquid hydrogen moderator but the pulse shape is narrower. Solid methane is the most efficient cold moderator material.

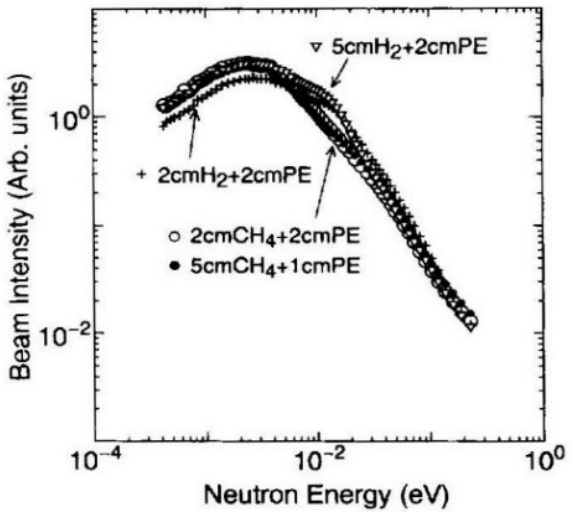

FIG. 33. Comparison of neutron energy spectra from coupled moderators of liquid hydrogen and solid methane. (Reproduced from Ref. [228] copyright (1995) with permission courtesy of Elsevier.)

However, methane is an explosive material, so requirements for handling and regulation are rather severe. 'Methane-like' materials such as mesitylene (1,3,5 trimethylbenzene) have been used in cold moderators at CANS [229, 230]. Cold neutron intensities from such materials are not as high as from methane, but mesitylene's aromatic ring increases resistance against radiation induced decomposition due to free radical formation, as the attached methyl groups retain some of the rotational disorder present in solid methane. Furthermore, mesitylene is liquid (not gaseous) at room temperature, and the flash point is far higher than that of methane. Trimethylbenzene is another material, solid at room temperature, that is being examined with similar moderating properties and radiation resistance [231].

For liquid hydrogen cold sources, attention has to be paid to the nuclear spin state of the hydrogen molecule. The hydrogen molecule has two nuclear spin isomers: para and ortho, and the ratio is temperature dependent, with the para state dominating at the typical temperature range of a liquid-hydrogen cold moderator at 20K, the para:ortho ratio at equilibrium is >99%, whereas at room temperature it is only 25%. However, conversion from ortho to para forms is slow as there is no effective radiative conversion mechanism, only a slow relaxation, although catalysts are available to speed this conversion. The ratio of spin isomers of hydrogen molecules can be monitored inline by Raman spectroscopy.

The reason for the interest in para hydrogen is the 'filter-like' behaviour in the scattering cross section, with a drop off of at least 30-fold below the thermal energy range (see Fig. 34). This is not present in ortho hydrogen. The advantage is that if an incoming neutron is thermalized to 'cold' temperatures and comes into kinetic equilibrium with a para hydrogen moderator at 20 K, there is very little chance of any further interaction within the moderator; this would quite likely involve up-scattering (re-gain of energy from the moderator material). Cold moderators have been designed and constructed that achieve a variable well-defined ortho-to-para ratio [232]

Very cold and ultracold neutrons are used for fundamental physics experiments such as the determination of the neutron electric dipole moment and the free neutron lifetime. Moderators used for this at spallation sources include solid ortho-D_2 (as used in Paul Scherrer Institute) [233] and superfluid He (as used at TRIUMF) [234, 235]. To date, CANS have not been designed specifically with this application in mind.

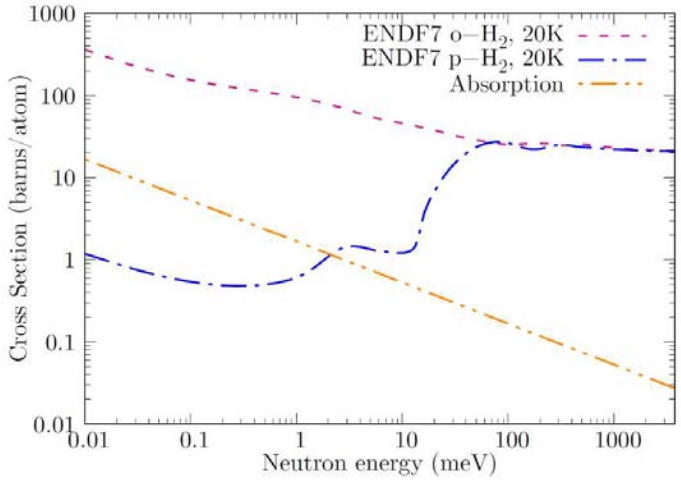

FIG. 34. Scattering and absorption cross sections for ortho (ortho-) and para (para-) H_2 at 20 K produced from the ENDF-B library [236] is licensed by K. B. Grammar and J. D. Bowman under CC BY 4.0.

4.3.4. Reflectors

A reflector is an important component of the TMR system. All components in this system need to be optimized together to optimize overall performance of a CANS. The reflector's function is to reflect neutrons that would otherwise be lost back towards the moderator and beamlines. Various materials have been considered as candidates [237]. The reflector can often itself also act as a moderator. Beryllium and graphite are effective materials for neutron sources for neutron scattering experiments. Beryllium is more effective than graphite, but graphite has been used at CANS in the past, since it is much cheaper than Be. Recently nano-diamond has been studied since it increases the intensity in the very cold neutron region [238, 239]. For BNCT, where epithermal neutrons (not thermal and below) are required, a non-moderating reflector material, Pb, is used [240, 241], see the discussion on BSAs for BNCT (Section 4.3.1).

4.3.5. Moderator geometry

Traditionally, the moderator shape was relatively bulky and block-like. Later improvements, particularly for hydrogen moderators in research reactors, included annular or re-entrant shapes, which allow illuminating neutron guides with the brightest possible cold flux [242].

Attention is being paid to hydrogen moderators in both reactors and accelerator sources due to the filter-like drop in cross section of para hydrogen (Fig. 34) and the resulting high mean free path of a cold neutron within this moderator. This has opened the possibility of building low dimensional moderators, such as rods, pancakes, and butterflies, potentially allowing to direct the emission of cold neutrons or allow more instruments to be packed around a single target [243, 244] (Section 4.3.3).

Various other ideas have been proposed to increase the neutron intensity at the sample position by changing the moderator shape. One method is to use a grooved surface moderator [245, 246]. This method is effective for thermal and cold moderators and increases the intensity by about 1.5 times. However, the neutron emission time distribution has a step like structure on the rising side due to the flight time difference of neutrons from the top and the bottom of the grooves, which may complicate time-of-flight methods.

5. ADDED VALUE AND LIMITATIONS OF CANS

Compact accelerator based neutron sources can be considered as complementary to reactor-based neutron sources, although the number of research reactors is much larger. Depending on the requirements of particular applications, certain types of CANS may be preferred. In the following, specific advantages of CANS are highlighted, and, towards the end of this section, some focus is put on advantages for (research) applications.

5.1. TECHNICAL ASPECTS

Advanced CANS can be built on many different scales. They feature intrinsic flexibility, scalability, and upgradability.

Not only the size and power, and thus the scale of the investment, can be chosen from a very wide range of options, but every specific implementation offers diverse options. Starting from the selected accelerated particles (protons versus deuterons), target materials can be optimized for specific demands.

Depending on the choices of geometries and moderators, performance can be tailored to rather varied and specific needs, and the neutron spectra can cover a broad range (cold, thermal, epithermal, fast). The versatility of CANS and the ability of even small installations to compete with large, general purpose facilities comes from this flexibility. Concentrating on selected demands and optimizing the whole chain from TMR to instrument can yield optimized fluxes and competitive performance for the intended purposes. For example, neutron scattering has traditionally been associated with large sample volumes (~cm^3). But advanced materials can often be difficult to synthesize in large volumes, or equipment such as pressure cells cannot handle large volumes. As the size of the samples to be investigated shrinks, Liouville's theorem helps: the requirement for point-like sources cannot benefit from very large TMRs (scales of m) at powerful spallation neutron sources.

The possibility to implement a flexible time structure is also helpful for specific applications.

As CANS are operated at lower energies (3–70 MeV), the energy of the secondary particles (gammas or neutrons) is limited by the incident particle kinetic energy. On the other hand, at spallation sources, where the incident proton energy is in the GeV range, very high energy secondary particles are emitted. The shielding of CANS is thus significantly reduced (typically tens of tons compared to 6000 tons of steel at ESS). Background radiation and activation issues are also significantly smaller at CANS than at spallation sources or research reactors.

The TMR for a CANS can be rather simple and thus be rather easily modified or upgraded. Besides, due to the limited γ radiation production, the thermal load on cold moderators is significantly reduced so that the cooling power required for cold sources is in the mW range compared to kWs around spallation sources or research reactors. This makes the construction of cold moderators far simpler.

The performance of a CANS may be upgraded by increasing the beam energy or by increasing the beam current. While this usually requires early provision in the accelerator design and construction, the upgrade of the facility can be spread over a long period.

5.2. INVESTMENT ASPECTS

Accelerators have found wide use in industry and in health applications. As a result, some can be ordered as off-the-shelf equipment from industrial suppliers. On the other hand, there are no complete 'standard' installations such as TRIGA or Materials Test Reactor research reactors on the market. If CANS are to replace research reactors on a broad scale for certain applications, dedicated governmental or organizational support will be required.

There are several advantages of CANS when it comes to financial analysis of such a project that reduce their risk in comparison to reactor sources:

- *Capital phase* – The potential modularity of designs of CANS and their future upgrades (Section 5.1) permits spreading cash flow demands over time and adapting financial requirements to realized demand, not early projections, reducing the risk of unproductive investment. As the risks associated with constructing and operating a CANS are lower than those for a research reactor, the regulatory aspects with respect to safety are less stringent, and a lower overall cost and shorter capital project duration (e.g., for construction) may result.
- *Operational phase* – Risks during the operational phase (see Section 5.3) are reduced: at least one fuel supplier needs to be in the market over the lifetime of a research reactor, whereas CANS require only guaranteed electrical supply. Maintenance of accelerators is usually simpler, less demanding and less costly than for a research reactor.
- *Decommissioning phase* – A large uncertainty in any financial projection are the decommissioning costs. From a financial point of view, the risk surrounding the decommissioning charges is high: potentially large cash flow requirements, decades in the future with large uncertainties around their size, as it is unknown what regulations and requirements will need to be complied with at that point. The decommissioning costs of any project scale somewhat with the investment, so decommissioning costs and risks may be expected to be lower for a CANS than for research reactors or spallation sources (see Section 7.3 for more detailed discussion). In some countries, it is mandatory that a decommissioning fund or bond be developed so that the operation is adequately financed ahead of time and the financial burden of an abandoned facility does not fall to future taxpayers [247]. This may be required before construction or may also be built up during the operational life.

Most CANS will not be profit making ventures, requiring financial support for capital and operational budgets, usually from a government-funded institution. The initial investment can be scaled to finely match the near- to medium-term scientific needs and thus over-investment is not necessary. While there are some 'world prices' for commonly available equipment with multiple suppliers (such as cyclotrons), the overall price of any facility depends strongly on the economic cycle (e.g., raw materials costs) on the location (which affects land and labour prices). Therefore, while some intercomparison between facility prices around the world is possible, the investment required for any proposed CANS facility must be individually calculated. Some of the aspects that decision makers often require to be addressed in such a project are outlined below:

(a) *Financial feasibility* – One tool available for financial feasibility analysis of such prospective investments is UNIDO's COMFAR [248], which offers discounted cash flow modelling and classical financial measures such as net present value. This modelling provides initial capital and operational budget estimates. It can also be used to model

different funding models, such as joint ventures between private corporations and government funding sources.

(b) *Macroeconomic feasibility* – A common approach to justify government investment for non-profit-making ventures to measure the macroeconomic value of activities is by input–output modelling. Examples of research facilities and activities where input-output modelling has been used to justify investment include TRIUMF [249] in Canada and fusion research in the UK [250]. A free extended input–output modelling tool called EMPACT is currently being developed within the IAEA.
IAEA has developed teaching cases for both COMFAR and EMPACT to assist in financial and economic feasibility analysis for accelerator projects.

(c) *Socio-economic justification* – The OECD Global Science Forum has several reports on socio-economic justification and optimization of major research infrastructure that may be consulted when developing arguments for a CANS [252–254].

5.3. OPERATIONAL ASPECTS

The radioactive inventory of a CANS is much less than that of a research reactor of comparable performance. The amount and diversity of produced radioactive isotopes is very restricted and confined in the comparatively small target. Depending on the power level, the demands for cooling, shielding and component handling may be more relaxed.

There is no nuclear fuel involved, so there is no risk of a criticality incident. At CANS, the radioactive inventory in secondary structures like shielding is also much less than in big and very powerful facilities. Compared to a research reactor this results in less waste, easier handling and reduced disposal (long term storage) cost; in particular, there are no long-lived actinides.

Small CANS, and even big spallation neutron sources, are not considered nuclear installations by law in some countries. Security management thus poses smaller challenges than at research reactors, while, at the same time, requirements on nuclear reactors keep increasing. The demands on highly qualified operational teams are smaller, including their education and licensing for shift crews.

In the case of a commercial accelerator used as a CANS, the reliability is high, and the maintenance costs are well known.

5.4. USERS' PERSPECTIVES

Easy and fast access is a key strength of CANS facilities. This is particularly useful under several perspectives; CANS are the perfect test bed for experiments, which can later be more efficiently performed at high-flux neutron sources, where access is more difficult as availability is at a premium. The lower security requirements in a CANS facility compared to those of a research reactor (Section 5.3) may also ease access for students from abroad.

With (small) moderators and instruments simultaneously optimised to one purpose, overall radiation levels can remain low, and hands-on experiments are possible that cannot even be thought of at larger, more powerful facilities.

Fast and low-threshold access is also important for industrial use. This applies in particular to local, small and medium size enterprises, which would not so easily travel to a big source. Short turn-around times from proposal to results is often most important for such businesses.

With easy hands-on access, moderator and instrument developments are most efficiently done at a small source. The same applies to general development of methods. Given the intrinsic flexibility and upgradability of CANS, any such installation also offers significant prospects for growth (the advantages of modularity described in Sections 5.1 and 5.2). Starting from one target station and only a few instruments, the incident particle beam can be multiplexed to a second target, possibly with a different time structure, and the whole chain optimized for new and additional applications.

There are even applications, where CANS offer opportunities, which appear (almost) in principle not accessible at large installations: having more than one target station relatively close to one another permits the intersection of neutron beams at large angles on one sample. This could be of particular value when the two neutron beams differ significantly in their time structure, spectra, or when a sample exhibits strong asymmetries.

For specific applications, CANS might be dedicated to and supported by purely commercial activities, as shown for commercial irradiation purposes of electronic systems (see Section 3.1.2), on-site production of radioisotopes for medical purposes (Section 3.2), or industrial neutron imaging[7].

5.5. OTHER ADVANTAGES

General public acceptance, at least in some parts of the world, make it hard to build new research reactors. With accelerator driven sources, ‘neutron physics’ and ‘neutron use’ can be decoupled from ‘nuclear reactors’ in the perception of the public. Compared to a research reactor there are several advantages regarding hazards:

- No uncontrolled chain reaction or criticality accident is possible;
- After the Fukushima-Daichi accident, greater focus has been placed on seismic hazard for all reactors: beam tubes that penetrate the biological shield in research reactors represent one possible source of a major loss of coolant accident. Decay heat from the targets in CANS do not lead to the same kinds of risks as in the case of nuclear fuels in research reactors as the source term for the worst case scenario accident for a typical CANS is much more limited;
- There is no spent fuel as nuclear waste.

The risk for an accident at any scale is comparable to that at other industrial facilities, but usually significantly smaller than at any chemical plant.

5.6. LIMITATIONS

The highest power CANS are likely to be based around proton or deuteron linacs (Section 4.1.5). These are currently limited to about 100 mA current. Most currently operating CANS have nominal primary neutron yields on the order of 10^{12} to 10^{14} n/s. This is at least an order of magnitude below medium and high flux reactors and spallation based neutron sources. The main limitation to increasing the neutron yield and reaching higher neutron production is the

[7] https://phoenixwi.com/neutron-radiography/

thermal load on the target. Increasing the power of the beam increases the number of released neutrons but the target has to withstand the increased heat load. Using water cooled systems, engineering limitations set a limit of ~500 W/cm^2 on solid targets. A solution can be liquid targets as used at the SARAF facility with a liquid Li or Ga target aiming for a neutron yield of 10^{15} n/s [254]. Another solution discussed is micro fluidic cooling which has been shown to allow cooling power of several kW/cm^2 [255]. Such systems are under development at various projects aiming to achieve a neutron yield at the target in the order of 10^{15} n/s [256, 257].

6. REGULATORY ASPECTS

6.1. REGULATING ACCELERATORS

Accelerators are devices that can produce nuclear reactions. The hazard encountered will depend on the energy and type of the accelerated particles and target. An assessment of the hazard created will provide the baseline requirements for the operation of the accelerator. The operator of the accelerator will have to implement mitigation measures to ensure safe operation of the accelerator. This section will be subdivided into two kinds of operation: accelerators within a facility, and accelerators in the field. Other aspects of regulating accelerators will be discussed in the final subsection.

6.1.1. Fixed accelerator within a facility

This subsection considers an accelerator that is a fixed device within a facility, which is by far the most common scenario. For the purpose of this report, we will consider that the accelerator is able to produce prompt gamma and neutron radiation and as such the facility has to encompass safety measures to protect the workers and the people around the accelerator.

The facility will typically require shielding that will reduce the radiation (γ and neutron) to an acceptable level in accordance with the ALARA principle. Depending on the Member State, the acceptable level may have been specified in the regulatory regime. In order to determine the shielding needed, the worst-case scenario of operation has to be considered. With this information, the operator will be able to select the shielding type and thickness required for the safe operation of the accelerator (within the safe regulatory specific dose level). All types of radiation (direct, scattering, leakage, activated material) produced by the accelerator need to be considered, and the facility shielding designed appropriately. The facility design also needs to take into account the dose rate coming from any access point (staff access or service ducts).

In addition to the facility shielding, the operator has to consider the necessary safety systems for the operation of the accelerator in a facility. The following safety systems for such a facility:

- Access control interlock which will terminate operation if the accelerator room is accessed;
- Emergency stop system to terminate unwanted operation;
- Area monitoring devices to measure radiation levels around the facility;
- Last-person-out system to ensure nobody is left in the accelerator room;
- Operation display (beam On or Off).

Over its lifetime, a facility will undergo the following stages:

- A planning phase where the design and location of the facility, how it may be constructed, operated and decommissioned are all considered.

which leads to the following stages which often require separate licencing approval:

- A construction phase where the final design of the facility is built;
- A commissioning phase where the facility's expected performance and behaviour will be validated through radiation surveys and safety system function tests;
- An operation phase for routine operation including routine maintenance;
- A decommissioning phase.

6.1.2. Mobile accelerators

In the case of an accelerator operated outside of a facility, there is typically no external shielding involved. However, depending on the hazards produced, additional mitigation measures need to be considered, including:

- Temporary physical barriers to limit access to the irradiation area with clear indications at the boundary that there is a high level radiation field (e.g., warning signs);
- Portable shielding, if feasible;
- Audible or visible alarm, or status indicator, to notify workers and the general public around the accelerator of operations;
- Operator oversight of field operations.

6.2. OPERATING PROCEDURES

For the two type of accelerators, operating procedures need to be developed. The procedures need to describe:

- Routine operation including the operating conditions;
- Radiation hazard mitigation measures taken;
- Mitigation measures for any other hazards (fire, chemical, electrical);
- Any anticipated non-routine operation;
- Any personnel dose monitoring (direct or indirect monitoring);
- Any area dose monitoring;
- Training of users and operators;
- Frequency of radiation survey;
- Frequency and method of testing the safety systems.

In addition, mobile accelerators have no engineered access controls; therefore, a procedure describing the level of supervision required for safe operation of the accelerator is very important (e.g., defined operator responsibilities and multiple staff overseeing the barriers, if necessary).

To complete the list of procedures, any servicing of the accelerator or the facility need also to be documented. This procedure needs to provide details on the protection required for servicing and any limitations on servicing.

6.3. NATIONAL EXAMPLE: ARGENTINA

Nuclear activity in Argentina is regulated by the National Regulatory Authority (ARN) that directly reports to the National President office. ARN has established a set of norms which users and developers of CANS need to consider [258], even though there is no explicit and specific treatment for these devices or the facilities that house them (cf. the case for fission reactors).

The first norm to consider is the Basic Norm of Radiological Safety (Norma AR 10.1.1., Rev. 4 [259]). This gives the general framework for radiation protection and nuclear safety. For example, it:

(a) Classifies particle accelerators as Class I or Class II facilities depending on characteristics;
(b) Classifies irradiation plants and radioactive source production plants as Class I facilities;

(c) Classifies as Class II facilities the following: facilities that use radiation sources in the oil industry and well profiling, nuclear medicine facilities, and facilities that use radiation sources for calibration and verification;
(d) Establishes dose limits to workers: 20 mSv/y effective dose (averaged over 5 y with a maximum below 50 mSv for a single year); 20 mSv/y equivalent dose to the lens of the eye (averaged over 5 y with a maximum below 50 mSv for a single year); 500 mSv/y equivalent dose to skin or extremities;
(e) Establishes dose limits to general public: 1 mSv/y effective dose; 15 mSv/y equivalent dose to the lens of the eye; 50 mSv/y equivalent dose to skin or extremities;
(f) Establishes the definition of 'non routine practice' which can be used for testing (especially in the development stages).

One needs to follow Licencing of Class I facilities (Norma AR 0.0.1., Rev. 2 [260]) which, on top of the above mentioned, includes Class I particle accelerators with energy above 1 MeV (other than those for medical purposes). This puts almost all CANS in this class, regardless of the application, except for small neutron generators. The norm enumerates several steps, aspects, and criteria for the complex licencing of Class I facilities, for instance: (a) licence to construct; (b) licence to operate; (c) licence to commission; and (d) licence to decommission. Conversely, Class II facilities only require a licence to operate. Electron linacs for medical (clinical) purposes with energies between 4 and 40 MeV are considered in 'Operation of Linear Accelerators for Medical Use' (Norma AR 8.2.2., Rev. 1 [261]) which considers special aspects of clinical applications. Class I accelerator facilities are also regulated by 'Worker Exposure in Class I Particle Accelerators' (Norma AR 5.1.1., Rev. 1 [262]) which provides specific requirements, as well as some non-radiological aspects (such as protection from high voltages).

A paradigmatic case in Argentina is the CNEA project for the Accelerator Based BNCT facility and Accelerator Development Laboratory in Constituyentes Atomic Center. The associated facility and accelerator, which are in the building stages, has been classified as Class I and, therefore, complete licencing is a multi-step process that is still ongoing. 'Nonroutine practice' permissions have been obtained for testing at different stages of the accelerator development.

7. COST CONSIDERATIONS

This section deals with the capital, operating, and decommissioning costs of CANS, the targets and moderators, instruments, and support infrastructure.

7.1. CAPITAL INVESTMENT

For a typical CANS facility, the basic investment costs mainly comprise the accelerator system including the ion source, the TMR assembly, the various instruments optimized to the source, and the building and infrastructure investment. Depending on the size and power of the installation, total investments may range from a few million Euros to several hundred million Euros. The cost also strongly depends on options to reuse existing equipment, buildings and infrastructure. A rough overview of the costs of individual components is given in the following paragraphs. The costs given in the conceptual design reports for NOVA ERA and HBS may also prove useful [4, 6, 257].

7.1.1. Accelerator costs and availability

One of the key elements of a CANS is the accelerator. There are several suppliers of electron linacs. There are also commercially available proton accelerator technologies which provide CW proton beams, such as cyclotrons or electrostatic accelerators. As these latter accelerators usually operate in CW mode with relatively low peak currents, they are less efficient than pulsed proton linear accelerators. Commercial systems with low energies up to some 10 MeV and currents up to ~1 mA, are usually below 10 million Euros.

For high peak current, pulsed proton beam accelerators with beam energies of 25 MeV or more, the cost scales more or less linearly with the proton energy. With respect to the accelerator current however, the cost does not scale linearly, as a high power accelerator with high peak current is technically more challenging to build. Typically, the cost of a pulsed proton linac is in the region of 1–1.5 million Euros per MeV (Section 4.1.5.3). Hence, such kinds of pulsed accelerator systems are in the 10–100 million Euro range of investment [3]. An overview is given in Table 11.

7.1.2. Target – Moderator – Reflector (TMR) monolith

The TMR, which is surrounded by biological shielding, has to be optimized for the needs of the experiments expected to be performed at the CANS. The shielding will scale with the power of the target and the released radiation. The overall power of the target system will also require the installation of auxiliary equipment such as cooling systems and handling tools for activated material. Based on these requirements the cost of a TMR assembly can vary between a few hundred thousand Euros up to ca. 3 million Euros [3].

7.1.3. Neutron instruments

Instruments for neutron scattering at a CANS will mostly follow designs similar to time-of-flight instrument designs at spallation neutron sources such as ISIS (UK), SNS (USA), J-PARC (Japan), or ESS (Sweden). An advantage of a CANS is that the source will be tuned to the instruments' needs. Hence, the need for T_0 and pulse shaping choppers, which modify the properties of a given TMR assembly, will be reduced. The length of the instruments can also be reduced if the source is optimized for the instruments' resolution. This can be expected to

lead to savings in optics and shielding costs. Instruments for neutron imaging or prompt gamma activation analysis will be less costly than time-of-flight spectrometers and diffractometers.

TABLE 11. APPROXIMATE COSTS FOR THE ACCELERATOR COMPONENTS OF A CANS FACILITY – ADDITIONAL COSTS ARE REQUIRED FOR TARGETS, MODERATORS AND INSTRUMENTS

Source type	Energy [MeV]	Yield n/s	Time structure	Investment cost [M USD]	Availability
DD, DT generators	0.01–0.3	10^6–10^{10}	CW or pulsed	0.05–0.5	Commercial companies
DD, DT electrostatic	0.2–0.3	10^{11}–10^{14}	CW	0.05–5	Commercial companies
Electrostatic accelerator	2–10	10^{12}–10^{14}	CW or pulsed	1–10	Commercial companies
Cyclotron	13–70	10^{11}–10^{14}	CW	1–30	Commercial companies
Electron accelerator	3–200	10^{11}–10^{15}	CW or pulsed (short)	5–50	Commercial companies
Proton Linac (P<10kW)	3–100	10^{11}–10^{13}	CW or pulsed	1–5	Commercial companies
Proton Linac (P>10kW)	3–100	10^{14}–10^{15}	CW or pulsed	3–100	R&D laboratories
Laser	-	10^{11}–(10^{13})	Pulsed (very short)	10–100	R&D laboratories

As the counting efficiency of most instruments scales with the coverage of the detectors (except for SANS, reflectivity, imaging) installation of a detector system can be quite expensive. Little progress has been made in reducing the cost of neutron detectors in the last 20 years. However, the boron detector technology developed for ESS may eventually reduce the costs of neutron detectors slightly, if this technology is commercialised [263]. An overview of the modern neutron detector technology for many applications, including neutron scattering, is given in Ref. [140].

As a rule of thumb, the cost of a neutron scattering instrument at a CANS can be expected to be lower than at other pulsed neutron sources, but only by 30–50% at most. Additional savings could be made by focussing the purpose of the instruments on a CANS with the possible benefit of improved performance, although this would be with reduced functionality; e.g., lower resolution, no polarization. As a result, the cost of an instrument may lie in the range 0.5–7 million Euros [257], depending on its complexity.

7.1.4. Common buildings and support infrastructure

Overall, there are 5 main parts of buildings to be provided for a CANS:

- Accelerator building including support systems;
- TMR-shielding unit;
- Experimental / Instrument area;

- Auxiliary buildings for infrastructure such as pumping systems, electronic bays, control rooms, cooling tower;
- Office building.

The required area for all buildings depends heavily on the facility being built. The space required for instruments can best be estimated by examining analogous instruments elsewhere, and Refs [3, 6, 10] provide some guidance. Additional space for laboratories, workshops and workspaces have to be added.

In addition, special requirements have to be taken into account regarding radiation shielding and safety at the buildings in particular regarding the accelerator system and the TMR monolith. For handling of activated components during operation, special rooms and equipment will have to be foreseen. To handle shielding components or other parts of higher weight appropriate cranes and storage areas will have to be provided.

As construction costs will vary drastically between countries and regions, as an order of magnitude estimate one may calculate the same amount of investment for buildings and infrastructure as for technical equipment foreseen (accelerator, target, instruments).

7.2. OPERATIONAL COSTS

The estimation of operation costs based on comparisons to existing facilities is difficult since what is included in reported costs from other facilities may be unclear, and costs vary substantially from one country to another. A rough estimate leads to the assumption that the annual operational costs of a facility is often on the order of 4% of the initial capital investment for the facility. An estimate can be made regarding the annual operational costs of an individual instrument as 0.2% of the initial investment [5]. Taking these numbers for a larger CANS based neutron facility operating 20 instruments would lead to total operational costs on the order of 8% of the initial investment, with half of the cost being dedicated to the source operation and half of the cost used to run the suite of instruments.

7.2.1. Electricity costs

Electricity costs for a CANS are rather limited as the accelerator energy remains low. The typical requirement is a few hundred kW up to a few MW for the most ambitious sources. This is incommensurate compared to the electrical costs of spallation sources. Total electrical demand scales with the planned operation time, although some systems consume power even when the CANS is not operating. In addition, the installed instruments and target will consume electricity for cooling, heating and vacuum requirements, which can be of the same order as the consumption of the accelerator.

As the costs of electricity per kWh vary substantially between different countries, a generic cost estimate is very difficult. Again, reference to the electrical demand of existing accelerator installations and laboratories (kWh/year) are often a reliable basis to calculate costs based on local unit costs of power.

Guidance regarding the specific electrical costs for the operation of neutron generators, cyclotrons, and electron linacs are given in Sections (4.1.1.2), (4.1.2.3) and (4.1.3.3), respectively.

7.2.2. Staffing requirements for operation

The size of the staff required for operation depends strongly on the size of the facility and the planned operational time; e.g., if a 24/7 operation as a national or international user facility is considered, the number of staff operating the accelerator, the instruments, and on duty service at the facility may double or triple compared to a site-specific (e.g. university) facility only in operation during standard working hours. On a medium flux source providing services to users, it can be considered that the support at each instrument might consist of 2 instruments scientists, 1 technician and 1–2 person-year from the general support (radiation safety, administration, electronics, computing…). At a larger facility, staff requirements for radiation safety, maintenance and administrative issues need to be taken into account that are not necessary at a small CANS; e.g., at a university level.

Hence, for a small university based CANS, only a few people are necessary to operate the facility, likely in the range of 4–10, depending on the number of instruments to be installed, while for a large user facility with standard user service up to 100 staff or more may be required.

It is frequently better to take staffing plans from other facilities and cost them locally. However, a basic estimation can be given using comparative figures of operational costs of existing sources during early stages of planning.

7.3. DECOMMISSIONING COSTS

When performing a financial feasibility analysis for a neutron source, there is a potentially large cost at the end of life in the form of decommissioning costs that need to be accounted for during the project proposal and development stages (Section 5.2).

Unlike a research reactor, decommissioning a typical CANS does not involve disposal of spent fuel or fissionable material waste, which considerably reduces the costs and uncertainties of decommissioning. In common between CANS and research reactors is a volume of activated material, including device components and shielding. Waste separation reduces the volume of material that is to be transferred to a radioactive waste facility, and allows for resale of non-radioactive, high value components, such as copper piping, partially offsetting the costs.

Decommissioning needs to be considered during facility design, as the volume of activated materials, and therefore, the costs, can be minimized by the appropriate choice of technologies, construction materials, and local shielding: the choice of accelerated particle can make a difference; e.g. proton cyclotrons produce more internal activation than cyclotrons accelerating H^- ions, and linacs accelerating protons rather than deuterons typically become less activated over time.

The preliminary decommissioning plan, developed during the planning stage before construction, is typically refined during the active lifetime of the facility. The desired end-state is usually defined well ahead of time (i.e. as part of the decommissioning plan) and budgeted for. The end state may be to create a condition that is as close as possible to that which existed before the facility was built or to repurposing the site for a new use (e.g. a new facility).

The IAEA recently issued a report dedicated to the issue of decommissioning particle accelerators and divided them into different classes based largely on accelerating energy [247]. Most of the CANS technologies discussed in Ref. [247] would fit into its definition of Class 1 or Class 2 facility. The typical activation products, their locations, and activity concentrations

are identified and listed in this report. Ref. [247] also provides methods for how to go about estimating the cost of such activities based on costing components of a work breakdown structure; some component estimates may be provided by outside experts. A staged approach to decommissioning will often be chosen for a CANS, allowing for decay of some relatively short-lived activation products. Deferred decommissioning also allows for spreading out the expenditure required into a greater number of smaller cash flows (Section 5.2).

A detailed report [264], issued by the European Commission, gives decommissioning experience at a variety of accelerators, and provides an overview of sources of activation, technologies available for decommissioning, and detailed ways of making estimates of costs and volumes of materials generated, including waste.

7.4. NATIONAL EXAMPLES OF INVESTMENTS

7.4.1. Investments in Argentina

Nuclear activity in Argentina is strongly biased towards fission reactors and focussed on the National Atomic Energy Commission (CNEA). Other areas like medical applications of nuclear energy have a considerable share. Activities concerning CANS struggle to find substantial support.

A paradigmatic case is the project of CNEA for the development of an accelerator based BNCT facility and accelerator laboratory in Constituyentes Atomic Center, including the design and construction of a 100% locally made electrostatic quadrupole accelerator (see Section 4.1.4.1 and Refs [147, 149]). After substantial efforts from the Department of Accelerator Technologies, it is reaching the final construction stage. In fact, this initiative, mainly supported by CNEA is the first effort to initiate a systematic activity in the development of accelerator technology in Argentina. There is no other such integral approach to CANS in the country. Nevertheless, a few groups are found that are working on topics that can be associated with CANS. Then, there is a 25 MeV linac at Bariloche Atomic Center that began operations at the end of the 1960s and was extensively used by neutron physics groups until reaching its useful life span more than forty years later. Since the start of the 2010s, there have been important efforts by the Neutron Physics Department in Centro Atómico Bariloche to replace it without yet reaching that goal [265, 266].

Available investment comes from a mix of federal government funding opportunities: grants for research and development assigned to researchers; funding for overall institutional operations and projects; fellowships and permanent positions in institutions covering human resources. This investment is mainly channelled through federal offices and agencies. The most relevant are the National Council for Science and Technological Research (CONICET), the National Agency for Promoting Science, Technological Development and Innovation (Agencia I+D+i) and CNEA. The first two are currently under the Ministry of Science, Technology and Innovation and the last one under the Secretary of Energy of the Ministry of Economy.

Private investment is negligible and largely limited to the purchase of devices or renting of services. Recent development in oil industry projects may increase private participation via demand for nuclear technology in diagnostics at oil facilities [19]. In addition, the projected demand for diagnostic and therapeutic nuclear medicine, which will require new production facilities (Section 3.2), might also boost interest in CANS. Finally, there also exist collaborations with groups from foreign countries and support from international institutions

that can favour access to a variety of resources from acquisition of equipment to training of human resources.

7.4.2. Investments in the Republic of Korea

In the Republic of Korea, neutron research and application has been performed with the 30 MW_{th} HANARO research reactor at the Korea Atomic Energy Research Institute since 2005, whose construction started in 1995. HANARO has been successfully used for neutron science, imaging, medical and industrial isotopes production, materials irradiation testing, and so on, until its temporary shutdown in 2014. Recently, due to increased industrial demand, neutron production based on the 100 MeV pulsed proton linac, KOMAC, for soft error testing of semiconductor devices has begun (see Section 3.1.2.2).

In order to continue neutron research with the restart of HANARO and increasing demand in the industrial, defence and medical sectors, the Korea CANS (better known as KCANS) was established to share information and encourage collaboration by holding several meetings since 2016. Currently, about 50 members are showing their interest in neutron research, its application as well as in neutron source development.

Recently, several projects are on-going or being proposed for new neutron source developments at the existing accelerators, industrial applications of DD neutron sources, and broadening the applications of HANARO have been submitted to, or prepared for, the government:

(a) In 2020, a 30 MeV cyclotron based neutron source and on-site neutron imaging development started at KAERI. The main objectives are to develop the TMRS for a 30 MeV cyclotron to produce over 10^{12} n/s, and to provide user service for imaging.
(b) An upgrade project proposal for the 100 MeV linac of KOMAC to 200 MeV is being prepared for soft error testing, which includes proton and high energy neutron irradiation in two separated target rooms.
(c) On-site application of neutrons from sources such as DD generators, cyclotrons, or linacs for the development of a nuclear fuel examination system.

Also, a proton accelerator based BNCT facility (A-BNCT) is under development in which neutrons are produced from a Be target and a 10 MeV (80 kW max.) proton beam. The project was launched in 2016 by a consortium initiated by a private company with a medical school and a large hospital, and several institutes' groups under government support. The accelerator and the dedicated building has been constructed, and low power operation testing and tuning are almost finished.

Currently, the shift from government-oriented investment to joint ventures including public-private partnerships for industrialization is beginning, as in other countries (Section 5.2).

8. SUMMARY AND CONCLUSIONS

As the number of research reactors is declining around the world, the number of neutron sources is dwindling. Historically, large spallation sources have been the main competition for research reactors for neutron beam research.

On the other hand, over the years, a variety of accelerators that do not use spallation as the neutron producing reaction have served as CANS, although their power has been limited to date. Recently, due to developments in a variety of accelerator technologies, it has become apparent that CANS have the potential to provide not only local sources of neutrons (e.g. for a large research university), but may also be competitive with research reactors as national sources for certain neutron beam techniques and applications. This potentially opens up neutron beam techniques to countries for which building a research reactor is not considered an option, and for which the costs or complexity of building and operating a spallation source remain out of reach.

In addition to neutron beam research, there are a number of other applications of CANS. For example, at the moment, there is a resurgence in the interest in accelerator based BNCT. This is driving the development of several high current electrostatic CANS that can also be of interest to the neutron beam community. As has been the case with research reactors, there is the possibility of building CANS with a mixed mandate; e.g. for materials research as well as applications in BNCT, which may be helpful in maintaining continuous operating funding in the longer term.

Finally, there have been developments in the larger spallation sources that are of relevance to CANS. The increases in proton current in the low energy sections of high powered linear accelerators that have been developed for the large modern spallation sources and the IFMIF-DONES materials damage facilities for fusion may benefit larger CANS sources based around proton linacs that are being considered as candidates for national neutron scattering facilities.

Due to the variety of possible accelerator technologies, the size and cost of building a CANS facility can be chosen to suit the mandates and budgets of individual research institutions within a country. When compared to the alternative of building a research reactor, the lower decommissioning liabilities, generally lower licensing and security requirements (and corresponding easier access), combined with a lack of public opposition to accelerators are making CANS attractive as neutron sources in many countries. It is hoped that this publication may be useful when such projects are being considered.

REFERENCES

[1] INTERNATIONAL ATOMIC ENERGY AGENCY, Research Reactor Database (RRDB) (2021), https://nucleus.iaea.org/RRDB/RR/ReactorSearch.aspx.

[2] GAROBY, R., et al., The European Spallation Source design, Phys. Scr. **93** (2018) 014001.

[3] JOINT INSTITUTE FOR NUCLEAR RESEARCH, Frank Laboratory of Neutron Physics (2021), http://flnph.jinr.ru/en/facilities/ibr-2.

[4] MAUERHOFER, E., et al., Conceptual Design Report NOVA ERA (Neutrons Obtained Via Accelerator for Education and Research Activities) A Jülich High Brilliance Neutron Source project, Vol. 7, Forschungszentrum Jülich, Jülich (2017).

[5] LEAGUE OF ADVANCED EUROPEAN NEUTRON SOURCES, LENS Report: Low Energy Accelerator-driven Neutron Sources, LENS Ad-hoc Working Group CANS Nov. 2020 (2020).

[6] RÜCKER, U., The Jülich high-brilliance neutron source project. Eur. Phys. J. Plus **131** (2016) 19.

[7] INTERNATIONAL ATOMIC ENERGY AGENCY, Interactive Map of Accelerators (2021), https://nucleus.iaea.org/sites/accelerators/Pages/Interactive-Map-of-Accelerators.aspx.

[8] DRESDEN TECHNNOLOGY TRAINING PORTAL (2021), https://dresden-technologieportal.de/en/equipment/view/id/1472.

[9] INTERNATIONAL ATOMIC ENERGY AGENCY, Seibersdorf Laboratories (2021), https://www.iaea.org/about/organizational-structure/department-of-nuclear-sciences-and-applications/seibersdorf-laboratories.

[10] INTERNATIONAL ATOMIC ENERGY AGENCY, Introduction to Neutron Scattering with Low and Medium Flux Neutron Sources. IAEA TECDOC No. 1961, IAEA, Vienna, (2021).

[11] INTERNATIONAL ATOMIC ENERGY AGENCY, Interactive Map of Neutron Beam Instruments (2021), https://nucleus.iaea.org/sites/accelerators/Pages/Interactive-Map-of-NB-Instruments.aspx.

[12] EUROPEAN STRATEGY FORUM ON RESEARCH INFRASTRUCTURES, Neutron scattering facilities in Europe Present status and future perspectives, Vol. 1, Dipartimento di Fisica–Università degli Studi di Milano, Milan (2016).

[13] WATSON, G., Neutron Compton scattering, J. Phys. Condens. Matter **8** (1996) 5955–5975.

[14] ISIS NEUTRON AND MUON SOURCE, Vesuvio (2008), https://www.isis.stfc.ac.uk/Pages/vesuvio.aspx.

[15] SCHLUMBERGER, Log Interpretation Principles/Applications. Schlumberger Wireline & Testing (1991).

[16] ELLIS, D.V., SINGER, J.M. (Eds.), Well Logging for Earth Scientists. 2nd Edn, Springer, Dordrecht, The Netherlands (2007).

[17] MONDOL, N.H., "Well logging: principles, applications and uncertainties", Petroleum Geoscience (BJØRLYKKE, K. Ed.), Springer, Berlin, Heidelberg (2015).

[18] ROSE, D., et al., "An innovative slim pulsed neutron logging tool", Society of Petrophysicists and Well Log Analysts, 56th Annual Logging Symp. Long Beach, California, USA (2015).

[19] HERRERA, M.S., et al., Detectability of smart proppants traced with gadolinium and samarium in the Vaca Muerta formation, J. Petrol. Sci. Eng. **179** (2019) 312–320.

[20] INTERNATIONAL ATOMIC ENERGY AGENCY, Neutron Generators for Analytical Purposes, Radiation Technology Reports No. 1, IAEA, Vienna (2012).
[21] INTERNATIONAL ATOMIC ENERGY AGENCY, Neutron Imaging: A Non-destructive Tool for Materials Testing, IAEA TECDOC No. 1604, IAEA, Vienna (2008).
[22] OLIVEIRA, G.J.R., et al., Probing the 3D molecular and mineralogical heterogeneity in oil reservoir rocks at the pore scale, Sci. Rep. **9** (2019) 1–10.
[23] MARTINS, R.M., et al., Dinosaur and crocodile fossils from the Mesozoic of Portugal: neutron tomography and synchrotron-radiation based micro-computed tomography, Mater. Res. Soc. Symp Proc. **1319** (2011) Mrsf10-1319-ww02-03.
[24] ZHANG, P., et al., Neutron imaging of water penetration into cracked steel reinforced concrete, Physica B: Condens. Matter **405** (2010) 1866–1871.
[25] PERFECT, E., et al., Neutron imaging of hydrogen-rich fluids in geomaterials and engineered porous media: a review, Earth Sci. Rev. **129** (2014) 120–135.
[26] WARREN, J.M., et al., Neutron imaging reveals internal plant water dynamics, Plant Soil **366** (2013) 683–693.
[27] NAKANISHI, T.M., MATSUBAYASHI, M., Nondestructive water imaging by neutron beam analysis in living plants, J. Plant Physiol. **151** (1997) 442–445.
[28]TAYLOR, M., et al., Thermal neutron radiography using a high-flux compact neutron generator, Phys. Procedia **88** (2017) 175–183.
[29] MANKE, I., et al., Characterization of water exchange and two-phase flow in porous gas diffusion materials by hydrogen-deuterium contrast neutron radiography, Appl. Phys. Lett. **92** 24 (2008) 244101.
[30] KARDJILOV, N., et al., Three dimensional imaging of magnetic fields with polarized neutrons, Nat. Phys. **4** (2008) 399–403.
[31] KIYANAGI, Y., SATO, H., KAMIYAMA, T., SHINOHARA, T., A new imaging method using pulsed neutron sources for visualizing structural and dynamical information, J. Phys. **340** (2012) 012010.
[32] SCHILLINGER, B., CRAFT, A., Epithermal neutron radiography and tomography on large and strongly scattering samples, Mater. Res. Forum **15** (2020) 142–148.
[33] CARREL, F., et al., Characterization of old nuclear waste packages coupling photon activation analysis and complementary non-destructive techniques, IEEE Trans. Nucl. Sci. **61** (2014) 2137–2143.
[34] SARI, A., CARREL, F., LAINÉ, F., Characterization and optimization of the photoneutron flux emitted by a 6- or 9-MeV electron accelerator for neutron interrogation measurements, IEEE Trans. Nucl. Sci. **65** (2018) 2539–2546.
[35] SKALYGA, V.A., et al., A powerful pulsed “point-like” neutron source based on the high-current ECR ion source, Rev. Sci. Instrum. **91** (2020) 013331.
[36] BIRJUKOVS, M., et al., Argon bubble flow in liquid gallium in external magnetic field, Int. J. Appl. Electromagnet. Mech. **63** S1 (2020) S51–S57.
[37] SATO, H., KAMIYAMA, T., KIYANAGI, Y., A Rietveld-type analysis code for pulsed neutron Bragg-edge transmission imaging and quantitative evaluation of texture and microstructure of a welded α-iron plate, Mater. Trans. **52** (2011) 1294–1302.
[38] PEETERMANS, S., et al., A new transmission based monochromator for energy-selective neutron imaging at the ICON beamline, Nucl. Instrum. Methods Phys. Res. A **757** (2014) 28–32.
[39] LEHMANN, E., et al., The energy-selective option in neutron imaging, Nucl. Instrum. Methods Phys. Res. A **603** (2009) 429–438.

[40] SATO, H., et al., Relation between Vickers hardness and Bragg-edge broadening in quenched steel rods observed by pulsed neutron transmission imaging, Mater. Trans. **56** (2015) 1147–1152.
[41] SHINOHARA, T., et al., The energy-resolved neutron imaging system, RADEN, Rev. Sci. Instrum. **91** (2020) 043302.
[42] KIYANAGI, Y., Neutron imaging at compact accelerator-driven neutron sources in Japan, J. Imaging **4** 4 (2018) 55.
[43] KAMIYAMA, T., et al., Sliced neutron tomography using neutron resonance absorption spectrometer, Nucl. Instrum. Methods Phys. Res. A **600** (2009) 107–110.
[44] SCHILLEBEECKX, P., et al., Neutron resonance spectroscopy for the characterization of materials and objects, J. Instrum. **7** (2012) C03009.
[45] KIYANAGI, Y., et al., Pulsed neutron imaging using 2-dimensional position sensitive detectors, J. Instrum. **9** (2014) C07012.
[46] ORGANIZATION FOR ECONOMIC COOPERATION AND DEVELOPMENT–NUCLEAR ENERGY AGENCY, Working Party on International Nuclear Data Evaluation Cooperation (2017), https://www.oecd-nea.org/science/wpec/.
[47] PLOMPEN, A., et al., The NEA high priority nuclear data request list for future needs, (Int. Conf. Nucl. Data for Science and Technology, Nice, France, 2007), EDP Sciences (2008) 765–768.
[48] GRAND ACCÉLÉRATEUR NATIONAL D'IONS LOURDS, NFS – Neutrons for Science (2021), https://www.ganil-spiral2.eu/scientists/ganil-spiral-2-facilities/experimental-areas/nfs/.
[49] MYRRA, Multi-purpose hYbrid Research Reactor for High-tech Applications (2021), https://myrrha.be/.
[50] BEYER, R., et al., Characterization of the neutron beam at nELBE, Nucl. Instrum. Methods Phys. Res. A **723** (2013) 151–162.
[51] KÄPPELER, F., et al., The *s* process: nuclear physics, stellar models, and observations, Rev. Mod. Phys. **83** (2011) 157.
[52] ARNOULD, M., GORIELY, S., TAKAHASHI, K., The *r*-process of stellar nucleosynthesis: astrophysics and nuclear physics achievements and mysteries, Phys. Rep. **450** (2007) 97.
[53] ARNOULD, M., GORIELY, S., The *p*-process of stellar nucleosynthesis: astrophysics and nuclear physics status, Phys. Rep. **384** (2003) 1.
[54] SCHATZ, H., et al., *rp*-process nucleosynthesis at extreme temperature and density conditions, Phys. Rep. **294** (1998) 167.
[55] HARISSOPULOS, S.V., Cross-section measurements of capture reactions relevant to *p*-process nucleosynthesis, Eur. Phys. J. Plus **133** (2018) 332.
[56] BELGYA, T., MOLNÁR, G., YATES, S.W., Analysis of Doppler-shift attenuation measurements performed with accelerator-produced monoenergetic neutrons, Nucl. Phys. A **607** (1996) 43.
[57] WISSHAK, K., et al., The Karlsruhe 4π barium fluoride detector, Nucl. Instrum. Methods Phys. Res. A **292** (1990) 595–618.
[58] WINTERBON, K.B., An analytic theory of Doppler-shift attenuation, Nucl. Phys. A **246** (1975) 293.
[59] UNIVERSITY OF KENTUCKY ACCELERATOR LABORATORY, University of Kentucky Accelerator Lab Home (2021), http://www.pa.uky.edu/accelerator/index.php.

[60] ARIMA, A., OHTSUKA, T., IACHELLO, F., TALMI, I., Collective nuclear states as symmetric couplings of proton and neutron excitations, Phys. Lett. **66B** (1977) 205.
[61] OTSUKA, T., ARIMA, A., IACHELLO, F., TALMI, I., Shell model description of interacting bosons, Phys. Lett. **76B** (1978) 139.
[62] MOLNÁR, G, GATENBY, R.A., YATES, S.W., Search for mixed-symmetry states in the O(6) nucleus ^{134}Ba, Phys. Rev. C **37** (1988) 898.
[63] GARRETT, P.E., et al., Properties of ^{112}Cd from the (n, n′γ) reaction: Levels and level densities, Phys. Rev. C **64** (2001) 024316.
[64] FRANSEN, C., et al., Investigation of low-spin states in ^{92}Zr with the (n,n'γ) reaction, Phys. Rev. C **71** (2005) 054304.
[65] YATES, S.W., Microscopic quasiparticle-phonon model in the study of the beta decay of Cd-115, J. Phys. G: Nucl. Part. Phys. **31** (2005) S1393–S1397.
[66] GARRETT, P.E., WARR, N., YATES, S.W., Nuclear structure studies with the inelastic neutron scattering reaction and gamma-ray detection, J. Res. Natl. Inst. Stand. Technol. **105** (2000) 141.
[67] GREENBERG, R., BODE, P., FERNANDES, E., Neutron activation analysis: a primary method of measurement, Spectrochim. Acta Part B **66** 3 (2011) 193–241.
[68] REVAY, Z., In situ determination of hydrogen inside a catalytic reactor using prompt γ-activation analysis, Anal. Chem. **80** (2008) 6066–6071.
[69] SUEKI, K., et al., Nondestructive determination of major elements in a large sample by prompt γ-ray neutron activation analysis, Anal. Chem. **68** (1996) 2203–2209.
[70] BERGAOUI, K., et al., Development of a new deuterium–deuterium (D–D) neutron generator for prompt gamma-ray neutron activation analysis, Appl. Radiat. Isot. **94** (2014) 319–327.
[71] BERGAOUI, K., et al., Prompt gamma-ray neutron activation analysis of boron using Deuterium–Deuterium (D–D) neutron generator, J. Radioanal. Nucl. Chem. **303** (2015) 115–121.
[72] ZHANG, X., et al., "A computerized concrete raw meal analyzer using a D-D neutron generator", (Proc. 4th Int. Conf. Comput. Sci. Educ., Nanning, China, 2009) IEEE (2009) 464–468.
[73] WAKABAYASHI, Y., et al., Feasibility study of nondestructive diagnostic method for chlorine in concrete by compact neutron source and PGA, J. Adv. Concr. Technol. **17** (2019) 571–578.
[74] HEE-JUNG, I., et al., Explosives detection using deuterium-deuterium neutron generator, J. Nucl. Sci. Technol. Suppl. **5** (2008) 364–366.
[75] CHE, Q., et al., "An imaging method utilizing PGNAA gadolinium prompt gamma to determine propped fracture parameters and its application" (SEG Int. Exposition and Annual Mtg., Anaheim, California, USA, October 2018) OnePetro Conf. Proc. (2018) SEG-2018-2998216.
[76] INTERNATIONAL ATOMIC ENERGY AGENCY, Practical Aspects of Operating A Neutron Activation Analysis Laboratory, IAEA TECDOC No. 564, IAEA, Vienna (1990).
[77] LIU, Y., et al., A compact DD neutron generator–based NAA system to quantify manganese (Mn) in bone in vivo, Physiol. Meas. **35** (2014) 1899.
[78] REIJONEN, J., et al., First PGAA and NAA experimental results from a compact high intensity D–D neutron generator, Nucl. Instrum. Methods Phys. Res. A **522** (2004) 598–602.
[79] SAYRE, E.V., LECHTMAN, H.N., Neutron activation autoradiography of oil paintings, Stud. Conserv. **13** (1968) 161–185.

[80] RADEL, R.F., et al., Detection of highly enriched uranium using a pulsed DD fusion source, Fusion Sci. Technol. **52** (2007) 1087–1091.
[81] BENTOUMI, G., et al., Investigation of in-beam prompt and delayed neutron counting techniques for detection and characterization of special nuclear material, Ann. Nucl. Energy **152** (2020) 108001.
[82] FOULON, F., et al., IAEA nuclear science and instrumentation laboratory: support to IAEA member states and recent developments, EPJ Web of Conf. **225** (2020) 10005.
[83] FINK, D., Neutron Depth Profiling (1996), https://sites.google.com/site/nistndp/home.
[84] OUDENHOVEN, J., et al., In situ neutron depth profiling: a powerful method to probe lithium transport in micro-batteries, Adv. Mater. **23** (2011) 4103–4106.
[85] CHEN, C., Origin of degradation in Si-based all-solid-state Li-ion microbatteries, Adv. Energy Mater. **8** 30 (2018) 1801430.
[86] WAS, G., PETTI, D., UKAI, S., ZINKLE, S., Materials for future nuclear energy systems, J. Nucl. Mater. **527** (2019) 151837.
[87] INTERNATIONAL FUSION MATERIALS IRRADIATION FACILITY DEMO ORIENTED NEUTRON SOURCE (IFMIF-DONES) (2021), https://ifmifdones.org/.
[88] MUROGA, T., et al., Users' perspective on D-Li neutron sources (A-FNS and IFMIF-DONES) or DEMO and beyond, J. Nucl. Mater. **535** (2020) 152186.
[89] NATIONAL ACADEMIES OF SCIENCES, ENGINEERING, AND MEDICINE Testing at the Speed of Light: The State of U.S. Electronic Parts Radiation Testing Infrastructure, The National Academies Press, Washington, D.C., USA (2018).
[90] ISIS NEUTRON AND MUON SOURCE, ChipIR (2021), https://www.isis.stfc.ac.uk/Pages/ChipIR.aspx.
[91] ACOSTA URDANETA, G.C., et al., ANEM: a rotating composite target to produce an atmospheric-like neutron beam at the LNL SPES facility, Int. J. Modern Phys.: Conf. Ser. **44** (2016) 1660207.
[92] IWASHITA, H., Accelerated tests of soft errors in network systems using a compact accelerator-driven neutron source, IEEE Trans. Nucl. Sci. **64** (2017) 689–696.
[93] INTERNATIONAL TELECOMMUNICATIONS UNION, New ITU standards to prevent soft errors caused by cosmic rays (2018), https://news.itu.int/new-itu-standards-to-prevent-soft-errors-caused-by-cosmic-rays/.
[94] ALI, F., et al., Dosimetric and microdosimetric analyses for blood exposed to reactor-derived thermal neutrons, J. Radiol. Prot. **38** (2018) 1037–1052.
[95] EL-JABY, S., et al., Method for the prediction of the effective dose equivalent to the crew of the International Space Station, Adv. Space Res. **53** (2018) 1037–1052.
[96] KUMAWAT, S., et al., Expanding avenue of fast neutron mediated mutagenesis for crop improvement, Plants **8** 6 (2019) 164.
[97] GAGNON, K.M., Cyclotron Production of Technetium-99m, PhD Thesis, University of Alberta, Canada (2011).
[98] JALILIAN, A. et al., Direct technetium radiopharmaceuticals production using a 30MeV Cyclotron, DARU J. Pharm. Sci. **19** (2011) 187–192.
[99] INTERNATIONAL ATOMIC ENERGY AGENCY, Planning a Clinical PET Centre, Human Health Series No. 11, IAEA, Vienna (2010).
[100] SCHMOR, P., Review of cyclotrons for the production of radioactive isotopes for medical and industrial applications, Rev. Accel. Sci. Technol. **4** (2011) 103–116.
[101] NUCLEAR ENERGY AGENCY, The Supply of Medical Radioisotopes: An Economic Study of the Molybdenum-99 Supply Chain, NEA No. 6967, NEA, Paris (2010).

[102] INTERNATIONAL ATOMIC ENERGY AGENCY, Cyclotron Produced Radionuclides: Guidance on Facility Design and Production of Fluorodeoxyglucose (FDG), Radioisotopes and Radiopharmaceuticals Series No. 3, IAEA, Vienna (2012).
[103] INTERNATIONAL ATOMIC ENERGY AGENCY, Cyclotron Produced Radionuclides: Guidelines for Setting Up a Facility, Technical Reports Series No. 471, IAEA, Vienna (2009).
[104] MASSACHUSETTS INSTITUTE OF TECHNOLOGY–NUCLEAR REACTOR LABORATORY, Neutron Transmutation Doping of Silicon (2020), https://nrl.mit.edu/facilities/ntds.
[105] RESEARCH NEUTRON SOURCE HEINZ MAIER–LEIBNITZ, Silicon Doping (2020), https://www.frm2.tum.de/en/industry-medicine/silicon-doping/.
[106] INTERNATIONAL ATOMIC ENERGY AGENCY, Neutron Transmutation Doping of Silicon at Research Reactors, IAEA TECDOC No. 1681, IAEA, Vienna (2012).
[107] PYEON, C., et al., Perspectives of research and development of accelerator-driven system in Kyoto University Research Reactor Institute, Prog. Nucl. Energy **82** (2015) 22–27.
[108] GOHAR, Y., Accelerator-driven subcritical facility: conceptual design development, Nucl. Instrum. Methods Phys. Res. Sect. A **562** (2006) 870–874.
[109] SAUERWEIN, W., WITTIG, A., MOSS, R., NAKAGAWA, Y. (Eds.), Neutron Capture Therapy–Principles and Applications, Springer, Heidelberg (2012).
[110] BLUE, T., YANCH, J., Accelerator-based epithermal neutron sources for boron neutron capture therapy of brain tumors, J. Neuro-Oncol. **62** 1–2 (2003) 19–31.
[111] DROSG, M., Monoenergetic neutron production by two-body reactions in the energy range from 0.0001 to 500 MeV (Overview), TCM-Meeting of IAEA, Debrecen, Hungary (1999), https://pdfs.semanticscholar.org/b577/dadd3f5d27adfaf64686a47f5404aeebc36a.pdf.
[112] VALKOVIĆ, V., 14 MeV Neutrons–Physics and Applications, Taylor & Francis Group, Boca Raton (2016).
[113] HAMM, R., HAMM, M. (eds.), Industrial Accelerators and their Applications, World Scientific, London (2012).
[114] HANNA, S., RF Linear Accelerators for Medical and Industrial Applications, Artech House, Norwood, MA (2012).
[115] MOSS, C., et al., Survey of Neutron Generators for Active Interrogation, Los Alamos National Laboratory, Los Alamos (2017).
[116] HELLBORG, R. (ed.), Electrostatic Accelerators–Fundamentals and Applications, Springer, Heidelberg (2005).
[117] MILEY, G., MURALI, S., Inertial Electrostatic Confinement (IEC) Fusion–Fundamentals and Applications, Springer, New York (2014).
[118] DOLAN, T., Fusion Research; Principles, Experiments and Technology, Pergamon Press, Oxford (1982).
[119] MORSE, E., Nuclear Fusion, Springer Nature Switzerland, Cham (2018).
[120] INTERNATIONAL ATOMIC ENERGY AGENCY, Regulations for the Safe Transport of Radioactive Material, IAEA Safety Standards Series No. SSR-6 (Rev.1), IAEA, Vienna (2018).
[121] STELZER, K.J., et al., Fast neutron radiotherapy: the University of Washington experience, Acta Oncologica **33** 3 (1994) 275–280.
[122] BÉM, P., et al., High-power TR-24 cyclotron-based p-n convertor cooled by submerged orifice jet, EPJ Web of Conf. **231** (2020) 03005.

[123] PAPASH, A., ALENITSKY, Y., On commercial H^- cyclotrons up to 30 MeV energy range for production of medicine isotopes, Probl. At. Sci. Technol. No. 5. Ser. Nucl. Phys. Invest. **50** (2008) 143–145.
[124] DYMOVA, M.A., et al., Boron neutron capture therapy: current status and future perspectives, Cancer Commun. **40** (2020) 406–421.
[125] INTERNATIONAL ATOMIC ENERGY AGENCY, Radiation Oncology Physics: A Handbook for Teachers and Students, IAEA, Vienna (2005).
[126] GRANADA, J.R., et al., The sciences and applications of the electron LINAC-driven neutron source in Argentina, Eur. Phys. J. Plus. **1316** (2016) 216.
[127] FURUSAKA, M., et al., Activity of Hokkaido University neutron source, HUNS. Phys. Procedia **60** (2014) 167–174.
[128] SANO, T., et al., Analysis of energy resolution in the KURRI-LINAC pulsed neutron facility, EPJ Web of Conf. **146** (2017) 03031.
[129] AUDITORE, L., et al., Study of a 5 MeV electron linac based neutron source, Nucl. Instrum. Methods Phys. Res. B **229** 1 (2005) 137–143.
[130] HUANG, W., LI, Q., LIN, Y., Calculation of photoneutrons produced in the targets of electron linear accelerators for radiography and radiotherapy applications, Nucl. Instrum. Methods Phys. Res. B **229** (2005) 339–347.
[131] HUANG, W., et al., Measurement of photoneutrons produced by a 15 MeV electron linac for radiography applications, Nucl. Instrum. Methods Phys. Res. B **251** (2006) 361–366.
[132] VEGA-CARILLO, H., BALTAZAR-RAIGOSA, A., Photoneutron spectra around an 18 MV LINAC, J. Radioanal. Nucl. Chem. **287** (2011) 323–327.
[133] TORABI, F., MASOUDI, S., RAHMANI, F., Photoneutron production by a 25 MeV electron linac for BNCT application, Ann. Nucl. Energy **54** (2013) 192–196.
[134] KOSAKO, K., et al., Angular distributions of photoneutrons from copper and tungsten targets bombarded by 18, 28, and 38 MeV electrons, J. Nucl. Sci. Technol. **48** 2 (2011) 227–236.
[135] AUDITORE, L., et al., Design of a photoneutron source based on a 5 MeV electron linac, (Proc. EPAC 2004, Lucerne, Switzerland) (2004) 2347–2349.
[136] PETWAL, V., et al., Optimization studies of photoneutron production in high-*Z* metallic targets using high energy electron beam for ADS and transmutation, Pram. J. Phys. **68** 2 (2007) 235–241.
[137] KIM, J. K., KIM, K.-O., Current research on accelerator-based boron neutron capture therapy in Korea, Nucl. Eng. Technol. **41** 4 (2009) 531–544.
[138] HODGES, M., BRAZILOV, A., CHEN, Y., LOWE, D., Characterization of a 6 MeV accelerator driven mixed neutron/photon source, Phys. Procedia **90** (2017) 164–169.
[139] BECKER, J., Simulation of neutron production at a medical linear accelerator, Diploma Thesis, University of Hamburg (2007).
[140] INTERNATIONAL ATOMIC ENERGY AGENCY, Modern Neutron Detection: Proceedings of a Technical Meeting. IAEA TECDOC No. 1935, IAEA, Vienna (2020).
[141] SALEHI, D., SARDARI, D., JOZANI, S., Characteristics of a heavy water photoneutron source in boron neutron capture therapy, Chin. Phys. C **37** (2013) 078201.
[142] GALLMEIER, F., General purpose photoneutron production in MCNP4, ORNL/TM 13073, Oak Ridge National Laboratory, Tennessee (1995).
[143] ELLER, L., An Investigation on Photoneutron Production from Medical Linear Accelerators, M.S. Thesis, Oregon State University, USA (2012).

[144] TSUCHIKAWA, Y., et al., "Construction of the 2nd beamline of Nagoya University Accelerator-driven Neutron Source (NUANS)", (Proc. Inter. Conf. Neutron Optics NOP2017, Nara, Japan), J. Phys. Soc Jpn. Proc. Conf. Proc. **22** (2018) 011024.
[145] KREINER, A., et al., Accelerator-based BNCT, Appl. Radiat. Isot. **88** (2014) 185–189.
[146] CARTELLI, D., et al., Present status of accelerator–based BNCT: focus on development in Argentina, Appl. Radiat. Isot. **106** (2015) 18–21.
[147] KREINER, A., et al., Present status of accelerator-based BNCT, Rep. Pract. Oncol. Radiother. **21** 2 (2016) 95–101.
[148] CAPOULAT, M., et al., Neutron spectrometry of the ^{9}Be(d (1.45 MeV), n)^{10}B reaction for accelerator-based BNCT, Nucl. Instrum. Methods Phys. Res., Sect. B **445** (2019) 57–62.
[149] CAPOULAT, M., KREINER, A., A ^{13}C(d,n)-based epithermal neutron source for boron neutron capture therapy, Physica Medica **33** (2017) 106–113.
[150] KREINER, A.J., et al., A tandem-ESQ for accelerator-based boron neutron capture therapy, Nucl. Instr. Meth. B **261** (2007) 751–754.
[151] TASKAEV, S., Accelerator based epithermal neutron source, Phys. Part. Nucl. **46** (2015) 956–990.
[152] TASKAEV, S., Development of an accelerator-based epithermal neutron source for boron neutron capture therapy, Phys. Part. Nucl. **50** (2019) 569–575.
[153] BYKOV, T., et al., Use of a wire scanner for measuring a negative hydrogen ion beam injected in a tandem accelerator with vacuum insulation, Instrum. Exp. Tech. **61** (2018) 713718.
[154] BYKOV, T., et al., Measurement of the space charge effect of a negative hydrogen ion beam, AIP Conf. Proc. **2052** (2018) 070004.
[155] KASATOV, D., MAKAROV, A., TASKAEV, S., SHCHUDLO, I., Recording of current accompanying an ion beam in a tandem accelerator with vacuum insulation, Tech. Phys. Lett. **41** (2015) 139–141.
[156] IVANOV, A., et al., Suppression of an unwanted flow of charged particles in a tandem accelerator with vacuum insulation, JINST **11** (2016) 04018.
[157] TASKAEV, S., et al., Accelerator neutron source for boron neutron capture therapy, IPAC–2018, Vancouver (2018).
[158] KUZNETSOV, A., et al., First experiments on neutron detection on the accelerator-based source for boron neutron capture therapy, Tech. Phys. Lett. **35** (2009) 346–348.
[159] KASATOV, D., et al., Proton beam of 2 MeV 1.6 mA on a tandem accelerator with vacuum insulation, JINST **9** 12 (2014).
[160] IVANOV, A., et al., Obtaining a proton beam with 5-mA current in a tandem accelerator with vacuum insulation, Tech. Phys. Lett. **9** (2016) 608–611.
[161] KASATOV, D., et al., New feedthrough insulator of the compact tandem–accelerator with vacuum insulation (Proc. 28th Intern. Symposium on Discharges and Electrical Insulation in Vacuum (ISDIEV), Greifswald, Germany) IEEE (2018) 761–764.
[162] KOLESNIKOV, I., SOROKIN, I., TASKAEV, S., Increasing the electric strength of a vacuum-insulated tandem accelerator, Instrum. Exp. Tech. **63** (2020) 807–815.
[163] KOLESNIKOV, I., KOSHKAREV, A., TASKAEV, S., SHCHUDLO, I., Diagnostics of the effectiveness of a stripping target of the vacuum insulated tandem accelerator, Instrum. Exp. Tech. **63** (2020) 310–314.
[164] BADRUTDINOV, A., et al., In situ observations of blistering of a metal irradiated with 2-MeV protons, Metals **7** 12 (2017) 558.
[165] ZHANG, Z., Performance of the CMS precision electromagnetic calorimeter at LHC run II and prospects for high–luminosity LHC, JINST **13** (2018) C04013.

[166] KASATOV, D., et al., Fast neutron source based on a vacuum insulated tandem accelerator and a lithium target, Instrum. Exp. Tech. **63** (2020) 611–615.
[167] WANGLER, T., RF Linear Accelerators, 2nd edn, Wiley-VCH Verlag, Weinheim (2008).
[168] KAPCHINSKIY, I., Theory of Resonance Linear Accelerators (Vol. 5), Harwood Academic Publishers, Amsterdam (1985).
[169] SCHEMPP, A., Radio-frequency quadrupole linacs, CERN Accelerator School–Radio Frequency Engineering, Geneva, Switzerland. CERN (2005) 305–314.
[170] RINCKEL, T., et al., LENS operating experience. Phys. Procedia **26** (2012) 161-167.
[171] OTAKE, Y., RIKEN accelerator-driven compact neutron systems. EPJ Web of Conf. **231** (2020) 01009.
[172] GERIGK, F., "Review on trends in normal conducting linacs for protons, ions and electrons, with emphasis on new technologies and applications", (Proc. 28th Linear Accelerator Conf. (LINAC'16), East Lansing, MI, USA) JACoW (2016) 336–338.
[173] PODLECH, H., et al., The superconducting linac approach for IFMIF (Proc. IEEE Particle Accelerator Conference PAC07, Albuquerque, USA) IEEE (2007) 1434–1436.
[174] MARDOR, I., et al., The Soreq applied research accelerator facility (SARAF): overview, research programs and future plans, Eur. Phys. J. A **54** (2018) 1–32.
[175] HÖLTERMANN, H., et al., "Light ion linear accelerator up to 7 AMeV for NICA" (26th Russian Particle Accelerator Conf. RUOAC2018, Protvino, Russia) JACoW (2019) 68–71.
[176] PICARDI, L., et al., Beam commissioning of the 35 MeV section in an intensity modulated proton linear accelerator for proton therapy, Phys. Rev. Accel. Beams **23** (2020) 020102.
[177] DEGIOVANNI, A., STABILE, P., UNGARO, D., LIGHT: "A linear accelerator for proton therapy" (Proc. 2016 North American Particle Accelerator Conf. (NAPAC2016) Chicago, USA) JACoW (2016) 1282–1285.
[178] PODLECH, H., et al., "The MYRRHA-RFQ–status and first measurements" (Proc. 8th International Particle Accelerator Conf., IPAC2017, Copenhagen, Denmark) JACoW (2017) 2243–2245.
[179] GARNETT, R., ORNL D-Li Fusion Neutron Facility–Accelerator Systems Cost Report, Los Alamos National Lab (2019).
[180] LONE, M., FERGUSON, A., ROBERTSON, B., Characteristic of neutrons from Be targets bombarded with protons, deuterons and alpha particles, Nucl. Instrum. Methods **143** (1977) 331–523.
[181] KNASTER, J., et al., Overview of the IFMIF/EVEDA project, Nucl. Fusion **57** (2017) 10.
[182] GALES, S., SPIRAL2 at GANIL: next generation of ISOL facility for intense secondary radioactive ion beams, Nuclear Physics A **834** 1–4 (2010) 717c–723c.
[183] PENG, S., The deuteron accelerator preliminary design for BISOL, Nucl. Instrum. Methods B **376** (2016) 420–424.
[184] WEISSMAN, L., et al., Accurate measurements of the ^{63}Cu(d,p)^{64}Cu and ^{nat}Cu(d,x)^{65}Zn cross-sections in the 2.77–5.62 MeV energy range, Nucl. Instrum. Methods B **342** (2015) 7–12.
[185] SHOR, A., et al., Fast chopper for single radio-frequency quadrupole bunch selection for neutron time-of-flight capabilities, Phys. Rev. Accel. Beams **22** (2019) 020403.
[186] SNAVELY, R., et al., Intense high-energy proton beams from petawatt-laser irradiation of solids, Phys. Rev. Lett. **85** (2000) 2945–2948.

[187] BORGHESI, M., et al., Fast ion generation by high-intensity laser irradiation of solid targets and applications, Fusion Sci. Technol. **49** 3 (2006) 412–439.
[188] ROTH, M., et al., A bright, laser-neutron source based on relativistic transparency of solids, Phys. Rev. Lett. **110** (2013) 044802.
[189] HURRICANE, O., et al., Fuel gain exceeding unity in an inertially confined fusion implosion, Nature **506** (2014) 343–348.
[190] COWAN, T., et al., Photonuclear fission from high energy electrons from ultraintense laser-solid interactions, Phys. Rev. Lett. **84** (2000) 903.
[191] GUENTHER, M., et al., A novel nuclear pyrometry for the characterization of high-energy bremsstrahlung and electrons produced in relativistic laser plasma interactions, Phys. Plasmas **18** (2011) 083102.
[192] WILKS, S., et al., Absorption of ultra-intense laser pulses, Phys. Rev. Lett. **69** (1992) 1383–1386.
[193] POMERANTZ, I., et al., Ultrashort pulsed neutron source, Phys. Rev. Lett. **113** (2014) 184801.
[194] DITMIRE, T., et al., Nuclear fusion from explosions of femtosecond laser-heated deuterium clusters, Nature **398** (1999) 489–492.
[195] BANG, W., et al., Experimental study of fusion neutron and proton yields produced by petawatt-laser-irradiated D_2–^{3}He or CD_4–^{3}He clustering gases, Phys. Rev. E **87** (2013) 0033108–1.
[196] ROTH, M., et al., Energetic ions generated by laser pulses: a detailed study on target properties, Phys. Rev. ST-AB **5** (2002) 061301.
[197] WILKS, S., et al., Energetic proton generation in ultra-intense laser-solid interactions, Phys. Plasmas **8** (2001) 542.
[198] LANCASTER, K., et al., Characterization of ^{7}Li(p,n)^{7}Be neutron yields from laser produced ion beams for fast neutron radiography, Phys. Plasmas **11** (2004) 3404.
[199] HIGGINSON, D., et al., Laser generated neutron source for neutron resonance spectroscopy, Phys. Plasmas **17** (2010) 100701.
[200] HIGGINSON, D., et al., Production of neutrons up to 18 MeV in high-intensity, short-pulse laser matter interactions, Phys. Plasmas **18** (2011) 100703.
[201] KRYGIER, A., et al., Selective deuterium ion acceleration using the Vulcan petawatt laser, Phys. Plasmas **22** (2015) 053102.
[202] WAGNER, F., et al., Pre-plasma formation in experiments using petawatt lasers, Optics Express **22** (2014) 29505–29514.
[203] YIN, L., et al., GeV laser ion acceleration from ultrathin targets: the laser break-out afterburner, Laser and Part. Beams **24** 2 (2006) 291–298.
[204] YIN, L., et al., Monoenergetic and GeV ion acceleration from the laser breakout afterburner using ultrathin targets, Phys. Plasmas **14** (2007) 056706.
[205] HEGELICH, B., et al., Experimental demonstration of particle energy, conversion efficiency and spectral shape required for ion-based fast ignition, Nucl. Fusion **51** (2011) 083011.
[206] OPPENHEIMER, J., PHILLIPS, M., Note on the transmutation function for deuterons, Phys. Rev. **48** (1935) 500–502.
[207] JUNG, D., et al., Characterization of a novel, short pulse laser-driven neutron source, Phys. Plasmas **20** (2013) 056706.
[208] ZOU, J., et al., High power laser science and engineering design and current progress of the Apollon 10 PW project, High Power Laser Sci. Eng. **3** (2015) e2.

[209] KIYANAGI, Y., Accelerator-based neutron source for boron neutron capture therapy, Ther. Radiol. Oncol. **2** (2018) 55.
[210] CAPOULAT, M., et al., ^{9}Be(d,n)^{10}B-based neutron sources for BNCT, Appl. Radiat. Isot. **88** (2014) 190–194.
[211] HAYASHI, S., et al., Measurements of angular distributions and energy spectra of neutrons from photoneutron targets for fast neutron spectrum study, Annu. Rep. Res. Reactor Instrum. Kyoto Univ. **13** (1980) 23.
[212] HALFON, S., et al., Demonstration of a high-intensity neutron source based on a liquid-lithium target for accelerator based boron neutron capture therapy, Appl. Radiat. Isot. **106** (2015) 57–62.
[213] KIYANAGI, Y., SAKURAI, Y., KUMADA, H., TANAKA, H., Status of accelerator-based BNCT projects worldwide, AIP Conf. Proc. **2160** (2019) 050012.
[214] YAMAGATA, Y., et al., Development of a neutron generating target for compact neutron sources using low energy proton beams, J. Radioanal. Nucl. Chem. **305** (2015) 787–794.
[215] GRAND ACCELERATEUR NATIONAL D'IONS LOURDS, NFS–Neutrons for Science (2020), https://www.ganil-spiral2.eu/scientists/ganil-spiral-2-facilities/experimental-areas/nfs/.
[216] INTERNATIONAL ATOMIC ENERGY AGENCY, Current Status of Neutron Capture Therapy, IAEA TECDOC No. 1223, IAEA, Vienna (2001).
[217] CARRON, N.J., An Introduction to the Passage of Energetic Particles Through Matter. CRC Press, Boca Raton, Florida (2007).
[218] FANTIDIS, J.G., Beam shaping assembly study for BNCT facility based on a 2.5 MeV proton accelerator on Li target. J. Theor. Appl. Phys. **12** (2018) 249–256.
[219] CEBALLOS, C., et al., Towards the final BSA modeling for the accelerator-driven BNCT facility at INFN LNL. Appl. Radiat. Isot. **69** (2011) 1660–1663.
[220] URITANI, A., et al., "Design of beam shaping assembly for an accelerator–driven BNCT system in Nagoya University", (Proc. Inter. Conf. Neutron Optics NOP2017, Nara, Japan). J. Phys. Soc Jpn. Proc. Conf. Proc. **22** (2018) 011002.
[221] HASHIMOTO, Y., HIRAGA, F., KIYANAGI, Y., Optimal moderator materials at various proton energies considering photon dose rate after irradiation for an accelerator-driven ^{9}Be (p, n) boron neutron capture therapy neutron source. Appl. Radiat. Isot. **106** (2015) 88–91.
[222] KIYANAGI, Y., IWASA, H., Pulsed neutron intensity from rectangular shaped light water moderator with fast-neutron reflector, J. Nucl. Sci. Tech. **19** (1982) 352–358.
[223] KIYANAGI, Y., Neutronics of polyethylene thermal moderator of wing and slab geometries on pulsed neutron source, J. Nucl. Sci. Tech. **22** (1985) 934–938.
[224] INOUE, K., OTOMO, N., IWASA, H., KIYANAGI, Y., Slow neutron spectra in cold moderators, J. Nucl. Sci. Tech. **11** (1974) 228–229.
[225] INOUE, K., KIYANAGI, Y., IWASA, H., An accelerator-based cold neutron source, Nucl. Instrum. Methods Phys. Res. **192** (1982) 129–136.
[226] INOUE, K., KIYANAGI, Y., IWASA, H., Accelerator-based pulsed cold neutron source, J. At. Energy Soc. Japan **21** (1979) 865–867.
[227] CARPENTER, J., LOONG, C., Elements of Slow-Neutron Scattering: Basics, Techniques, and Applications, Cambridge University Press, Cambridge, United Kingdom (2015).
[228] KIYANAGI, Y., et al., Comparison of coupled liquid hydrogen and solid methane moderators for pulsed neutron sources, Physica B **213–214** (1995) 857–859.

[229] UTSORO, M., SUGIMOTO, M., Pulsed cold neutron source of solid methylbenzene, J. Nucl. Sci. Tech. **14** (1977) 390–392.
[230] CRONERT, T., et al., Compact and easy to use mesitylene cold neutron moderator for CANS, Physica B **551** (2018) 377–380.
[231] CANTARGI, F., et al., New scattering kernels for some materials of interest as advanced cold neutron moderators, Physica B **385** (2006) 1312–1314.
[232] EISENHUT, S., et al., Cryostat for the provision of liquid hydrogen with a variable ortho–para ratio for a low-dimensional cold neutron moderator, EPJ Web of Conf. **231** (2020) 04001.
[233] LAUSS, B., et al., A new facility for fundamental particle physics: the high–intensity ultracold neutron source at the Paul Scherrer Institute, AIP Conf. Proc. **1441** (2012) 576–578.
[234] AHMED, S., et al., First ultracold neutrons produced at TRIUMF, Phys. Rev. C **99** (2019) 025503.
[235] SCHREYER, W., et al., Optimizing neutron moderators for a spallation-driven ultracold-neutron source at TRIUMF, Nucl. Instrum. Methods Phys. Res. Sect. A **959** (2020) 163525.
[236] GRAMMER, K.B., BOWMAN, J.D., Monte Carlo calculation of the average neutron depolarization for the NPDGamma experiment, Nucl. Instrum. Methods Phys. Res. Sect. A **942** (2019) 162336.
[237] KIYANAGI, Y., Effect of reflector on intensity of thermal neutrons emitted from moderator for pulsed neutron source, J. Nucl. Sci. Tech. **24** (1987) 490–497.
[238] NESVIZHEVSKY, V., et al., Fluorinated nanodiamonds as unique neutron reflector, J. Neutron Res. **20** (2018) 81–82.
[239] TESHIGAWARA, M., et al., Measurement of neutron scattering cross section of nano-diamond with particle diameter of approximately 5 nm in energy range of 0.2 meV to 100 meV, Nucl. Instrum. Methods Phys. Res. **929** (2019) 113–120.
[240] TANAKA, H., et al., "Measurement of the thermal neutron distribution in a water phantom using a cyclotron based neutron source for boron neutron capture therapy", IEEE Nucl. Sci. Symp. Conf. Rec. (2009) 2355–2357.
[241] KUMADA, H., et al., Development of LINAC-based neutron source for boron neutron capture therapy in University of Tsukuba, Plasma Fusion Res. **13** (2018) 2406006.
[242] WILLIAMS, R.E., ROWE, J.M., KOPETKA, P., The liquid hydrogen moderator at the NIST research reactor (Proc. Int. Workshop on Cold Moderators for Pulsed Neutron Sources, Argonne National Laboratory, Illinois, USA) NIST Neutron Center for Neutron Research (1997).
[243] BAXTER, D.V., SWAINSON, I., Activities of an IAEA coordinated research project on advanced cold moderators, Neutron News **30** (2019) 19–25.
[244] MEZEI, F., et al., Low dimensional neutron moderators for enhanced source brightness, J. Neutron Res. **17** (2014) 101–105.
[245] OGAWA, Y., KIYANAGI, Y., FURUSAKA, M., WATANABE, N., Experimental studies on neutronics of coupled grooved liquid-hydrogen moderator for long pulse spallation sources, J. Neutron Res. **6** (1997) 197–204.
[246] KIYANAGI, Y., Optimization of grooved thermal moderator for pulsed neutron source, and its characteristics, J. Nucl. Sci. Tech. **21** (1984) 735–743.
[247] INTERNATIONAL ATOMIC ENERGY AGENCY, Decommissioning of Particle Accelerators, Nuclear Energy Series No. NW-T-2.9, IAEA, Vienna (2020).
[248] UNITED NATIONS INDUSTRIAL DEVELOPMENT ORGANISATION. COMFAR: Computer Model for Feasibility Analysis and Reporting (COMFAR) (2021), https://www.unido.org/resources-publications-publications-type/comfar-software.

[249] MAIR, G., MACKAY, S., COOK, T., Economic and Social Impacts of TRIUMF, MMK Consulting, Vancouver, Canada (2009).
[250] HERR, D., et al., The impact of the UK's public investments in UKAEA fusion research, 2020/049, London Economics, United Kingdom (2020).
[251] ORGANISATION FOR ECONOMIC CO-OPERATION AND DEVELOPMENT, Strengthening the effectiveness and sustainability of international research infrastructures, OECD Science, Technology and Industry Policy Papers No. 48, OECD Publishing, Paris (2017).
[252] ORGANISATION FOR ECONOMIC CO-OPERATION AND DEVELOPMENT, Reference framework for assessing the scientific and socio-economic impact of research infrastructures, OECD Science, Technology and Industry Policy Papers No. 65, OECD Publishing, Paris (2019).
[253] ORGANISATION FOR ECONOMIC CO-OPERATION AND DEVELOPMENT /SCIENCE EUROPE, Optimising the operation and use of national research infrastructures, OECD Science, Technology and Industry Policy Papers No. 91, OECD Publishing, Paris (2020).
[254] PAUL, M., et al., Reactions along the astrophysical s-process path and prospects for neutron radiotherapy with the Liquid-Lithium Target (LiLiT) at the Soreq applied research accelerator facility (SARAF), Eur. Phys. J. A **55** (2019) 44.
[255] MASTINU, P., et al., Microchannel-based high specific power lithium target, Il Nuovo Cimento **38C** (2015) 193.
[256] OTT, F., et al., The SONATE project, a French CANS for materials sciences research, EPJ Web Conf. **231** (2020) 01004.
[257] BRÜCKEL, T., et al., Conceptual design report, Jülich high brilliance neutron source (HBS), Schriften des Forschungszentrums Jülich, Volume 8 (2020).
[258] ARGENTINA UNIDA, Normas regulatorias (2020), https://www.argentina.gob.ar/arn/marco-regulatorio/normas-regulatorias.
[259] AUTORIDAD REGULATORIA NUCLEAR, ARGENTINA, Norma Básica de Seguridad Radiológica, Norma AR 10.1.1., Revisión 4. Resolución Nº 521/19 (2019).
[260] AUTORIDAD REGULATORIA NUCLEAR, ARGENTINA, Licenciamiento de Instalaciones Clase I, Norma AR 0.0.1., Revisión 2. Resolución Nº 39/01 (2001).
[261] AUTORIDAD REGULATORIA NUCLEAR, ARGENTINA, Operación de Aceleradores de Lineales de Uso Médico, Norma AR 8.2.2., Revisión 1. Resolución Nº 18/02 (2002).
[262] AUTORIDAD REGULATORIA NUCLEAR, ARGENTINA, Exposición ocupacional en aceleradores de partículas Clase I, Norma AR 5.1.1., Revisión 1. Resolución Nº 36/01 (2002).
[263] PISCITELLI, F., et al., The multi-blade boron-10-based neutron detector for high intensity neutron reflectometry at ESS, J. Instrum. **12** 3 (2017) P03013.
[264] VRIJE UNIVERSITEIT BRUSSEL, Nuclear Safety and the Environment: Evaluation of the Radiological and Economic Consequences of Decommissioning Particle Accelerators, EUR 19151, European Commission, Luxembourg (1999).
[265] GRANADA, R., Proyecto ALBA: propuesta de un nuevo acelerador lineal de electrones en el Centro Atómico Bariloche, Comisión Nacional de Energía Atómica, Bariloche (2014).
[266] GRANADA, R., MAYER, R., Proyecto: Reemplazo del Acelerador Lineal de Electrones del CAB, Comisión Nacional de Energía Atómica, Bariloche (2017).

ANNEX

Table A-1 provides a list of many of the training schools for neutron beam methods that are or have been active in recent years.

TABLE A-1. NEUTRON TRAINING SCHOOLS

School	Location	Country	Duration / Frequency	No. students	Details
HERCULES[a]	Univ. Grenoble Alpes	FR	4 weeks, yearly	40	Neutron and X-ray practicals
FANs[b]	Lab. Léon Brillouin	FR	4 days, yearly	30	Neutron practicals
JCNS Laboratory Course on Neutron Scattering	FZ Jülich	DE	10 days, yearly	50	Neutron practicals
CETS Central European Neutron School[c]	KFKI	HU	6 days, yearly	30	Neutron practicals
Oxford School of Neutron Scattering[d]	ISIS	UK	12 days, every 2 years	60	Neutron practicals
Berlin Neutron School	HZB Berlin	DE			Stopped in 2018
SONS School of Neutron Scattering. Scuola Neutroni	Erice	IT			Stopped in 2016
School on Neutron Scattering	LANSCE, Los Alamos	US			Stopped in 2015
SwedNESS Swedish Neutron School (NNSP)[e]	Swedish Foundation for Strategic Research (SSF)	SE		20	
National School on Neutron and X-Ray Scattering	Argonne NL - Oak Ridge NL	US	11 days, yearly	60	Virtual in 2021
PSI Summer School on Condensed Matter Research.	Zuoz	CH			Stopped
Summer School on Fundamentals of Neutron Scattering[f]	NIST, Gaithersburg, MD	US		35	
Canadian Neutron Scattering Summer School[g]	Chalk River, CNL	CA	5 days, yearly	40	Virtual in 2020
Neutron and Muon School[h]	J-PARC	JP			

TABLE A-1. NEUTRON TRAINING SCHOOLS (cont.)

School	Location	Country	Duration / Frequency	No. students	Details
ANSTO-HZB Neutron School[i]	ANSTO	AU			
AONSA Neutron School[j]	AONSA		5 days, yearly	30	Location changes every year
Bilbao Neutron School	ESS Bilbao, Bilbao	SP			
The All-Russian School for Young Scientists and Students and International Student Practice Summer School		RU			
The All-Russian School for Young Scientists on Boron Neutron Capture Therapy	Novosibirsk	RU	3 days, yearly	80	

Notes:

[a] Hercules European School, http://hercules-school.eu/.

[b] Laboratoire Lėon Brillouin, http://www-llb.cea.fr/fanLLB/.

[c] Central European Training School, https://www.kfki.hu/cets/.

[d] Oxford School on Neutron Scattering, https://www.oxfordneutronschool.org/.

[e] SWEDNESS, https://www.swedness.se/.

[f] CHRNS Summer School on the Fundamentals of Neutron Scattering–Scattering, https://www.nist.gov/ncnr/2019-chrns-summer-school-fundamentals-neutron-scattering-spectroscopy.

[g] Canadian Institute for Neutron Scattering, http://cins.ca/ss2017/.

[h] The 4th Neutron And Muon School & Mirai PhD School, https://neutron.cross.or.jp/4th-nms/.

[i] ANSTO–HZB Neutron School, https://www.ansto.gov.au/whats-on/ansto-hzb-neutron-school.

[j] AONSA School, http://aonsa.org/aonsa-school/.

LIST OF ABBREVIATIONS

ADS	Accelerator Driven System
ALARA	As Low As Reasonably Achievable
BGO	Bismuth Germanium Oxide
BNCT	Boron Neutron Capture Therapy
BPA	Boronophenylalanine
BSA	Beam Shaping Assembly
CANS	Compact Accelerator based Neutron Source
CERN	European Organization for Nuclear Research
CNEA	Comisión Nacional de Energía Atómica (Argentina)
CP	Charge Parity
CW	Continuous Wave (continuous beam)
D–D (DD)	Deuteron–Deuteron nuclear reaction
DGNAA	Delayed Gamma Neutron Activation Analysis
D–T (DT)	Deuteron–Triton nuclear reaction
DSAM	Doppler Shift Attenuation Method
DTL	Drift Tube Linac
ECR	Electron Cyclotron Resonance
ESS	European Spallation Source
FWHM	Full Width Half Maximum
GDR	Giant Dipole Resonance
HPRL	High Priority Request List
HPGe	High Purity Germanium
IECF-NG	Inertial Electrostatic Confinement Fusion Neutron Generator
INAA	Instrumental Neutron Activation Analysis
INS	Inelastic Neutron Scattering
LINAC	LINear ACcelerator
MS	Mixed symmetry
NAA	Neutron Activation Analysis
NDP	Neutron Depth Profiling
NEA	Nuclear Energy Agency
NG	Neutron Generator
OECD	Organisation for Economic Co-operation and Development
PGAA	Prompt Gamma Neutron Activation Analysis
PIG	Penning Ionization Gauge
RF	RadioFrequency
RFQ	RadioFrequency Quadrupole
SANS	Small Angle Neutron Scattering
SCL	SuperConducting Linac
TESQ	Tandem ElectroStatic Quadrupole
TMR	Target-Moderator-Reflector
TOF	Time-of-Flight
TRIGA	Training, Research, Isotopes, General Atomics (research reactor)
TT	Triton-Triton nuclear reaction
UCANG	Ultra-compact Neutron Generator
UNIDO	United Nations Industrial Development Organisation
VITA	Vacuum Insulated Tandem Accelerator

CONTRIBUTORS TO DRAFTING AND REVIEW

Berkovits, D.	Soreq Nuclear Research Centre, Israel
Brown, P.	Mevex Corporation, Canada
Chai, J.	Sungkyungkwan University, Korea
Charisopoulos, S.	International Atomic Energy Agency
Fritzsche, H.	Canadian Nuclear Laboratories, Canada
Gutberlet, T.	Forschungszentrum Jülich, Germany
Kardjilov, N.	Helmholtz Zentrum Berlin, Germany
Kiyanagi, Y.	Nagoya University, Japan
Klujber, G.	Budapest University of Technology and Economics Institute of Nuclear Techniques, Hungary
Kreiner, A.J.	Comisión Nacional de Energía Atómica, Argentina
Lee, C-H.	Korea Atomic Energy Institute, Korea
Lee, D.W.	Korea Atomic Energy Institute, Korea
Mavric, H.	International Atomic Energy Agency
Ott, F.	Commissariat à l'énergie atomique et aux énergies alternatives, France
Plante, J.	Canadian Nuclear Safety Commission, Canada
Roth, M.	Institut für Kernphysik, Germany
Sengbusch, E.	Phoenix Corporation, United States of America
Swainson, I.P.	International Atomic Energy Agency
Sztejnberg, M.	Comisión Nacional de Energía Atómica, Argentina
Tanaka, H.	Kyoto University, Japan
Taskaev, S.	Budker Institute for Nuclear Physics, Russian Federation
Thomsen, K.	Paul Scherrer Institut, Switzerland
Verma, R.	Bhabha Atomic Research Centre, India

Technical Meeting
Venna, Austria: 4–7 November 2019

Consultants Meeting
Vienna, Austria: 26–27 November 2018

IAEA
International Atomic Energy Agency

No. 26

ORDERING LOCALLY

IAEA priced publications may be purchased from the sources listed below or from major local booksellers.

Orders for unpriced publications should be made directly to the IAEA. The contact details are given at the end of this list.

NORTH AMERICA

Bernan / Rowman & Littlefield

15250 NBN Way, Blue Ridge Summit, PA 17214, USA
Telephone: +1 800 462 6420 • Fax: +1 800 338 4550

Email: orders@rowman.com • Web site: www.rowman.com/bernan

REST OF WORLD

Please contact your preferred local supplier, or our lead distributor:

Eurospan Group

Gray's Inn House
127 Clerkenwell Road
London EC1R 5DB
United Kingdom

Trade orders and enquiries:

Telephone: +44 (0)176 760 4972 • Fax: +44 (0)176 760 1640
Email: eurospan@turpin-distribution.com

Individual orders:

www.eurospanbookstore.com/iaea

For further information:

Telephone: +44 (0)207 240 0856 • Fax: +44 (0)207 379 0609
Email: info@eurospangroup.com • Web site: www.eurospangroup.com

Orders for both priced and unpriced publications may be addressed directly to:

Marketing and Sales Unit
International Atomic Energy Agency
Vienna International Centre, PO Box 100, 1400 Vienna, Austria
Telephone: +43 1 2600 22529 or 22530 • Fax: +43 1 26007 22529
Email: sales.publications@iaea.org • Web site: www.iaea.org/publications

International Atomic Energy Agency
Vienna